DISSERTATION

THE CARDIAC JELLY EXTRACELLULAR MATRIX CONTRIBUTES TO VALVE DEVELOPMENT AND OVERALL CARDIAC FUNCTION

Submitted by

Paige Ostwald

Graduate Degree Program in Cell and Molecular Biology

In partial fulfillment of the requirements

For the Degree of Doctor of Philosophy

Colorado State University

Fort Collins, Colorado

Summer 2022

Doctoral Committee:

Advisor: Deborah Garrity

David Bark
Patricia Bedinger
Erin Nishimura
Graham Peers

ABSTRACT

THE CARDIAC JELLY EXTRACELLULAR MATRIX CONTRIBUTES TO VALVE DEVELOPMENT AND OVERALL CARDIAC FUNCTION

Nearly 2.6 million infants are born every year with a congenital cardiac anomaly across the entire globe. Congenital heart defects (CHDs) within the valve occur in over 50% of cases. 56% of heart defects have an unknown etiology, illuminating the need for continuous research on heart development and potential causes. Before the valve is a mature structure with established leaflets, the heart forms two endocardial cushions that press together to occlude blood flow between chambers. The cushions are composed of an extracellular matrix called the cardiac jelly (CJ). Previous studies have found evidence of the vital role the cardiac jelly plays within the developing valve for structure, genetic signaling and cell organization. Here, we present a specific role the cardiac jelly plays in valve function and overall cardiac output. To alter the cardiac jelly, we used a morpholino approach in a zebrafish model to increase, decrease and structurally compromise the cardiac jelly. By doing so, we found decreased valve cell differentiation with decreased CJ and increased valve cell differentiation with increased CJ. Using high-speed video technology, we also found decreased valve opening regardless of cardiac jelly alteration, resulting in reduced overall cardiac function. Our results suggest that the function of the endocardial cushions relies on an appropriate presence of CJ. We next investigated just how the cardiac jelly may be altered during development. To do so, we exposed zebrafish embryos to hyperglycemic conditions during the initial and critical heart development period. We found that when embryos absorb over 1.5-fold more D-glucose due to high-glucose conditions, they exhibit significant alterations to CJ width. Altered CJ due to hyperglycemic conditions affected valve differentiation, valve opening, and cardiac function,

particularly when embryos have absorbed over a 2-fold increase of glucose. Together, these results show the structural role of the cardiac jelly to support endocardial cushion opening which will supply enough oxygenated blood to the embryo.

ACKNOWLEDGMENTS

I would like to thank my advisor, Dr. Deborah Garrity. She has been a constant source of knowledge, support, and inspiration ever since I was undergraduate student in her lab. Throughout the many years, she has provided an environment for personal growth and professional exploration which I know has shaped me into the scientist I am today. I would also like to thank my committee who have supported me through this entire endeavor with their insightful feedback and advice.

I would also like to thank the many members of the Garrity Lab I have had the honor of working with. I have had the pleasure of mentoring undergraduates who have helped me complete this project. I'd like to thank John Reed and Jordan Crowther who have taught me just as much as I have taught them. I would also like to thank my fellow graduate students (past and present) who have worked alongside me and have also supported me; Dr. Rasha Alnefaie, Areej Alshahrani, Dr. Andrea Kingcade, Dr. Neha Ahuja, Alex Gendernalik, Brandon Hylton, and Beth Wittmann. I especially need to thank Neha for being an incredible scientist, student, mentor, and friend. You have helped me more than you know, and I would not be here today without you.

Finally, I need to thank my friends and family for providing the support system I needed to complete this journey. To my fiancé Jared, you have been my number one fan before I even began graduate school and you never stopped believing I could do this even when I stopped believing. To my parents, Don and Donna, and my brother, Alex, you have always been there for me while I pursued this degree, and your support has been unrelenting. To the Collins family, thank you for being my home away from home. I'm blessed to have even more people who are not specifically mentioned that have been by my side, rain, or shine. Thank you.

TABLE OF CONTENTS

Chapter 1 – Congenital Birth Defects and Heart Development

SUMMARY

Globally, 7.9 million infants are born with a serious birth defect. Of those defects, cardiac anomalies are the most prevalent, accounting for nearly one-third of reported cases (Lobo 2008, van der Linde, Konings et al. 2011). As a result, many children are disabled for life or their affliction results in death (Lobo 2008). Congenital heart defects (CHDs) may be caused by inherited genetic mutations, spontaneous mutations, or nongenetic experiences associated with increased risk. However, for nearly half of all reported cardiac birth defects the causes remain unknown (Christianson, Howson et al. 2006). Over the years, surgical repair has been the primary option for repair for severe defects. The technology and techniques available have improved and grown but success is still low with a mortality rate of roughly 10.4%. Although heart development has been studied for many years, much remains to be learned about the intricate molecular and cellular processes required for heart field migration, organ morphogenesis and cardiac cell differentiation. A contributing factor to these processes is the extracellular matrix cell environment. Although studies have established strong connections between the extracellular matrix and cell and molecular aspects of heart development, there remains a gap in knowledge about how the extracellular matrix may play a role in pumping mechanics of the embryonic heart. The more we understand, the better we can detect, diagnose, and correct detrimental defects that affect many people around the world.

1.1 CONGENITAL HEART DEFECTS

Congenital heart defects are defined as anatomical malformations of the heart and/or great vessels during intrauterine development, regardless of the age of presentation (Rao 2012). In the United States, congenital heart defects occur in approximately 8 out of 1000 live births (Shuler, Black et al. 2013). A meta-analysis performed by Liu et al. accessed published studies from 1970-2017 reporting the birth prevalence of CHD. This analysis provided a much

needed review of how risk factors contribute to CHD and how the prevalence of CHD has changed over time (Liu, Chen et al. 2019). Liu et al. reviewed the global impact of CHDs and their distribution. Incidences in Europe are reported to occur in 6.9 out of 1000 births, in Asia 9.3 out of 1000 births, and Africa 2.3 out of 1000 births (van der Linde, Konings et al. 2011, Liu, Chen et al. 2019). It should be noted that global variation could be due to the age of detection in affected individuals paired with availability of prenatal care. Some serious defects are apparent using ultrasound technology within the prenatal and neonatal stage whereas less severe defects may not be detectable until adulthood, providing a challenge in accurately detecting and reporting the frequency of congenital heart defects (Mozaffarian, Benjamin et al. 2015).

In their analysis, Liu et al. showed that variation in global reports of CHDs may be influenced by the level of accessibility of prenatal healthcare. Between the years 1970 and 2017, only 4 of the 260 studies contained data collected from Africa. It is likely that the limited access to healthcare in those regions resulted in fewer diagnoses and fewer reported occurrences (Liu, Chen et al. 2019). However, accuracy in reporting is not always related to gross national income. For example, in the United States, data support an association of uninsured women with decreased prenatal care (Shoff, Yang et al. 2012). Fewer uninsured women receive the vital prenatal care necessary for proper detection, diagnoses, and treatment of congenital birth defects. The rate of CHD incidence has increased by 10% from 2010 to 2017 due to improved echocardiography technology. 90% of this increase is due to higher detection rates of mild CHDs that would have previously gone unnoticed (Liu, Chen et al. 2019). As improved technology becomes available to pregnant women worldwide, more will women receive the prenatal care they need and deserve. As a result, more accurate and consistent reports of different CHDs will provide a better understanding why these defects are occurring.

Types of Congenital Heart Defects

Congenital heart defects exhibit a spectrum of severity. Some birth defects, such as small ventricular septal defects, can correct themselves, usually within the first year of the

patient's life. On the other end of the spectrum lie critical congenital heart defects. 1 in 4 babies born with a heart defect have a critical congenital heart defect. These defects are characterized by the dangerously low levels of oxygen in the newborn and require surgical repair (Oster, Kim et al. 2014). In 2019, Mai et al. published a review of a report on data from United States birth defects from the years 2010-2014 (Mai, Isenburg et al. 2019). These data reported the most common birth defects in the United States which are listed and described below.

Ventricular septal defect (VSD)

Ventricular septal defects (VSDs) are the most commonly occurring congenital heart defects worldwide. This defect is a hole in the septum separating the right and the left ventricles (Figure 1.1, 1). This opening results in inappropriate blood flow from the left ventricle into the right, forcing more blood pumped to the lungs, requiring more work from the heart. If this defect is not repaired, it can contribute significantly to a patient's risk of heart failure, pulmonary hypertension, arrhythmia, or stroke (Mavroudis, Dearani et al. 2019). As with many CHDs, VSDs can be detected prenatally using echocardiogram technology. VSDs can be diagnosed after birth if patients exhibit shortness of breath, fast/heavy breathing, sweating, tiredness while feeding or poor weight gain (Anderson, Stevens et al. 2013). Every year, 16,800 babies are born each year with a VSD. This number is so high because VSDs comprise 20% of all forms of CHD (Mavroudis, Dearani et al. 2019). Almost 80% of patients presenting a VSD will have spontaneous closure of the defect, often not requiring surgery. Those diagnosed will be closely monitored for signs of heart failure until potential spontaneous closure. If the septal defect does not close on its own, surgical repair is necessary. Fortunately, VSD correction surgery is the

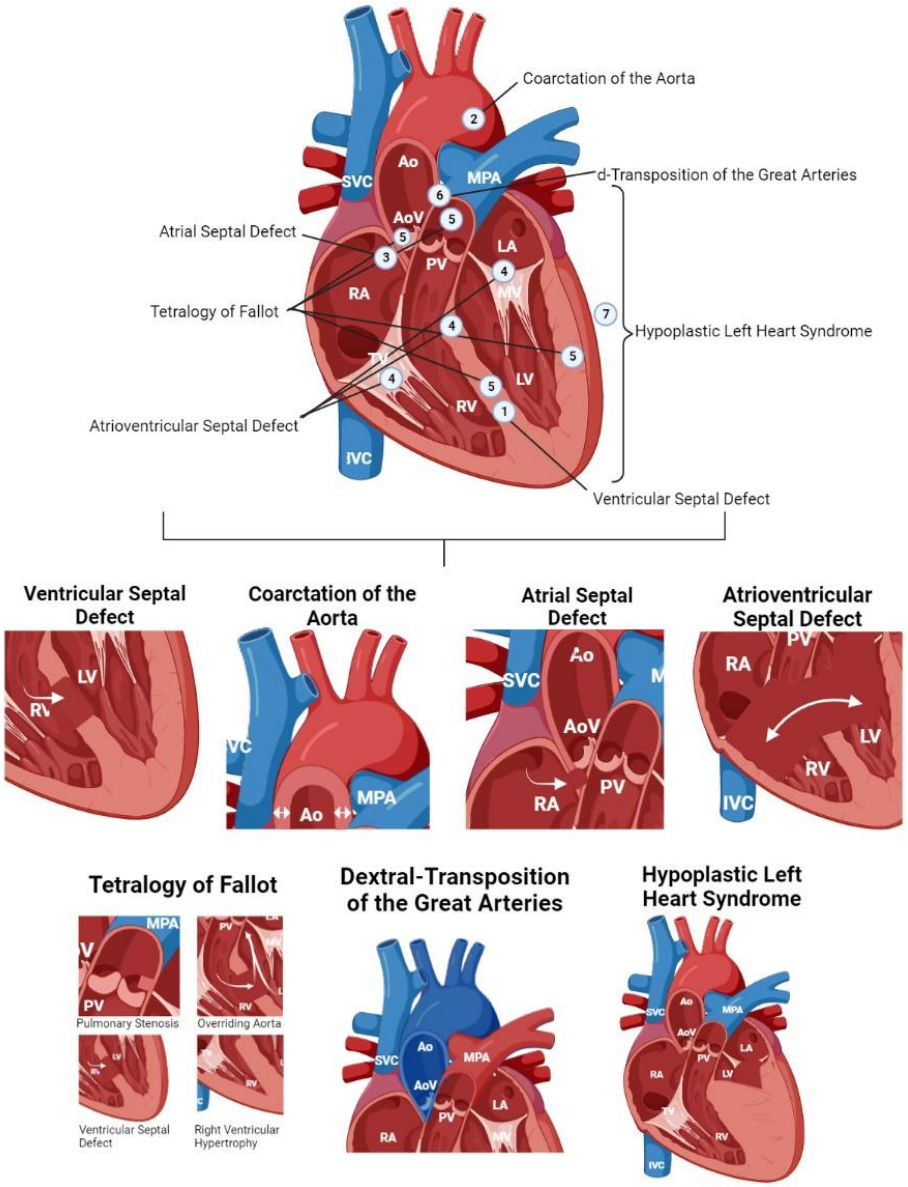

Figure 1.1: *Anatomical positions of common birth defects.* Pictured is a diagram of the adult heart with major structures labeled with white text and locations of common birth defects in blue circles. Common birth defects are ordered in order of most common (1- Ventricular Septal Defect) to less common (7- Hypoplastic Left Heart Syndrome). RA: Right Atrium, RV: Right Ventricle, LA: Left Atrium, LV: Left Ventricle, Ao: Aorta, AoV: Aortic Valve, IVC: Inferior Vena Cava, MPA: Main Pulmonary Artery, MV: Mitral Valve, PV: Pulmonary Valve, SVC: Superior Vena Cava, TV: Tricuspid Valve. Created using BioRender. (Mai, Isenburg et al. 2019)

most common pediatric cardiac surgical procedure and mortality due to surgery is less than 1% (Anderson, Stevens et al. 2013, Rao and Harris 2018).

Coarctation of the aorta (CoA)

Coarctation of the aorta is classified as a critical congenital heart defect. A narrowing of the aorta near the patent ductus arteriosus blocks blood flow to the body and also backs up blood flow into the left ventricle, leading to ventricular hypertrophy (Figure 1.1, 2) (Reifenstein, Levine et al. 1947). Prenatal diagnosis of CoA is often difficult. At the typical time of a routine anomaly scan, CoA is undetectable. Diagnosis of CoA would be easier to detect in the third trimester; however, anomaly scans are not universally performed unless other complications are expected (Familiari, Morlando et al. 2017). In the US, 2,200 babies are born each year with this defect and surgery is required for the infant to survive (Mai, Isenburg et al. 2019).

Atrial septal defect (ASD)

An atrial septal defect is a hole (varying in size) in the septum dividing the upper chambers (atria) of the heart (Figure 1.1, 3). Similar to a ventricular septal defect, the size of the hole determines the severity of the defect, with a smaller hole resulting in a less severe defect and vice versa (Fraisse, Latchman et al. 2018). Prenatally, ASDs may be detectable via ultrasound or echocardiogram. However, if the hole is too small, it may be undetectable. After birth, infants may be diagnosed with ASD after detection of a murmur. Incredibly, some individuals will not be diagnosed with an ASD until adulthood. In the United States, 2,118 babies are born with ASD every year in the (Mai, Isenburg et al. 2019). Sometimes ASDs can close spontaneously. If spontaneous closure does not occur, surgery may be required. Lower mortality is associated with early closure compared to closure later in life (Nyboe, Karunanithi et al. 2018).

Atrioventricular septal defect (AVSD)

Atrioventricular septal defects are holes between the chambers of the right and left sides of the heart (Figure 1.1, 4). Sometimes, valves may also be malformed. Due to this, blood will have less oxygen content which results in extra blood being pumped to the lungs. Structural defects such as this puts a strain on the lungs and may result in congestive heart failure. This is also the most common defect in individuals with Down syndrome (Rao and Harris 2017). Similar to VSDs and ASDs, suspected AVSDs can be confirmed prenatally using an echocardiogram. 2,118 babies are born with AVSD every year in the US (Mai, Isenburg et al. 2019). Ventricular septal defects contribute to 51% of CHD phenotypes in Down syndrome patients (Pfitzer, Helm et al. 2018). Unlike VSDs and ASD, an atrioventricular septal defect cannot correct itself. These defects must be repaired surgically (Rao and Harris 2017).

Tetralogy of Fallot

Tetralogy of Fallot is another condition that is considered a critical congenital heart defect. This heart disease is comprised of four different defects in the heart and its vessels: pulmonary stenosis, overriding aorta, malalignment ventricular septal defect and right ventricular hypertrophy (Figure 1.1, 5) (van der Ven, van den Bosch et al. 2019). This condition may be diagnosed during pregnancy (via echocardiogram) or after the baby is born. If not detected prenatally, tetralogy will be considered if the baby has an episode during which they turn blue while crying or feeding. Skin may appear bluish-looking and/or the heart will have a murmur (Chelliah, Moon-Grady et al. 2021). 1,660 babies are born with tetralogy of Fallot in the United States every year (Mai, Isenburg et al. 2019). To correct this defect, surgeons will either widen or replace the pulmonary valve and place a patch over the ventricular septal defect. Usually, an expedited surgery will result in a more successful outcome. Symptomatic individuals require prompter surgical repair than those non-presenting (van der Ven, van den Bosch et al. 2019).

Dextral-transposition of the great arteries (d-TGA)

D-transposition of the great arteries is a condition in which the main pulmonary artery and the aorta are transposed (Figure 1.1, 6). Because of this juxtaposition, unoxygenated blood does not go to the lungs, rather it goes to the rest of the body. Concomitantly, the oxygenated blood from the lungs goes straight back to the lungs resulting in a lack of oxygenated blood in the rest of the body (Schoeneberg and Adebo 2021). This defect can be detected during pregnancy or soon after the baby is born with two-dimensional echocardiography (Schoeneberg and Adebo 2021). Every year, 1,153 babies are born with TGA in the United States (Mai, Isenburg et al. 2019). D-TGA is classified as a critical congenital heart defect, so surgery is mandatory. Two potential corrective procedures would be the atrial switch procedure (most common, done in the first month of life) or arterial switch operation (less common) (Schoeneberg and Adebo 2021).

Hypoplastic left heart syndrome (HLHS)

Another critical congenital heart defect is hypoplastic left heart syndrome. When the left side of the heart develops abnormally, multiple structures are affected; the left ventricle is underdeveloped, mitral and aortic valves are very small or nonexistent, and the ascending portion of the aorta is underdeveloped (Figure 1.1, 7) (Feinstein, Benson et al. 2012). This birth defect has a known association with atrial septal defect (Chin, Weinberg et al. 1990). To diagnose HLHS prenatally; tests and/or echocardiograms are required. After the baby is born, symptoms such as breathing issues, pounding heart and a weak pulse may be detectable during a physical examination (Feinstein, Benson et al. 2012). Each year, 1,025 babies are born with HLHS in the United States (Mai, Isenburg et al. 2019). Prior to surgery, patients will need medication to help lower blood pressure (Feinstein, Benson et al. 2012). Surgical treatment is possible, but is performed in three separate operations; the Norwood Procedure (Norwood, Lang et al. 1983), the Bi-directional Glenn Shunt Procedure (Mavroudis, Backer et al. 1999), and the Fontan Procedure (d'Udekem, Iyengar et al. 2007). The Norwood procedure is

performed the first two weeks of the baby's life. Using a shunt, blood flow is redirected in a way that the right ventricle is the primary pump to the lungs and the body. Although effective, this procedure still permits oxygen-rich and oxygen-poor blood to mix within the chambers (Norwood, Lang et al. 1983). When the infant is 4 to 6 months old the circulatory load on the right ventricle is alleviated by connecting the pulmonary artery to the superior vena cava (Mavroudis, Backer et al. 1999). Later, when the patient is 18 months to 3 years of age the Fontan Procedure is performed to connect the pulmonary artery and the inferior vena cava. After this procedure oxygen-rich and oxygen-poor blood are no longer mixed (d'Udekem, Iyengar et al. 2007).

Etiologies of Congenital Heart Defects

Due to the extensive amount of research on CHDs, innovative diagnostic techniques have allowed earlier identification of alterations within the first days/weeks of life. However, the etiology of the identified heart defects can remain a mystery. A review published by Zaidi and Brueckner was able to break down the main etiologies of congenital birth defects. 34% of heart defects have a genetic basis. Only 1% of these genetic causes are from a known inherited mutation of a single gene. Other genetic etiologies of heart defects stem from aneuploidies (13%), copy number variations (10%), *de-novo* chromatin single nucleotide variants (SNV) (3%) or other de-novo SNVs (7%). 10% of all heart defects are linked to environmental factors, leaving 56% of CHDs with an unknown etiology (Zaidi and Brueckner 2017). Genetic mutations can exist as a stand-alone defect (isolated defect), but roughly a quarter of diagnoses are associated with a genetically based syndrome disorder (Marín-García 2009). Genetic mutations can also result in epigenetic changes causing the diagnosed CHD. It is important to note that CHDs are not only caused by genetic mutations but there are significant nongenetic risk factors closely associated with CHDs.

Isolated CHD genetic etiology

Heart development involves multitudes of genetic pathways meaning that there are multiple opportunities for gene mutations to lead to CHDs. Using published data, Diz et al compiled a concise list of genes that showed strong association with the most common CHDs as described in Figure 1.1 and Table 1.1. Many of these genes influence early heart development stages such as early heart patterning (*CITED2, NKX2.5, NKX2.6*), cell differentiation (*GATA4, GJA1, NKX2.5*), and chamber development (*CRELD1, GATA6, NOTCH1*); (Diz, Toro et al. 2021). Many common genes associated with CHDs have been linked to multiple malformations, but surprisingly some genes are associated with only a single anomaly (Table 1.2). Further elucidation of unique genes associated with CHDs will lead to faster detection and repair to improve or even save the lives of many.

Table 1.1 Common genes, protein function and associated CHDs

Gene	**Protein function in heart development**	**Associated CHDs**	**References**
CITED2	Controls left-right patterning with transcriptional activation in left lateral plate mesoderm.	Atrial septal defect Ventricular septal defect	(Yahata, Shao et al. 2001, Bragança, Eloranta et al. 2003, Tien, Davis et al. 2004)
CRELD1	Cell adhesion molecule involved in the development of the lower atrial septum and upper ventricular septum	Atrial septal defect Atrioventricular septal defect	(Robinson, Morris et al. 2003) (Zatyka, Priestley et al. 2005)
GATA4	Transcriptional activator in coordination with TBX5 to promote cardiomyocyte gene expression while downregulating endocardial and endothelial gene expression.	Atrial septal defect Ventricular septal defect Tetralogy of Fallot Transposition of great vessels Ventricular septal defect	(Yang, Gharibeh et al. 2013, Ang, Rivas et al. 2016)
GATA6	Transcription factor activating pathways involving BMP-mediated gene expression and outflow tract development.	Atrial septal defect Atrioventricular septal defect Coarctation of the aorta Tetralogy of Fallot	(Kodo, Nishizawa et al. 2009)

GJA1	Ventricular cardiomyocyte gap junction protein	Atrioventricular septal defect Hypoplastic Left Heart Syndrome	(Vincentz, Barnes et al. 2011)
NKX2.5	Homeobox protein expressed in early heart progenitor cells. Involved in heart looping morphogenesis and myocyte differentiation.	Atrial septal defect Atrioventricular septal defect Coarctation of the aorta Hypoplastic Left Heart Syndrome Tetralogy of Fallot Transposition of great vessels Ventricular septal defect	(Lints, Parsons et al. 1993, Lyons, Parsons et al. 1995, Benson, Silberbach et al. 1999)
NKX2.6	Transcription factor in the NK-2 gene family that controls left right patterning and heart tube development.	Atrial septal defect Coarctation of the aorta Tetralogy of Fallot Ventricular septal defect	(Biben and Harvey 1997, Bartlett, Veenstra et al. 2010, Zhao, Ni et al. 2014)
NOTCH1	Paracrine signal involved in the regulation of myocardial gene expression which stimulates proliferation and differentiation of surrounding cells during ventricle development. Also associated with ECM degradation during the trabeculation process.	Coarctation of the aorta Hypoplastic Left Heart Syndrome Tetralogy of Fallot	(Grego-Bessa, Luna-Zurita et al. 2007, Del Monte-Nieto, Ramialison et al. 2018)
NR2F2	Transcription factor that plays a key role atrial differentiation and identity in developing chambers as well as patterning between atrium and atrioventricular canal.	Atrial septal defect Atrioventricular septal defect Tetralogy of Fallot	(Pereira, Qiu et al. 1999, Duong, Ravisankar et al. 2018)
TBX1	Transcription factor that regulates second heart field proliferation and differentiation. It is also required for the recruitment of progenitor cells to the heart.	Coarctation of the aorta Tetralogy of Fallot	(Rana, Théveniau-Ruissy et al. 2014, Alfano, Altomonte et al. 2019)
TBX5	Transcription factor is highly associated with atrial and ventricle septation as	Atrial septal defect Atrioventricular septal defect	(Garrity, Childs et al. 2002, Steimle

	well as earlier chamber development.	Ventricular septal defect	and Moskowitz 2017)

Table 1.2 CHDs and their uniquely associated genes

Pathology	**Unique Associated Genes**
Atrial septal defect	*MYH6, ACTC1, TBX20, TLL1, TBX6, ACVR1/ALK2*
Coarctation of the aorta	*NR2F1, SMAD6*
Hypoplastic left heart syndrome	*PCDHA13*
Tetralogy of Fallot	*JAG1, GATA5, TAB2*
Transposition of great vessels	*MED13L, PITX2*
Ventricular septal defect	*ETS1, TBX1*

Syndromic CHD genetic etiology

Often, CHDs will be associated with genetically based syndromes that affect the heart as well as other tissues (Diz, Toro et al. 2021). Of the syndromes associated with CHDs, 20% are caused by a single variant; 70% of which are *de novo* mutations, and 30% are inherited mutations. 15% of syndromes associated with CHDs have copy number variants such as 22q11.2 chromosome deletion syndrome (DiGeorge syndrome) or 1p36 deletion syndrome (Diz, Toro et al. 2021). One of the key genes described in Table 1.1, *TBX1,* is a gene located within the 22q11.1 locus and has been extensively studied to evaluate its role in heart development (Lindsay, Vitelli et al. 2001). TBX1 is a transcription factor implicated in defects within the developing cardiac outflow tract and pharyngeal arches in individuals with DiGeorge syndrome (Baldini 2004)

Syndromes with chromosomic alteration comprise 10% of syndromes associated with CHDs, 75% of which are Down syndrome (Diz, Toro et al. 2021). Some syndromes associated with CHDs involve alteration of epigenetic regulation of heart development. Wolf-Hirschhorn

syndrome results cranio-facial malformations along with growth retardation, learning disability, and heart defects. These symptoms result from reduced trimethylation of H3K36 (Nimura, Ura et al. 2009). Holt-Oram syndrome, an autosomal dominant 'heart-hand' disorder, is caused by mutation in the *TBX5* gene which is required both in early heart tube patterning and in limb bud initiation and patterning (Table 1.1) (Basson, Bachinsky et al. 1997, Li, Newbury-Ecob et al. 1997). Heart defects include atrial septal defects and ventricular septal defects (Basson, Bachinsky et al. 1997, Li, Newbury-Ecob et al. 1997). TBX5 also functions to regulate epigenetic processes when it is recruited to enhancer sites to promote transcriptional activation for cardiac gene expression (Murakami, Nakagawa et al. 2005). A final syndrome to note is DiGeorge syndrome, which encompasses an interruption of the aortic arch, VSDs, persistent truncus arteriosus and tetralogy of Fallot (Carey, Kelly et al. 1992). Pathogenesis involves TBX1 and its regulation of cardiac gene expression. TBX1 cooperates with NKX2.5 to regulate the PITX2 enhancer. TBX1 also interacts with ASH2l known to epigenetically regulate transcription via methylation (Stoller, Huang et al. 2010).

Of all the syndromes associated with CHDs, it's important to note that 55% of heart defects will have an unknown etiology. This further emphasizes the need to study the developing heart and further understand the required processes for healthy development. The more that is understood, the more advantageous diagnoses become.

Nongenetic risk factors of CHDs

Further studies of the causes of CHDs have led the science community to understand that CHDs do not always have a genetic basis. Nongenetic risk factors such as biological parental age, maternal health, environmental factors, and socioeconomic status are associated with heart anomalies. Advanced maternal age (>40 years old) is associated with an increased risk of Ebstein anomaly, TGA, ASD, or coarctation of the aorta (Miller, Riehle-Colarusso et al. 2011, Patel and Burns 2013, Ntostis, Iles et al. 2021). A study in Egypt found an association between advanced paternal age (>40 years old) and VSDs (Bassili, Mokhtar et al. 2000,

Gonzalez, Ory et al. 2022). Younger maternal age (<30 years old) that is not classified as advanced has an increased risk of tricuspid atresia, total anomalous pulmonary venous return, and tricuspid atresia (Patel and Burns 2013).

Maternal health such as diabetes mellitus and hypertension are strongly associated with CHDs. Pre-gestational diabetes has been associated with a number of conditions including ASD, AVSD, CoA, TGA and Tetralogy of Fallot (Correa, Gilboa et al. 2008, Garne, Loane et al. 2012, Patel and Burns 2013). The underlying mechanisms are still not well understood, but hyperglycemia is believed to play a critical role (Correa, Gilboa et al. 2008). Mothers with hypertension during pregnancy will have pregnancies with a two-fold increased risk of CHDs. The correlation of hypertension to a specific defect has yet to be determined, nor is it understood if the hypertension itself or the medication used for its treatment is the basis for increased risk (Tikkanen and Heinonen 1990, Yauck, Malloy et al. 2004, Caton, Bell et al. 2009, Li, Yang et al. 2011). Environmental factors such as teratogens and infectious agents are often associated with CHD. Teratogens ingested by the mother such as alcohol, retinoic acid and doxycycline have been linked to alcohol-related birth defects, heart valve development and chamber septation, and cardiac hypertrophy (Sinning 1998, Streissguth, Bookstein et al. 2004, Errami, Galindo et al. 2008). Mothers infected with viruses may also put the developing embryo at risk. The Rubella virus is associated with septal defects, aortic stenosis, coarctation of the aorta, tetralogy of Fallot and many other CHDs (Stuckey 1956).

Finally, socioeconomic status of the biological parents is associated with an increased risk of CHD. Low maternal and paternal socioоccupational status was associated with infant CHDs (Kuciene and Dulskiene 2009). Socioоccupational status and a particular CHD have no specific associations, but many characteristics such as an unemployed mother or father, low education levels of either parent are associated with increased risks of CHDs (Yang, Carmichael et al. 2008). A related study found that maternal stress comes with an increased risk of embryonic CHD (Patel and Burns 2013). A possible mechanism includes an excess of

maternal corticosteroids. Animal studies show elevated corticosteroids are teratogenic in various organ systems including the heart (Rowland and Hendrickx 1983, Carmichael, Shaw et al. 2007). Studies have found a threefold greater risk of CHD in infants born to mothers who reported stressful life events compared to those less stressed (Liu, Zhou et al. 2009).

Surgical Outcomes for Congenital Heart Defects

For birth defects such as critical congenital defects and other severe abnormalities, surgical repair is the only option for treatment. Surgical repair has been an option since the 1930s, as evidenced by the first successful repair of a patent ductus arteriosus defect (Gross 1939). As science and medicine continued to progress throughout the years, the median age of patients undergoing their first operation decreased. Between 1971 and 1979, the median age of first operation was 1.6 years. In 1980-1989 the median age decreased to 0.35 years. In current times the median age is <3 weeks old for critical congenital heart defects. Patients with simpler defects have an average higher median age of 5.7 years at the time of surgery (Erikssen, Liestøl et al. 2015). In 2017, 135 hospitals across the United States reported 30,130 congenital cardiovascular operations (Jacobs, Shahian et al. 2018). Infants, children, and adults are all eligible for potential surgical repair. Although improved since the 1930s, the overall survival rate of individuals requiring surgical repair is 89.6% which leaves room for further advances in the field (Spector, Menk et al. 2018). It is important to understand the current options for CHD repair and treatment and how they may be improved for the future.

When an infant is diagnosed with a critical congenital heart defect, surgery will be performed as soon as possible, usually within the first year of the infant's life. Survival has been improving. However, mortality is still quite high (Oster, Lee et al. 2013). Along with mortality, adverse neurodevelopmental disorders have been associated with congenital heart defects. Data published evaluating neurodevelopmental damage post-surgery will be discussed later in this chapter (Clancy, McGaurn et al. 2003, Albers, Bichell et al. 2010, Marino, Lipkin et al. 2012). However, evidence suggests that prenatal brain abnormalities due to congenital heart

disease may also be present *in utero* (Khalil, Bennet et al. 2016). A comprehensive review of multiple studies showed that 28% of fetuses with CHD had structural brain abnormalities. Fetuses with CHD were more likely to have ventriculomegaly (abnormally large ventricles in the brain), white-matter abnormalities, delayed brain development, and other defects. These defects can be detected in the second or third trimester (Khalil, Bennet et al. 2016).

Sometimes CHDs are not severe enough to be repaired until the patient is past the infant stage. In a study of 26,856 children undergoing surgery from January 2012-December 2019, 1.9% of children died, which is a lower rate than the rate in 2012-2015 (Zhang, Luo et al. 2020). Of the children that died, 42.5% died of heart failure and 32.9% died of residual anatomic defects within the heart. In particular, patients diagnosed with transposition of the great arteries died from residual anatomic defects and those diagnosed with ventricular defects died from pulmonary hypertension and heart failure (Zhang, Luo et al. 2020).

Surprisingly, individuals can live well into adulthood before a congenital heart defect is detected. Once detected, some defects may have to be surgically repaired. Of all adult heart disease hospitalizations, around 20% are congenital heart surgery admissions (Kim, Gauvreau et al. 2011). Most of these surgeries occur in pediatric hospitals, primarily due to the local expertise in congenital heart defects (Kim, Gauvreau et al. 2011). In 2007, a European study of adult congenital heart surgery repair was published summarizing the outcomes of 2,012 participants of an average age of 35 years old. The top diagnoses were isolated atrial septal defect (32%), congenital aortic valve stenosis/regurgitation (8%), and pulmonary valve insufficiency (5.9%). The top three surgeries performed were isolated atrial septal defect closure (32.2%), conduit replacement (6.1%), and aortic valve replacement (5.5%). The most common postoperative complications included arrhythmias (154 patients), bleeding (63 patients), and low output syndrome (42 patients) (Vida, Berggren et al. 2007).

Thankfully, surgical repair for individuals with CHDs is an ever-growing and improving field of medicine, but it still requires some improvements. Infants and children are more

susceptible to adverse neurodevelopmental outcomes from CHD surgical repair than adults (Albers, Bichell et al. 2010). Impairments can be mild to severe, involving cognition, motor skills, visual construction, attention, and communication (Marino, Lipkin et al. 2012). Some measures are effective for cerebral protection such as the deep hypothermic circulatory arrest (DHCA) procedure. DHCA involves an induced hypothermic state of the patient while using a cardioplegia-induced cardiac arrest to perform the cardiac repair (S, JE et al. 2010). However, there still involves a risk of neurological damage and seizures (Clancy, McGaurn et al. 2003). A patient can be in a hypothermic state for a “safe” duration, between 39-65 minutes, resulting in a smaller chance of residual neural damage (Kirkham 1998). A higher chance of adverse neurodevelopmental outcomes in infants exists if the duration of circulatory arrest exceeds 41 minutes (Wypij, Newburger et al. 2003).

New techniques have been created to help alleviate the risk of adverse neural impairments. Retrograde cerebral perfusion (RCP) was introduced as a method to improve neurological outcomes in 1988 in which. Cold, oxygenated blood is perfused into the superior vena cava during DHCA (Ueda, Miki et al. 1992, Gatti, Benussi et al. 2017). 3D imaging is used for training, planning and execution of surgeries. These images are created using cardiac computed tomography angiograms, magnetic resonance imaging, rotational angiograms, and 3D ultrasounds. With advanced technologies, 3D images of the heart can be projected as a hologram rather than a flat (2D) screen (Brun, Bugge et al. 2019). Finally, models of congenital heart disease can be 3D printed and used for hands-on surgical training. Although the printing material is different from the human myocardium, the quality is adequate to help surgeons and trainees feel like they have improved their surgical skills (Yoo, Spray et al. 2017). As the technology improves to repair detrimental congenital heart defects is also important to focus on the potential prevention of CHDs. To do so, we must thoroughly understand how the heart develops and all the intricate processes involved for proper organ development and function.

Congenital defects in the valve

Reviewing the most common heart abnormalities and their etiologies illuminated a trending theme of defects occurring within the valve. Congenital abnormalities affecting the valve account for 50% of reported congenital heart defects (Le Gloan, Mercier et al. 2011). A defect in the valve means surgery is most often the only option for treatment (Lincoln and Garg 2014). Valve defects can be isolated to only a valve or they can be combined with other defects within the heart. Isolated valve defects involve a stenosis or regurgitation phenotype such as aortic stenosis, pulmonary stenosis or Ebstein anomaly (Holst, Said et al. 2017). A key example is bicuspid aortic valve disease (BAV), a valve-specific disease when patients develop two unequal-sized leaflets compared to three equal-sized leaflets in unaffected individuals (Siu and Silversides 2010). The unequal valve leaflets result in stenosis and regurgitation (Verma and Siu 2014). BAV is the most common congenital heart defect in adults, affecting 1.3% of the population worldwide. BAV results in more deaths and complications than other congenital heart defects combined (Fedak, Verma et al. 2002, Siu and Silversides 2010).

In conclusion, it is apparent that congenital heart defects affect more individuals than commonly thought. The physical, emotional, and financial burden on the patients and their families/ loved ones is not easy to bear. Although the medical field has innovative techniques and technologies, defects will continue to occur. That is why researchers are investigating why these defects are occurring. A better understanding of the complicated cellular and molecular processes that must occur during heart development could lead to better family planning, screening, detection, and diagnosis of these defects.

1.2 HEART DEVELOPMENT

Early in development, heart progenitor cells originate from bilateral cell populations in the lateral plate mesoderm. These cells will migrate towards the embryonic axis and fuse at the midline. Then the cells form a simple tube composed of 2 distinct cell layers: an interior endocardium and an exterior myocardium. The heart then undergoes a complex series of

morphological changes such as looping and chamber ballooning to form a two-chambered organ. Valve specification and development then begins along with chamber trabeculation and septation, forming a four-chambered heart in mammals (Figure 1.2).

Human development is marked by Carnegie stages (CS), a system of 23 stages used to describe the developmental chronology. Human embryos are not ideal for use in developmental studies due to long gestation periods, internal development, and strict ethical guidelines of use. Many animal models can be used to study heart development, and each has its own benefits and drawbacks. Often mouse models are used because their heart structure, physiology and development are highly conserved with humans. Mouse development is measured in embryonic days (E) and has a rapid timeline compared to humans (Figure 1.2). Most embryonic tissues and cells are accessible in mice, however surgery is required due to *in utero* development (Moon 2008). As a more accessible alternative, zebrafish have emerged as an optimal model for heart development. Zebrafish embryos are externally fertilized and can be collected as early as a single-celled zygote. They have a comparable developmental rate to mice which is measured in hours post fertilization (hpf) (Figure 1.2). Zebrafish embryos are not reliant on a functioning cardiovascular system for survival. Passive diffusion of oxygen is sufficient to keep the embryo alive regardless of cardiovascular failure, which is illuminating for heart development studies (Stainier 2001). Although other non-mammal model organisms, chick, *Xenopus,* etc., can be used, the remainder of this chapter will highlight key developmental stages of the embryonic heart using zebrafish as the primary model.

Migration of myocardial cells in heart tube formation

There are three main cell types in the linear heart tube, atrial cardiomyocytes, ventricular cardiomyocytes, and endocardial cells. These cell types trace back to cardiac progenitor cells (CPCs). In the zebrafish blastula (5 hpf), CPCs are in the lateral marginal zone. Cardiomyocyte progenitors separate into two different pools, those within the anterior lateral plate mesoderm and those within the medial pharyngeal mesoderm. The cardiomyocyte progenitors from the

anterior lateral plate are considered the first heart field (FHF) (Rydeen and Waxman 2016). During gastrulation, the FHF cells travel towards the posterior half of the anterior lateral plate mesoderm in two separate groups. These bilateral pools of CPCs fuse to form the cardiac crescent with an inner endocardial ring lined by ventricular and atrial myocytes, eventually resulting in a heart tube (Stainier 2001, Brown, Samsa et al. 2016). Meanwhile, progenitors from the medial pharyngeal mesoderm are labeled as the second heart field (SHF). This heart field gives rise to later-differentiating cardiomyocytes that contribute to the arterial and venous poles of the heart (Rydeen and Waxman 2016).

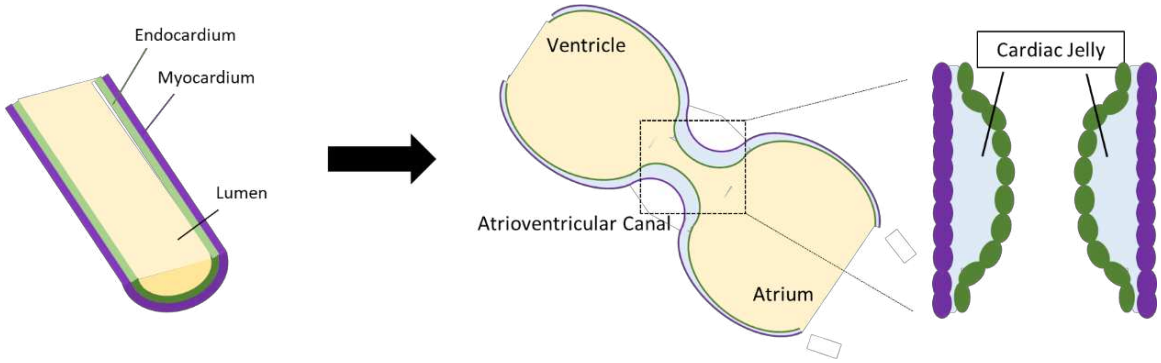

	Heart Tube Formation	Heart Looping and Chamber Ballooning	Valve Development
Zebrafish	24 hpf	36 hpf	36 hpf – 96 hpf
Mouse	E7.5	E8.75	E9 - Birth
Human	CS9	CS11	CS13-23

Figure 1.2: *Basic stages of vertebrate heart development.* The heart first forms a linear tube composed to two cell layers: the outer myocardium and inner endocardium. The tube then undergoes looping and chamber ballooning to form the atrium, ventricle and an early valve structure called the atrioventricular canal. Within this canal, an extracellular matrix called the cardiac jelly forms between the two cell layers to create valve cushions. These processes are conserved across species but have different developmental rates (Stainier 2001, Moon 2008, Sylva, van den Hoff et al. 2014).

Heart Tube Formation and Heart Looping

After the cardiac crescent forms, the cells will assemble to form a linear heart tube composed of two cell layers: an outer layer of myocardial precursors and an inner layer of

endocardial precursors (Figure 1.2). Starting at 19 hpf, the myocardial cells form a horse-shoe shaped structure which will transform into a cone. Ventricular cells are at the center of the cone and atrial cells are at its base. The cone will then telescope out to form the linear tube. The ventricular end of the heart tube will assemble first, followed by the atrial end. By 24 hpf the heart tube is parallel to the anteroposterior axis with the atrial end left of the embryonic midline. At this point the heart begins to beat and at 36 hpf the heart will undergo a substantial morphological change by looping and chamber ballooning. During these events, the heart will establish its left-right asymmetry (Stainier 2001).

Endocardial cushion formation and valve morphogenesis

Beginning at 36 hpf, the cardiac jelly begins to swell between the myocardial and endocardial cell layers at the atrioventricular canal (AVC) (Stainier 2001). In contrast, the extracellular matrix within the cardiac chamber boundaries gradually decreases (Figure 1.2, Figure 1.3A); (Rasouli and Stainier 2017). The cardiac jelly (CJ) is a transient form of cardiac ECM that emerges between the endocardial and myocardial cell layers in the heart tube. The myocardium secretes the components of the CJ, consisting of collagen, glycoproteins and glycosaminoglycans (Williams and Black III 2015). When the embryo reaches 72 hpf, the thick layer of cardiac jelly at the AVC provides necessary space for the movement of endocardial cells into the extracellular space. This movement of cells varies slightly between vertebrates. It has been found that in mice and humans, endocardial cells at the AVC undergo an epithelial-to-mesenchymal transition and invade the extracellular matrix. In zebrafish, the endocardial cells invaginate and fold into the extracellular matrix (Figure 1.3B). The migrating endocardial cells differentiate into valve interstitial cells at 96 hpf and the valves become more functional by occluding retrograde blood flow. The surrounding endocardial cells rely on spatiotemporal cues from the ECM to differentiate into valve-specific cells and create the general valve structure (Figure 1.3C). Genetic signaling between the two cell layers promotes ECM expansion localized to the AVC while minimizing expansion at the ballooning chamber surfaces, establishing the

boundaries between the cardiac chambers and the AVC. As the valve matures the ECM stratifies into three layers and transitions from a pliable, glycosaminoglycan-rich structure to a firmer structure with thick collagen bundles and denser collagen cross-links (5 days post fertilization) (Figure 1.3D) (Pagnozzi and Butcher 2017).

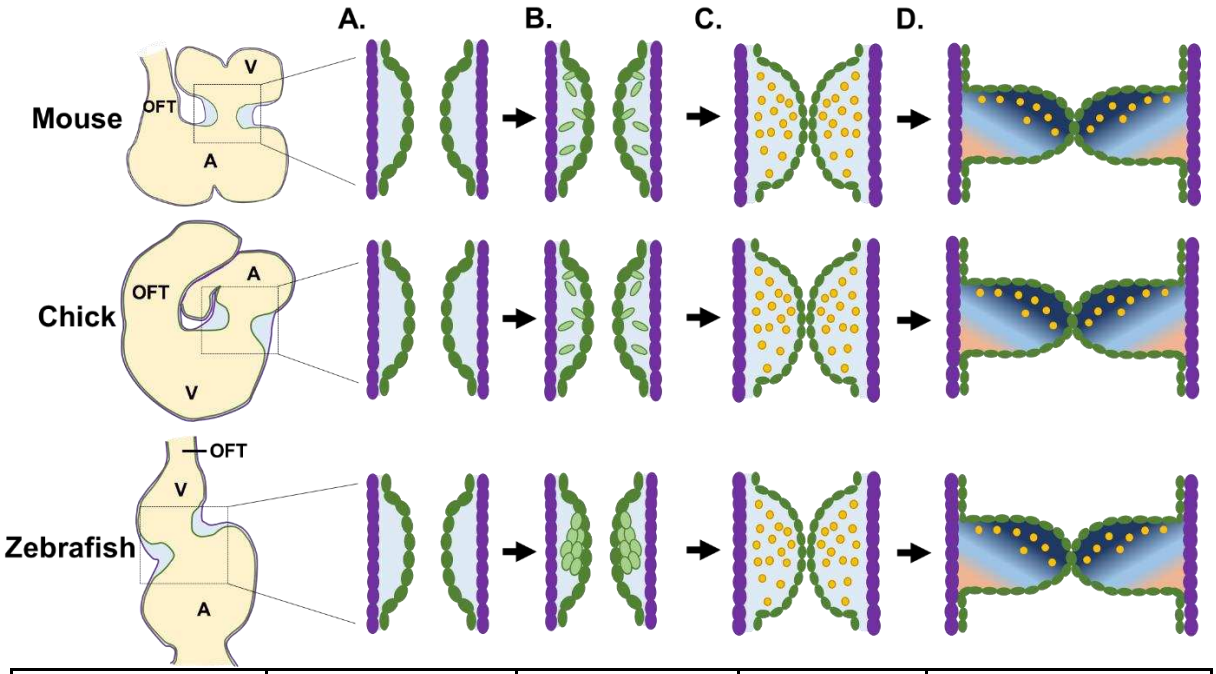

	Cardiac Jelly Accumulation	Endocardial Migration	Mature Cushions	Stratified Valve Leaflets
Mouse	E9	E9.5	E12.5	E14.5 - Birth
Chick	HH12	HH16	HH22	HH28 - 36
Zebrafish	36 hpf	72 hpf	96 hpf	Day 5 - Day 16

Figure 1.3: *Atrioventricular valve development across species*. **A)** Valve development begins with cardiac jelly accumulating between the myocardial (purple) and endocardial (green) cell layers. **B)** Endocardial cells begin the fill the space created by the cardiac jelly by epithelial to mesenchymal transition (mouse, chick) or endocardial cell folding (zebrafish). **C)** Valve interstitial cells then create the mature valve-like cushions. **D)** After remodeling the valve leaflets become stratified and mature. A, atrium; V, ventricle; OFT, outflow tract.[1]

[1] This figure was created by Paige Ostwald and previously published. Ahuja, N., P. Ostwald, D. Bark and D. Garrity (2020). "Biomechanical Cues Direct Valvulogenesis." J Cardiovasc Dev Dis **7**(2).

Chamber development and trabeculation

As the previous section focused on the development of the valve, it is important to include the processes occurring concomitantly within the chamber. Chamber development includes cardiac wall trabeculation and septation. Trabeculation increases myocardial surface area within chambers which in turn increases cardiac output. Within the chambers, a layer of cardiac jelly lies between the endocardium and myocardium. When trabeculation begins, the myocardial cells invade the cardiac jelly and protrude into the cardiac chamber. After trabeculation, myocardial cells proliferate and increase in size, resulting in remodeling and compaction (Williams and Black III 2015). Then, in mammalian species, septation of the atria and ventricles occurs. Research on developmental time points post valve development is more common in mammalian models due to their more precise relationship to human cardiac development. Zebrafish do not undergo septation, so they are not an ideal model for research on some chamber development studies.

1.3 EXTRACELLULAR MATRIX IN DEVELOPMENT

ECM Composition

There has been a significant increase in the amount of research on the extracellular matrix. With the increase in research comes further elucidation, but not complete knowledge, on the vital role of the ECM in development. The majority of findings identify many cellular and molecular functions the ECM is associated with in heart development. But the exact mechanisms remain to be established. What also remains is a solid understanding of how the ECM influences the mechanics of the heart and how the ECM may be a link between molecular and mechanical function during development.

Surprisingly, zebrafish have been a popular model for studying the precise mechanisms underlying the ECM's influence in development. Although the entire composition of zebrafish ECM has not been established, researchers have been able to identify key components that influence multiple developmental timepoints (Mundell and Jessen 2013, Jessen 2015). As

reviewed by Williams and Black, the components comprising the cardiac ECM can be categorized based on structure and/or function (Figure 1.4) (Williams and Black III 2015, Williams, Hsu et al. 2018). Categories include ECM receptors, glycoproteins, collagens, glycosaminoglycans, and proteoglycans along with other molecules that do not lie within these categories. Most substantially, the most studies on cardiac ECM focus on fibronectins, laminins, collagens, proteoglycans, integrins and matrix metalloproteinases (MMPs).

Integrins are type I transmembrane receptor glycoproteins for ECM proteins such as fibronectin, laminin, and collagen. When integrins bind to matrix proteins, tension in the ECM fibrils is created. This tension promotes further integrin binding and cross-linking of fibrils (Schwarzbauer and Sechler 1999). Zebrafish contain at least 17 integrin or integrin-like genes, including multiple *integrinβ1* homologs (Mould, McLeish et al. 2006). Integrins are essential for cell-cell interactions, and cell-environment interactions leading to cell migration, adhesion, proliferation, and survival (Figure 1.4); (Williams and Black III 2015).

Collagen is the most abundant extracellular matrix protein in the mammalian body. Mammals have 43 collagen genes that encode 28 distinct collagens. Based on function and structure, those distinct collagens are sorted into different families (Chan, Poon et al. 2008, Ricard-Blum 2011). Zebrafish encode at least 22 collagen isoforms representing 10 collagen family members (type I, II, IV, V, VI, VII, VIII, IX, X and XI) (Thisse, Heyer et al. 2004). Collagens have a very important role in structural stability. Collagen types I and III are needed for mechanical strength and elasticity during early cardiac morphogenesis. Collagen IV is found in cardiomyocyte basement membranes to maintain stability with an increases mechanical load (Figure 1.4); (Williams and Black III 2015).

Glycoproteins are proteins composed of polypeptide chains covalently bound to oligosaccharide chains. Fibronectins are large multidomain glycoproteins widely expressed in adult and embryonic tissues. Fibronectins exist in two forms: soluble and insoluble. The insoluble form is the major extracellular matrix protein (Schwarzbauer and Sechler 1999). The

zebrafish genome encodes two fibronectin isoforms, Fibronectin1 and Fibronectin1b (Zhao, Liu et al. 2001, Sun, Zou et al. 2005). Fibronectins mediate multiple cell functions for cardiac development and regeneration by interacting with other ECM molecules, cell surface receptors, and other Fibronectin molecules (Figure 1.4); (Williams and Black III 2015).

Laminins are also a part of the glycoprotein category. Laminins are composed of a combination of alpha, beta, and gamma subunits. Mammals contain at least 16 distinct complexes coded by 12 laminin genes. Zebrafish have 10 laminin orthologs compared to humans (Knöll, Postel et al. 2007). Laminin has a vital role in composing the basement membranes and aides in cardiomyocyte adhesion as they mature. Laminins will also bind integrins and other cell surface receptors (Williams and Black III 2015). Mutations in laminin have been shown to contribute to cardiomyopathies (Figure 1.4); (Sztal, Berger et al. 2011).

Proteoglycans (PGs) comprise protein cores covalently linked to glycosaminoglycan (GAG) chains that make up most of the molecular mass. Proteoglycans can be secreted, or membrane bound. Along with collagens, proteoglycans represent a vast number of proteins that make up the majority of the extracellular matrix (Mundell and Jessen 2013). Proteoglycans and glycosaminoglycans have a strong affinity to water, creating a hydrated matrix attributing to ECM structure. Glycosaminoglycans such as Hyaluronan are able to act independently of proteoglycans. Hyaluronan plays a key role in early valve development by promoting endocardial cell invasion into the ECM. Versican, a proteoglycan, will interact with other ECM proteins, cell surface receptors, and aide in ECM assembly (Figure 1.4); (Williams and Black III 2015).

Finally, matrix metalloproteinases (MMPs) are part of the metzincin superfamily of zinc-dependent endopeptidases. MMPs will cleave ECM and non-ECM targets and are inhibited by tissue inhibitors of metalloproteinases (TIMPs). Humans have 24 encoded MMPs and 4 TIMPs, compared to zebrafish who have a similar complement of *mmp* and *timp* genes. Zebrafish lack orthologs of human MMP1, 3, 7, 8, 10, 12, 26, and 27 and TIMP1 (Wyatt, Keow et al. 2009).

The ECM is a dynamic environment that requires remodeling and breaking down, particularly during heart development. MMPs and TIMPs ensure that the ECM has the appropriate structure and composition as the heart continues to develop (Figure 1.4); (Williams and Black III 2015).

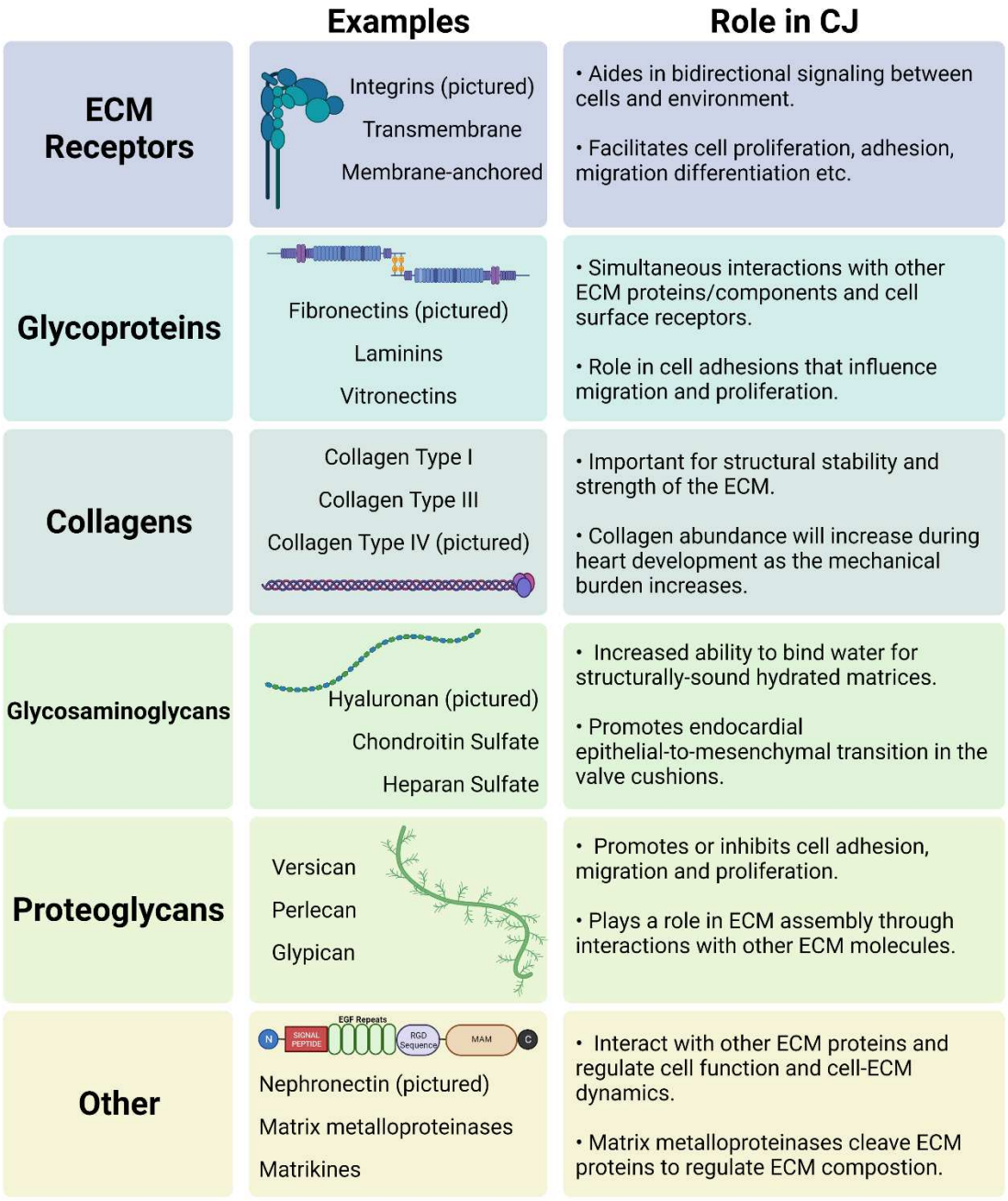

Figure 1.4 *Main components of the cardiac ECM*. The main categories of the ECM are listed, including key molecules and basic functions. Reviewed in (Williams and Black III 2015). Created using BioRender.com.

The role of Fibronectin during myocardial precursor migration in the heart field

The initial migration of the myocardial precursors has been extensively studied to understand the signaling and cues necessary for the cells to arrive at the right place at the right time. Recently, scientists have been investigating how the extracellular matrix surrounding these migrating cells influences their positioning and differentiation. Though particular cell signaling requirements have been revealed, little is known about how cells react to their environment during these migratory stages. Researchers use zebrafish to understand how the ECM may influence these morphogenic movements. Fibronectin plays a vital role for cell migration throughout gastrulation and neurulation stages. Trinh and Stainier were among the first to show that fibronectin is dynamically expressed during cell migration in zebrafish. At the onset of gastrulation, *fibronectin* (*fn*) expression is detected in marginal blastomeres within the mesoderm and is maintained throughout gastrulation. At the somitogenesis stage, *fn* expression is observed at the lateral plate mesoderm and tailbud until the 10-somite stage. At the 11-12 somite stage *fn* is now expressed in a few more medial cells around the yolk extension. Once the embryo reaches 15 somites, *fn* is expressed in two layers of cells at the ventral midline (Trinh and Stainier 2004).

Fibronectin is deposited in the midline between the endoderm and endocardial precursor cells, and it is deposited laterally around the myocardial precursors. Trinh and others showed that the myocardial precursors require the deposition of Fibronectin for proper timing for migration by knocking out the Fibronectin-encoding gene, *nat*. From this mutant analysis they also found the myocardial precursors do not depend on Fibronectin for the migration process itself but rather for maturation. Cell-substratum interactions are supported by adherens junctions and are required for epithelial organization. However, when Fibronectin is completely absent, adherens junctions between the myocardial precursors are malformed (Trinh and Stainier 2004). These studies show us that a Fibronectin-rich ECM plays a crucial role for the migration

of the myocardial cells towards the midline. Without this ECM-component, cells are not able to properly form the initial cardiac structures required.

Migrating cells adhere to the extracellular matrix for the traction necessary to form membrane protrusions and cell body translocation (Friedl and Gilmour 2009). During gastrulation, ectodermal and mesodermal cell populations must elongate and align themselves in a mediolateral fashion. This organization contributes to the convergence and extension of the embryo. Planar cell polarity (PCP) proteins are key regulators of this process. Polarized cell behaviors are necessary for these directed cell migration and intercalation events (Prince and Jessen 2019). PCP proteins are a conserved group of proteins that include VANGL planar cell polarity protein 2 (Vangl2). Vangl2 is a membrane protein known to transmit directional signals and loss of function leads to severe convergence and extension phenotypes. Underlying these normal morphogenetic movements are specific cellular migrations such as directed migration and mediolateral intercalation (Jessen, Topczewski et al. 2002). Cell migration occurs in the context of a fibronectin-containing ECM network. Early in gastrulation, before mesendodermal cells are polarized, they exhibit meandering migration patterns (Jessen, Topczewski et al. 2002). During early gastrulation, minimal fibronectin extracellular matrix localized between the epiblast and hypoblast germ layer, meaning the deep layer of mesendodermal cells are not in contact with the fibronectin ECM. As gastrulation progresses, mesendodermal cells are now classified as mesodermal cells and adopt a polarized morphology coupled with an underlying fibrillar fibronectin network (Love, Prince et al. 2018, Prince and Jessen 2019). When cells transition from a tumbling phase to directed migration, their membrane protrusions change from a bleb-like to filapodia-like and are characterized by localized Vangl2 expression to the cell membrane. Without Fibronectin, mesodermal cells fail to transition from bleb protrusions to filapodia protrusions and Vangl2 fails to translocate to the plasma membrane. Reduced Vangl2 translocation indicates that the cells are not adopting a directed migration phenotype partially because Vangl2 is not at the cell membrane. A fibronectin-rich ECM supports convergence and

extension movements with proper membrane-protrusive activity (Love, Prince et al. 2018). Fibronectin is a critical component for the migration of these cardiomyocyte progenitor cells.

The FHF and the SHF both rely on proper fibronectin levels for heart cell migration (Trinh and Stainier 2004, Mittal, Pulina et al. 2013). Without Fibronectin, the SHF cardiomyocytes fail to develop resulting in a shortened outflow tract (OFT) (Mittal, Pulina et al. 2013). A similar phenotype was also presented in a recent study evaluating the effects of excess retinoic acid (RA). Cyp26 enzymes are main regulators of RA levels within vertebrate embryos. Cyp26 deficient zebrafish embryos have decreased ventricular cardiomyocytes and shortened OFTs, indicating that excess RA disrupts SHF migration (Rydeen and Waxman 2016). In previous studies RA signaling has also been found to disrupt the extracellular matrix cushion within the OFT. It was then discovered that excess RA signaling increases the expression of *matrix metalloproteinase 9 (mmp9)*. MMP9 is known to break down collagen within the extracellular matrix, implicating that MMP9 levels must be limited in order to have an appropriate amount of ECM present for SHF migration (Rydeen and Waxman 2016).

Earlier studies have also demonstrated an inverse relationship between Hand2 and Fibronectin. Hand2 is a bHLH transcription factor necessary for fusion of the cardiac field prior to heart tube formation. The Hand2 pathway was found to provide a proper cell environment for cardiac fusion by limiting the expression of *fibronectin* (Garavito-Aguilar, Riley et al. 2010). Further studies elucidating this relationship have yet to be completed.

The role of Glypican in myocardial precursor migration

Along with fibronectin, Glypican, a proteoglycan, is thought to play a role during the convergence and migration stage of gastrulation (Strate, Tessadori et al. 2015, Love, Prince et al. 2018). Glypican4 is a heparan sulphate proteoglycan (HSPG) that is bound to the cell membrane by a glycosylphosphatidylinositol (GPI) anchor. While anchored to the cell membrane, Glypican4 interacts with various extracellular matrix, growth factors and receptors. Similar to Vangl2, Glypican4 is necessary for PCP and membrane-protrusive activity, however

the two proteins have distinct effects on how the protrusions form and directed cell movement (Love, Prince et al. 2018). The *knypek* zebrafish mutant is deficient for Glypican4 protein and exhibits severe cardiac defects along with a reduced anterior-posterior axis. In wildtype embryos, inhibition of Bone Morphogenetic Protein (BMP) signaling promotes differentiation of cardiac progenitor cells. *Knypek* mutants exhibit high levels of *bone morphogenetic protein (bmp)* expression within the cardiac field resulting in poor cardiomyocyte specification and differentiation which eventually leads to a reduction in heart chamber size. Glypican4 must attenuate Bmp signaling in the anterior lateral plate mesoderm to ensure sufficient cardiac progenitor cell differentiation. This is potentially done through by the interaction of Glypican4's heparin chains with BMP growth factor in the extracellular space but this hypothesis remains elusive in mesoderm-derived cells (Strate, Tessadori et al. 2015). In the endoderm, Glypican4 acts through matrix metalloproteinase 14 to control the levels of ECM optimal for cell migration (Hu, Gao et al. 2018). Yet, the exact mechanism as to how Glypican4 influences the ECM for mesoderm migration is not completely understood.

Cardiac jelly composition and influence on looping

The CJ is initially formless with some radially oriented fibers that become more concentrated and organized prior to heart looping. The CJ is initially acellular and thought to assist in maintaining heart tube structure and regulate blood flow as the organ begins to function. Due to their high affinity for water molecules the GAGs will play a role in the hydration of the matrix. In particular, the GAG Hyaluronan is a main component of the initial CJ. Later on, increased synthesis of this GAG will become a prominent player in endocardial cushion formation (Williams and Black III 2015). At the initial heart tube phase, the CJ is primarily used as structural support. When the heart begins looping, the CJ plays a much more vital role in aiding the morphological change. This process has been extensively researched using chick embryos. In a zebrafish model it has been found that Hyaluronan is required for zebrafish heart looping, but studies using chick have noted otherwise (Baldwin and Solursh 1989, Derrick,

Sanchez-Posada et al. 2019). Although the role of Hyaluronan in cardiac looping is up for debate, another GAG, Heparan sulfate, is vital. Cleavage of Heparan sulfate by heparinase occurs on the left side of the heart tube but not the right. If heparinase cleaves on the right side of the heart tube, then the heart will loop in the opposite direction (Yue, Schultheiss et al. 2004). This is one of the first examples of a constantly changing ECM. During development, scientists believe that the CJ changes its structure and composition to support the needs of the growing embryo, although the field is lacking in current research on this topic.

Of note, one study has been able to use zebrafish to examine chamber-specific expansion of the ECM during the cardiac looping and ballooning stages. At 26 hpf, zebrafish have an asymmetric ECM between the two cell layers. On the left side of the heart tube, in the venus pole/future atrium exists a thicker layer of CJ which is maintained throughout the cardiac cycle. This asymmetry is not caused by a change in synthesis of Hyaluronan but rather by a protein that modifies Hyaluronan cross-linking. Hyaluronan and proteoglycan link protein 1a (Hapln1a) is in the Hapln1 family. Hapln1a is secreted into the ECM and crosslinks Hyaluronan to proteoglycans. In the zebrafish heart tube, *hapln1a* expression is upregulated on the left side of the heart tube at 26 hpf and later barely expressed at 50 hpf within the precursor valve, indicating its function in heart looping and chamber development. Hyaluronan and Hapln1a must interact in a spatiotemporally-regulated manner to properly drive heart morphogenesis. Expression of *hapln1a* does not aide in ventricle morphogenesis, instead it is spatially restricted to the atrium to drive proper looping and ballooning. Furthermore, initiation of *hapln1a* expression is laterally dependent. Cells expressing *hapln1a* are determined by left-right positioning of the heart (Derrick, Sánchez-Posada et al. 2022).

Cardiac jelly expansion- Hyaluronan regulation

Hyaluronan (HA) stands out as a key component of the cardiac jelly. HA is a non-sulfated linear glycosaminoglycan known to promote the cellularization of the endocardial cushion (Lagendijk, Szabó et al. 2013, Williams and Black III 2015). HA within the cushion

creates a meshwork and binds water molecules, creating a stiff viscous structure (Necas, Bartosikova et al. 2008). Previous studies in mice have found that a homozygous mutation for the cardiac-specific enzyme Hyaluronan synthase 2 (Has2) results in a depleted cardiac jelly and embryonic lethality (Camenisch, Spicer et al. 2000). Further studies using zebrafish led to the conclusion that Has2 is downstream of the valve-specific BMP signaling cascade. Starting at 36 hpf myocardial Bmp4 binds to its receptor on endocardial cells, which then activates transcription factor Tbx2b to initiate HA synthesis by Has2 (Shirai, Imanaka-Yoshida et al. 2009).

The Mediator Complex (MC) is composed of multiple subunits that regulate transcription of valve-specific genes. Mediator complex subunit 10 and 12 (Med10 & Med12) are two specific MC subunits characterized in zebrafish (Segert, Schneider et al. 2018). Both subunits promote the synthesis of hyaluronan, contributing to the expansion of the CJ. Med10 acts through the transcription factor Forkhead box N4 (Foxn4) to activate Tbx2b leading to its downstream activation of Has2 (Just, Hirth et al. 2016). Med12 also promotes Tbx2b and its downstream affects. However, Med12 independently acts with Sox9 to activate Bmp4 expression. Both MC subunits play a critical role in ensuring the proper levels of HA are synthesized resulting in a properly formed endocardial cushion. Along with appropriate levels of HA, the Med10 and Med12 activation provide the necessary cues for endocardial cell differentiation and valve development (Segert, Schneider et al. 2018).

To assure CJ expansion at the AVC and not the chamber boundaries, other mechanisms are set in place to regulate HA synthesis. A novel extracellular matrix protein, Nephronectin (Npnt), was found to inhibit Bmp4 signaling between the two cell layers in the cardiac chambers. Inhibition of Bmp4 restricted *has2* expression to only the AVC along with proper valve-cell differentiation and CJ width (Patra, Diehl et al. 2011). More recently, *atrial natriuretic peptide* (*nppa*) and *brain natriuretic peptide* (*nppb*) have been found to play a similar role as *npnt*. In the ballooning surface of the atrium, *nppa* and *nppb* act redundantly to repress the AVC Bmp4

pathway. Conversely, in the AVC, Tbx2b inhibits the chamber genetic program including *Nppa* and *Nppb*. This mutually exclusive regulatory loop between Bmp4, Nppa/Nppb, and Tbx2b establishes a sharp boundary between atrium and AVC (Grassini, Lagendijk et al. 2018).

Endocardial cell migration – integrin-mediated focal adhesion

Defects in HA regulatory genes coincide with poor valve specification. Endocardial cells that should be invaginating and folding into the ECM space fail to differentiate leading to very little development (Patra, Diehl et al. 2011, Just, Hirth et al. 2016, Segert, Schneider et al. 2018). Like the migrating cardiac precursor cells, the endocardial cells rely on sensing the ECM to properly move to their desired location. Migrating cells within the endocardial cushion use a vital process called integrin-mediated focal adhesion (Sun, Guo et al. 2016). This consists of an integrin membrane receptor that mediates communication between the endocardial cell membrane and the ECM. During AVC endocardial cell migration focal adhesion (FA) factors such as integrin subunits *itga5* and *itgb1b* are upregulated encoding the two protein subunits that create Itgα5β1. When Itgα5β1 is activated, cytoplasmic regulators of actin organization are recruited, leading to cell membrane protrusions and cell translocation. These protrusions respond to physical tension of the ECM and guide the migrating cell (Gunawan, Gentile et al. 2019).

Adding to the similarities between precursor and endocardial cell migration, Fibronectin plays a crucial role in valve development. AVC-specific fibronectin synthesis aides in the organization of the folding endocardial cells during leaflet formation (Steed, Faggianelli et al. 2016). In fact, Itgα5β1 binds selectively to Fibronectin, leading to the proposed model that cardiomyocytes secrete Fibronectin when endocardial cells begin migrating. The migrating cells then respond to the extracellular Fibronectin through Itgα5β1 activation subsequently organizing and establishing a multilayered valve tissue (Huveneers, Truong et al. 2008, Gunawan, Gentile et al. 2019).

Trabeculation and ECM

In mice, the process of trabeculation requires five distinct steps; sprouting (E8.0), touchdown formation (E8.0-8.5), lateral ingression (E8.5), extension (E8.5-14) and termination (E14). At E8.0, the endocardium forms sprouts oriented towards the myocardium (sprouting). At the outer curvature of the ventricle, the endocardial cells progress through the cardiac jelly and the columns anchor to the myocardial cell layer (touchdown formation). Between the touchdowns, endocardial ridges form, creating multiple matrix-rich 'bubbles' creating the initial trabecular architectural units. The endocardial touchdowns then expand laterally (lateral ingression). Once these units are formed, cardiomyocytes grow radially, extending the trabeculae while decreasing the amount of extracellular matrix in a basal-to-apical manner (extension). At the peak of trabecular growth, the ECM is minimized and is continued to be reduced past trabecular events (termination); (Del Monte-Nieto, Ramialison et al. 2018).

When trabeculation begins (E8.0), *Hyaluronan synthase 2 (Has2)*, *Versican (Vcan)*, and a hyaluronan receptor, CD44 are upregulated in the initial laminar trabeculae, producing more Hyaluronan and Fibronectin. Interestingly, proteolytic genes known for extracellular matrix degradation *Adamts1*, *Mmp2* and *Hyal2* expression increases in the early touchdown endocardium. This expression then expands in a basal-apical pattern later in trabeculation to degrade ECM proteins. At the termination stage and beyond, expression of these genes occupies the entire endocardium. The expression patterns of both ECM expansion and degradation genes indicate a delicate balance between the presence and absence of the ECM. During trabeculation, when ECM synthesis is reduced and ECM degradation is excessive or vice versa, severe embryonic phenotypes in trabeculation occur. Studies found that NRG1 signaling promotes the synthesis of the ECM whereas NOTCH1 pathways promote ECM degradation. In fact, these pathways have a reciprocal relationship that determine the trabecular architecture during development (Del Monte-Nieto, Ramialison et al. 2018).

Medical applications of the cardiac ECM

As the role of the cardiac extracellular matrix becomes more elucidated, scientists have been striving to find an application of ECM properties to human medicine. In a review published by Derrick and Noël, single-cell analysis and high throughput sequencing have become valuable tools to help bridge the gap between animal models and human medicine (Derrick and Noël 2021). Single-cell transcriptomic analysis of human fetal hearts between 5 weeks and 25 weeks gestation suggest a dynamic expression profile of ECM molecules in cardiomyocytes linked to maturation. Derrick and Noël's review also compiled a list of ECM genes and loci linked to specific congenital heart defects (Table 1.3). Studies have found associations between human loci that encode ECM components and CHDs but a causational link is yet to be determined, emphasizing the need to continue research of the cardiac ECM to establish specific links.

Table 1.3- Valve-related CHDs and associated human genes/loci

Valve-related CHD	Human gene/loci	References
Bicuspid aortic valve	*ACAN* (aggrecan), *B3GAT3* (Glc-AT-I), *MMP2*	(Rambeau, Faure et al. 2017) (Baasanjav, Al-Gazali et al. 2011) (Tuysuz, Mosig et al. 2009)
Atrioventricular septal defect	*ADAMTS1, 2q13 (FBLN7)*	(Thorsson, Russell et al. 2015) (Russell, Raeker et al. 2014)
Aortic valve disease	*ADAMTS19*	(Wünnemann, Ta-Shma et al. 2020)
Cardiac-valvular Ehlers-Danlos syndrome	*COL1A2*	(Malfait, Symoens et al. 2006)
Tetralogy of Fallot	*2q13 (FBLN7), 13q31.1 – 13qter (GPC5), 11q13.1 (LTBP3), 5q14.1-q14.3 (VCAN and HAPLN1)*	(Russell, Raeker et al. 2014) (Quélin, Bendavid et al. 2009) (Glessner, Bick et al. 2014) (Soemedi, Wilson et al. 2012) (Silversides, Lionel et al. 2012)
Mitral valve prolapse and regurgitation	*UGDH*	(Hyde, Farmer et al. 2012)

Our knowledge of the cardiac ECM has the potential to help with genetic diagnosis, as described above, and it has the capacity to provide insight into the healing and repair of adult cardiac tissue. Silva and others reviewed the cardiac ECM and its role in development, homeostasis, and injury response (Silva, Pereira et al. 2020). The adult human heart has the lowest regeneration capacity compared to all organ systems in mammals (Virani, Alonso et al. 2020). The mammalian heart can regenerate in fetal-neonatal stages by triggering proliferation of existing cardiomyocytes. But, regeneration of cardiomyocytes does not happen in adult tissue, which causes build-up of fibrotic tissue, making the tissue stiffer (Silva, Pereira et al. 2020). Studies have evaluated cellular mechanisms behind regeneration, yet they have not evaluated the role of the extracellular matrix. Understanding more about the ECM in healthy and diseased hearts could have an impact on creating novel regenerative therapies (Bassat, Mutlak et al. 2017). After birth, the ECM in the heart undergoes a drastic change in composition, primarily by reducing the abundance of Fibronectin, Hyaluronic acid and proteoglycans and increasing the abundance of collagens and laminin. This results in a more structured ECM surrounding each individual cardiomyocyte (Silva, Pereira et al. 2020). This change in ECM composition coincides with the change in the tissue's regenerative capacity. Studies have provided evidence that the transition from a regenerative state to a reparative state is due to ECM composition alteration (Mammoto, Jiang et al. 2013, Yahalom-Ronen, Rajchman et al. 2015, Notari, Ventura-Rubio et al. 2018). Cardiac ECM-based strategies have been implemented for regeneration and repair in animal models and in human applications. Technical challenges remain preventing the movement of these therapies into clinical standards, but the more that is understood about the ECM will aide in applications in the future (Silva, Pereira et al. 2020).

CONCLUDING REMARKS

As this chapter has demonstrated, there has been significant progress in the study of heart development, congenital birth defects and surgical corrections. Even with these

tremendous advances, there remains many unanswered questions behind how congenital heart defects occur. Key genetic pathways, cell environment and non-genetic factors have been well-established regulators of heart development but the relationship between these regulators remains unclear. Specifically, a knowledge gap exists about the etiology and fundamental processes of the extracellular matrix and embryonic heart development and embryonic heart function. I hypothesize that an embryonic ECM, the cardiac jelly, plays a role in heart development physiologically by influencing normal structure development and relaying mechanical stimuli from the beating heart to the developing cells. Results from these studies will help elucidate the role of the cardiac jelly in heart development.

DISSERTATION AIMS

Aim 1: Determine whether the cardiac jelly provides mechanical cues for proper heart development. The cardiac jelly is an extracellular matrix known be vital for proper heart development however the exact mechanism remains unclear. We will utilize morpholinos targeted towards *hyaluronan synthase 2*, *nephronectin*, and *cadherin 5* to decrease, increase and compromise the cardiac jelly respectively. Resulting phenotypes in the chamber, valve and cardiac function will be evaluated using microscopy, immunofluorescence, and high-speed video analysis. We anticipate seeing developmental defects throughout the organ that coincides with decreased mechanical function.

Aim 2: Test the hypothesis that hyperglycemic conditions alter the cardiac jelly and overall heart development. Infants born from mothers with pre-gestational or gestational diabetes are at an increased risk for cardiac defects, including malformation of the valves. Others have found that zebrafish exposed to hyperglycemic conditions develop expanded CJ and expanded *has2* expression. Experiments will use immunofluorescence, embryonic free glucose measurements and live imaging approaches to explore a mechanistic connection between hyperglycemia, CJ composition and valve defects.

Chapter 2: Embryonic Formation of the Cardiac Jelly Extracellular Matrix Assists in Endocardial Cushion Opening for Proper Cardiac Function

SUMMARY

Aims: Many studies have shown that heart development does not solely rely on genetic signaling and regulation for development. Due to the mechanical nature of the heart, the resulting dynamic environment plays a crucial role in cardiac development. The precise mechanisms behind the mechanical cues require further elucidation. Within the developing heart valve there is a critical extracellular matrix called the cardiac jelly that is as dynamic as its surrounding environment. Without this extracellular matrix, embryonic cushions do not develop and, in mammalian models, results in embryonic mortality. Due to the cardiac jelly's dynamic nature, there is a possibility that the cardiac jelly assists in the heart's mechanical nature leading to appropriate development.

The objective of this work is to alter the amount of cardiac jelly and evaluate the resulting effect on heart development and overall function.

Methods and Results: Here we describe a zebrafish model exhibiting decreased, increased, and compromised cardiac jelly using morpholinos targeted towards *hyaluronan synthase 2* (*has2*), *nephronectin* (*npnt*), and *cadherin 5* (*cdh5*), respectively. We found that altering the cardiac jelly does not impact chamber development but has a substantial effect on valve cell differentiation and valve opening. Specialized high-speed video technology and analysis showed that any change to the cardiac jelly severely impacts overall cardiac function. We compared morpholino-induced phenotypes with those from a mechanically absent model and found similarities. Decreased amounts of cardiac jelly results in endocardial phenotypes like those from a heart with ceased heart function.

Conclusions: The cardiac jelly is a necessary structure for valve development and cardiac function. Our results suggest that the cardiac jelly relies on heart mechanics to properly develop

and in the absence of a cardiac jelly, mechanical cues from heart contractions do not relay to the developing endocardial cells, resulting in poor differentiation and valve function. With these data, the cardiac jelly should be considered as more than just an extracellular matrix needed for structure within the developing heart.

INTRODUCTION

Congenital heart defects occur in 8 out of 1000 live births (Shuler, Black et al. 2013). Some defects are auto-correcting, but many require surgical repair (Oster, Kim et al. 2014). The more severe the defect, the earlier surgery will be required, accompanied by increased risk of mortality (Oster, Lee et al. 2013, Erikssen, Liestøl et al. 2015). Therapeutic approaches require a fundamental understanding of how the heart develops. Along with genetic regulation, evidence increasingly supports a critical role for biomechanical forces within the developing heart (e.g., blood flow, contractility, and cardiac afterload) (Freund, Goetz et al. 2012, Boselli, Freund et al. 2015, Ahuja, Ostwald et al. 2022). Although several examples document how particular tissues sense or interpret aspects of their mechanical environment and respond accordingly, much remains to be learned about which signals are paired with which cellular changes. We focus here on cues impacting the cardiac jelly and its subsequent contribution to valve formation.

At 24 hours post fertilization (hpf) the early zebrafish heart forms a linear tube composed of two endothelial cell layers. Endocardial cells that line the lumen inside the tube come into direct contact with moving blood cells during each cardiac cycle. The myocardial cells which create the outer mechanical layers begin contracting concomitantly with the formation of the heart tube (Stainier, Lee et al. 1993). Following the linear heart tube phase, the heart undergoes looping and chamber ballooning starting around 36 hpf to develop an atrium, a ventricle and an early valve structure called the atrioventricular canal (AVC). Signals from the myocardium initiate extracellular matrix secretion to establish a dynamic layer of cardiac jelly (CJ) between the endocardium and myocardium. Within AVC boundaries, a thickened area of CJ leads to

formation of the endocardial cushions by 48 hpf (Männer and Yelbuz 2019). The cushions function as a primitive valve. When pressed together, they prevent ventricular blood from flowing back into the atrium (Stainier 2001). The firm yet deformable nature of the ECM allows the endocardial cushions to occlude the lumen during ventricular systole, then relaxing to allow blood flow into the ventricle during atrial systole (Barry 1948). Previous work demonstrated the cardiac jelly in the AVC influences heart patterning, structure, and function prior to endocardial migration at 52 hpf (Camenisch, Spicer et al. 2000, Patra, Diehl et al. 2011, Hatano, Kimata et al. 2012). However, studies have not fully determined what processes contribute to CJ regulation and development. After 52 hpf endocardial cells within the AVC differentiate further and migrate to form the valve leaflet. The CJ continues to change in its composition, structure and distribution as heart development proceeds (Männer and Yelbuz 2019) (Nair, Ngangan et al. 2012).

The development of the CJ in endocardial cushions depends on cell-to-cell communication via gene expression. Within the AVC boundaries Wnt signaling triggers myocardial cells to release Bone Morphogenetic Protein (BMP) ligands to bind to receptors located on the endocardium to initiate valve-specific development. T-box Transcription Factor 2 (Tbx2) and Hyaluronan Synthase 2 (Has2) are two key endocardial downstream targets that initiate deposition of hyaluronic acid (HA, a main component of the CJ) (Camenisch, Spicer et al. 2000, Shirai, Imanaka-Yoshida et al. 2009, Verhoeven, Haase et al. 2011). Has2 activity is essential for cardiac jelly formation and is restricted to the AVC during valve development (Camenisch, Spicer et al. 2000, Smith, Joziasse et al. 2009). Has2 synthesizes HA, a linear polymer, composed of thousands of linked glycosaminoglycan molecules (Ma, Lu et al. 2005, Smith, Joziasse et al. 2009). The HA meshwork extensively binds water, giving it a stiff viscous quality reminiscent of Jell-O (Necas, Bartosikova et al. 2008). HA polymers form expanded coils that entangle with each other and confer unique rheological properties (i.e., the ability to flow and deform). Previous studies demonstrated that *has2* knockdown in embryonic hearts resulted

in marked reduction of HA along with reduced CJ width and less cell differentiation within the valve (Patra, Diehl et al. 2011). The distribution of CJ throughout the heart (abundant in the AVC, less in the chambers) is negatively regulated as well. Nephronectin (Npnt) is an ECM protein transiently expressed in the cardiac chambers during development (Brandenberger, Schmidt et al. 2001) (Patra, Diehl et al. 2011). Npnt acts upstream of the BMP pathway, inhibiting the initiation of valve development in non-valve structures (Patra, Diehl et al. 2011).

In knockdown zebrafish embryos with reduced expression of *npnt*, the expression of *has2* expands beyond the AVC boundary, leading to the concomitant expansion of the thicker CJ characteristic of endocardial cushions to encompass the borders of the adjacent chambers (Patra, Diehl et al. 2011). Another player in that impacts the amount and quality of the CJ is VE-cadherin (Cdh5), a component of adherens junctions that adjoins endocardial and vascular endothelial cells (Mitchell, Brown et al. 2010). Between 48 and 72 hpf, *cdh5* expression decreases in the ventricle and becomes restricted to the AVC during the time the endocardial cushions form, consistent with a role of adherens junctions in facilitating proper CJ development (Wang, Yu et al. 2013). Mutants demonstrating reduced expression of *cdh5* develop less dense CJ within the AVC, suggesting that impaired integrity of the endocardial cell layer has consequences (Mitchell, Brown et al. 2010). The downregulation of *cdh5* when endocardial cells migrate into the extracellular matrix at the onset of leaflet formation may facilitate their movement (Steed, Faggianelli et al. 2016).

Valve development requires genetic and mechanical stimuli. We hypothesize that CJ plays an essential role in this morphogenetic process and relies both on mechanical and genetic cues. To investigate the formation and impact of CJ on valve development, we utilized the zebrafish model due to their external fertilization, quick development, and translucent embryos. The small size of embryos during the first days of life allows passive diffusion of oxygen, so they are not completely reliant on a functional cardiovascular system, thus lessening the likelihood of embryonic lethality in studies concerning the heart (Stainier 2001).

To investigate the impact of myocardial contraction on CJ formation, we treated embryos with contraction inhibitors and found that the CJ largely does require this type of mechanical input for proper formation. Genetic contributions from both endocardial and myocardial cells also facilitate CJ formation. *has2*, *npnt,* or *cdh5* knockdown embryos exhibited quantifiable changes in the width of the cardiac jelly within the developing endocardial cushion. We find that alterations to the CJ have consequences for the differentiation of the endocardial cushions and their functional abilities. When the width of the cardiac jelly was decreased, valve cell differentiation was impaired, valve opening was reduced, and cardiac function decreased. When the width of cardiac jelly was enlarged, valve cell differentiation proceeded normally, but valve opening was nevertheless impaired and cardiac function decreased. Lastly, we show that both the presence of CJ as well as cues generated by mechanical conduction are required for the CJ, once formed, to continue its differentiation and functional abilities.

METHODS

Zebrafish Husbandry

Zebrafish were raised as per Colorado State University Animal Care and Use Protocols. Zebrafish embryos were raised at 28.5°C until 52 hpf in E3 medium, and dechorionated.

Morpholino Microinjection

Morpholino solutions were made at 3.5 pmol (*has2, npnt* MO) and 1.75 pmol (*cdh5* MO). One-cell stage embryos were injected (0.5-1 nL; Eppendorf Femtojet 5247) into the yolk, directly under the cell. The efficacy of the *has2, npnt* and *cdh5* morpholinos has been validated as previously described (Bakkers, Kramer et al. 2004) (Patra, Diehl et al. 2011) (Mitchell, Brown et al. 2010).

Blebbistatin Application

Tg(fli1:eGFP) embryos were raised at 28.5°C until 24 hpf in E3 medium. Blebbistatin (BLE) was diluted to 8 µM in DMSO (Yang, Hartjes et al. 2014). 24 hpf embryos were

dechorionated and placed in solutions of E3 medium, 0.01% DMSO, or 8 μM BLE and 20mM BDM solubilized in DMSO. Embryos were incubated at 28.5°C until 52 hpf.

Immunofluorescence

Immunofluorescence was performed on dissected Tg(fli1:eGFP) zebrafish hearts as previously described (Yang and Xu 2012). In short, hearts were dissected at 52 hpf in an L15-10% FBS solution. The hearts were then placed on a polylysine-coated glass slide. Hearts were fixed in 4% PFA and permeabilized with a 1% Triton-X solution. Rhodamine phalloidin labelling was performed using a 1:200 dilution of Alex-546 conjugated-phalloidin. Activated Leukocyte Cell Adhesion Molecule (Alcam) labelling was performed using a zn8 antibody at 1:10 dilution. Embryos were washed 3X with PBST solution then incubated with Alexa-546 anti-goat IgG secondary antibody at a 1:200 dilution. 50% glycerol was added to the slide prior to a coverslip. Z-stack images were taken on the Zeiss LSM800 and analyzed.

Cardiac Jelly Width with Endocardial and Myocyte Imaging and Analysis

After immunohistochemistry and imaging, center slices of the z-stack were chosen to measure the maximal width of the cardiac jelly. In this assay the endocardium fluoresces green (Tg(fli1:eGFP)) and the myocardium fluoresces red (phalloidin). The space separating the myocardial and endocardial layers was measured at its widest point in the AVC for the superior and inferior valve cushions. For myocyte analysis, z-stack slices showcasing chamber myocytes were chosen and cell membranes were traced to measure cell area and circularity of cardiomyocytes in the outer curvature and inner curvature of the ventricle. Center slices of Tg(fli1:eGFP) and Alcam-labeled hearts were evaluated for valve cell differentiation. Endocardial cells expressing GFP and Alcam were considered “valve-specific”. The percentage of valve-specific cells among all the endocardial cells within the AVC region was calculated. Cells are considered within the AVC region if they lay within the narrowest point of the endocardial layer or 15 μm above or below. If valve-specific cells extended beyond the AVC region, the percentage was listed as above 100% (Patra, Diehl et al. 2011). Throughout the z-

stack, the number of endocardial cells were counted in the atrium, AVC, and ventricle. All image measurements and cell counts were performed using Fiji-ImageJ software.

Quantification of Cardiac Function and Chamber Volume

52 hpf embryos were mounted in low melt agarose. Videos of live hearts were captured using a Photon SA3 camera at 1200 frames per second, across at least 3 cardiac cycles. Videos analysis was performed as previously described using a line scan and spatiotemporal kymographs to quantify blood cell movement along the line scan (Johnson, Garrity et al. 2013).

RESULTS

CJ deposition relies on gene expression and mechanical input

After the linear tube phase, the embryonic heart loops and balloons creating the designated chamber the atrioventricular canal regions. Prior work demonstrated that biomechanical input of the heart plays a critical role in valve development and morphology (Boselli, Freund et al. 2015, Heckel, Boselli et al. 2015, Johnson, Bark et al. 2015), but no study has evaluated how the CJ specifically develops with respect to these mechanical stimuli. To determine if heart tube contractions influences the later development of CJ, we exposed embryos to Blebbistatin (BLE), a non-muscle myosin II inhibitor, close to the onset of early heart contractions (~20-22 hpf) (Straight, Cheung et al. 2003). Immunofluorescence was performed on 52 hpf embryo hearts and the CJ thickness assessed at the AVC. This value was determined by measuring the distance between the endocardial cell layer and myocardial cell layer in both the inferior valve cushion (IVC) and superior valve cushion (SVC) (Figure 2.1). Results showed that BLE-treated embryos developed a significantly thicker presumptive CJ compared to embryos in control embryonic media (Figure 2.1D,D',E) (BLE n = 11, WT n = 12, IVC p = <0.001, SVC p = <0.0001) and BLE's solvent DMSO (Figure 2.1B,B',E) (DMSO n =12, IVC p = 0.0126,

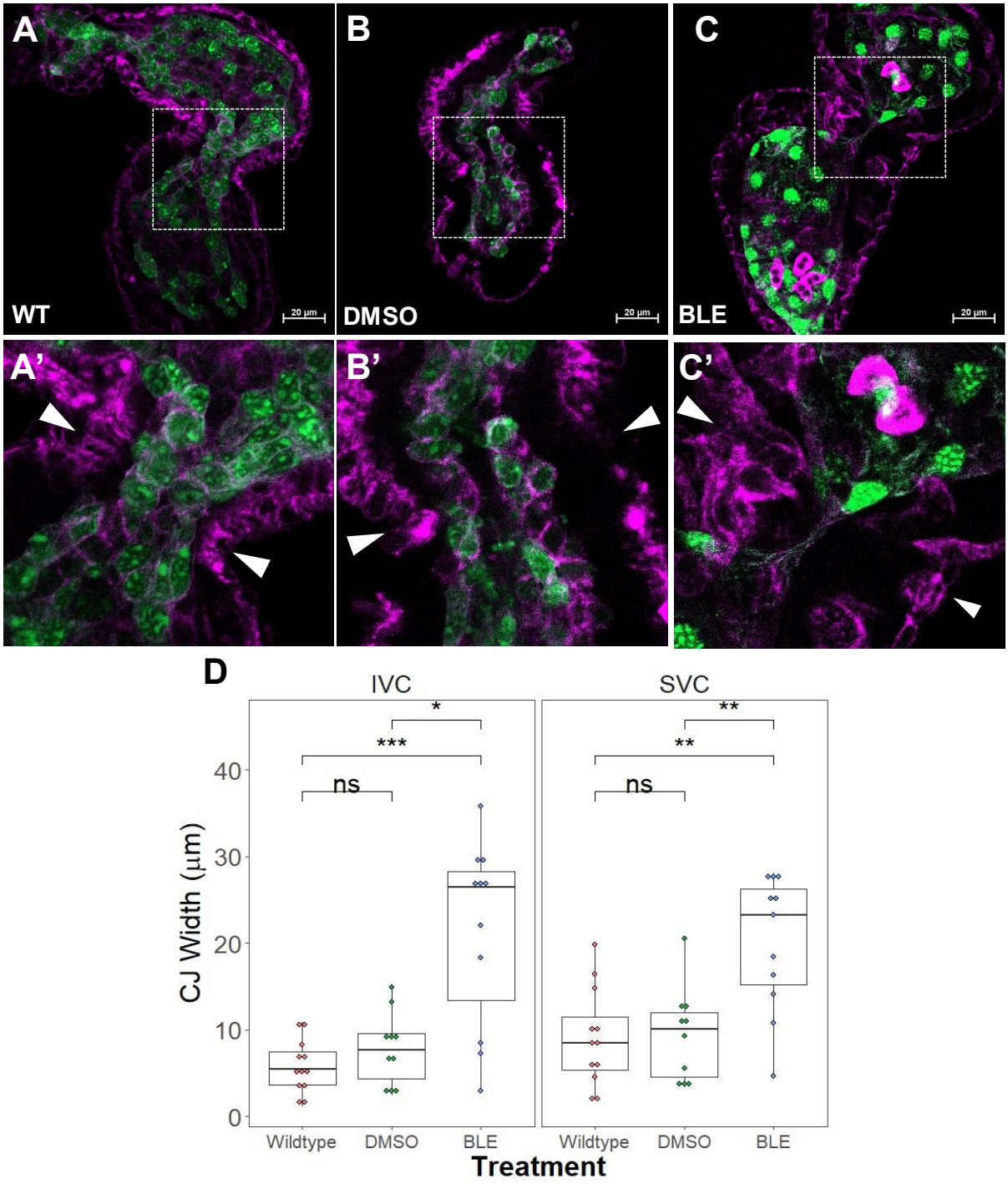

Figure 2.4. Cardiac jelly width is not dependent on mechanical function. (**A**) Wildtype and (**C**) BLE-treated dissected hearts with BLE solvent control DMSO (**B**). In the AVC region (indicated by white box, negative space is measured between the myocardial cells (purple) and endocardial cells (green) to evaluate the CJ width (**D**). (**A', B', C'**) depict the AVC region and white arrow heads indicate myocardial border of valve cushions. Hearts dissected at 52 hpf. Images are pseudo colored. Scale bar measures 20 µm. Kruskal Wallis test performed, * indicates $p \leq 0.05$, ** indicates $p \leq 0.01$, *** indicates $p \leq 0.001$.

SVC p = 0.006). These data are consistent with the conclusion that the distance between the two cell layers is due to increased CJ or fewer endocardial cells, or both. This leads us to the conclusion that heart contractions prior to CJ development play a role in its development, however there must be more factors that contribute.

To investigate the genetic factors responsible for cardiac jelly development, we examined embryos depleted for *hyaluronan synthase 2* (*has2)* and *nephronectin* (*npnt*)(Mitchell, Brown et al. 2010, Patra, Diehl et al. 2011). Previous studies observed an apparently larger separation between the AVC endo- and myocardial layers in *npnt* knockdown embryos and a decreased separation in *has2* knockdown embryos (Patra, Diehl et al. 2011). TEM images have confirmed that the space between endocardial and myocardial cells is occupied by the extracellular matrix layer, so we and others have used the separation of these two cells layers as representative of CJ width (Mitchell, Brown et al. 2010, Patra, Diehl et al. 2011, Grassini, Lagendijk et al. 2018). We revisited this approach to collect quantitative data on the degree of endo-myocardial separation at the AVC. In addition, we were motivated to compare the effects relative to each valve cushion due to recent data showing regionalized, asymmetric ECM expansion within the developing heart tube prior to 52 hpf (Derrick, Sánchez-Posada et al. 2022). Using the double-labeling immunohistochemistry procedure above (Figure 2.1), we analyzed the degree of endo-myocardial separation in both valve cushions at 52 hpf (Figure 2.2). Compared to non-injected (NI) siblings, *has2*-depleted embryos showed a decrease in endo-myocardial separation in both valve cushions (Figure 2.2B,B',D) (NI, n = 32 *has2*MO, n = 15, IVC p = 0.0566, SVC p = 0.0005). When *npnt* was depleted, the endo-myocardial separation significantly increased (Figure 2.2C, E) (*npnt*MO n = 10, IVC p = 0.0012, SVC p = <0.0001). These data provide statistical confirmation that endo-myocardial separation is altered by depletion of either *has2* or *npnt*, supporting the idea that both genes play a significant role in mediating CJ width within both valve cushions. independent analysis of the IVC and SVC at 52

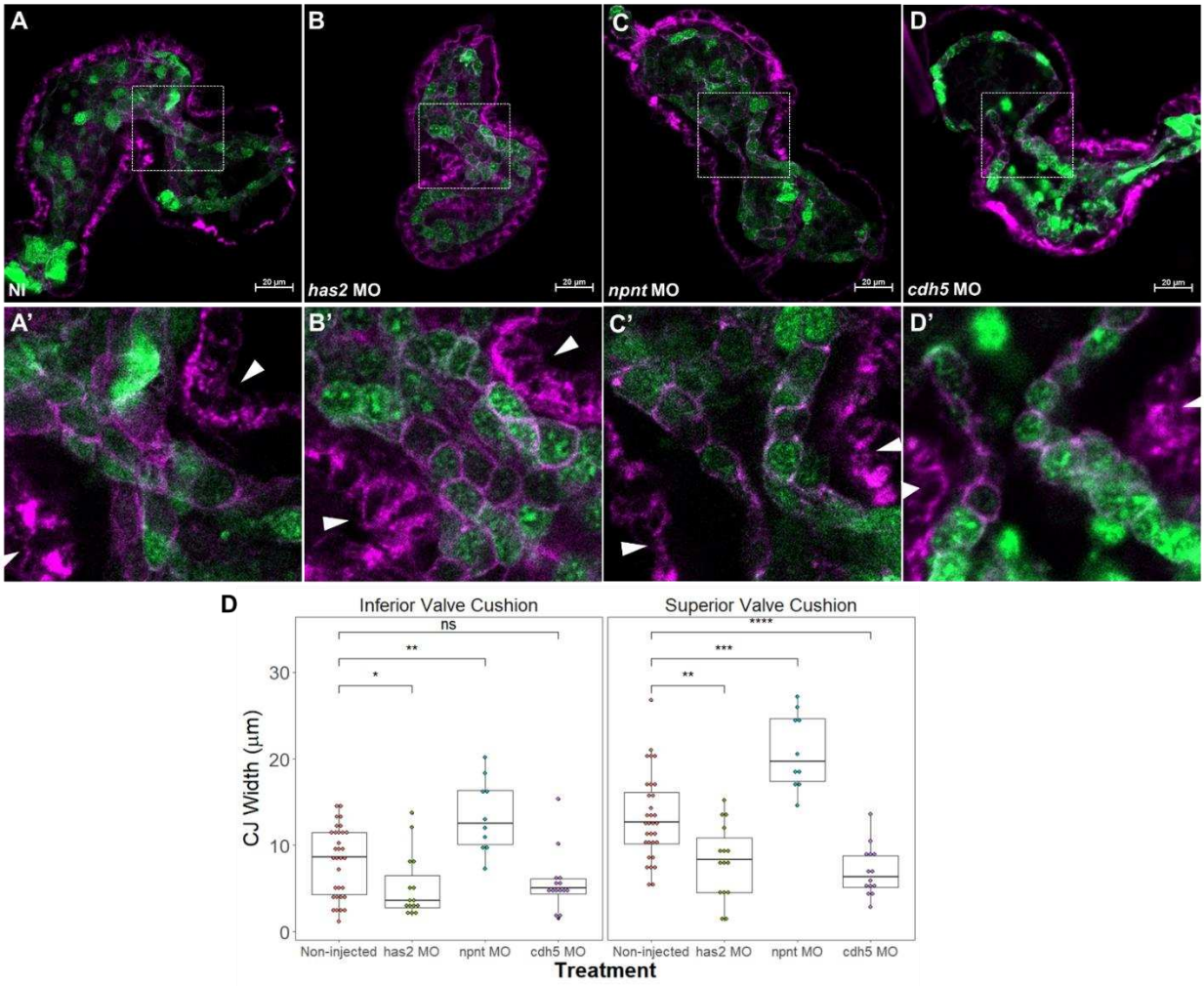

Figure 2.5. Cardiac jelly width depends on genetic expression. (**A**) Non-injected (NI) siblings, (**B**) *has2* MO, (**C**) *npnt* MO and (**D**) *cdh5* MO embryonic dissected hearts at 52 hpf. AVC regions (white boxes) of NI (**A'**), *has2* MO (**B'**), *npnt* MO (**C'**), and *cdh5* MO (**D'**) analyzed by measuring space between myocardial (purple, phalloidin stain) and endocardial (green, *kdlr:EGFP*) cells (**E**). Myocardial border of valve cushion indicated by white arrow heads. Images are pseudo colored. Scale bar measures 20 μm. Dunnett's comparison performed, * indicates $p \leq 0.05$, ** indicates $p \leq 0.01$, *** indicates $p \leq 0.001$.

hpf indicated that these knockdown treatments produced corresponding effects in both structures.

Another player that potentially contributes to CJ maturation is *cadherin 5* (*cdh5*). A study found that depletion of Cdh5 disrupted endocardial adherens junctions and that cardiac jelly in these embryos showed decreased electron density (Mitchell, Brown et al. 2010). We found *cdh5* depletion resulted in a non-significant decrease in CJ width in the IVC but a significant decrease

in the SVC (Figure 2.2,D,E) (*cdh5*MO n = 14, IVC p = 0.1659, SVC p = <0.0001). These data suggest that development of the superior valve cushion at 52 hpf is especially sensitive to the integrity of the CJ. In sum, the manipulation of the above gene products provides us a convenient approach to manipulate the quantity or quality of CJ present in a developing valve. We therefore used this strategy to further investigate how disruptions in the width and composition of cardiac jelly impacted in other morphological and functional aspects of heart development.

Alteration of AVC cardiac jelly does not impact chamber volume or chamber function

The cardiac jelly is not sequestered to only the AVC within the developing heart. Previous studies show CJ is present within the chambers at 52 hpf, albeit in much reduced quantity compared to the AVC (Derrick, Sánchez-Posada et al. 2022). Prior work indicated that during the period of chamber morphogenesis (~30-52 hpf), the expression of *has2* and *npnt* becomes increasingly retracted to the AVC. Moreover, the extent of CJ in the chambers at 52 hpf is small relative to the AVC. Others have noted that embryos depleted for *has2* show much reduced myocardial trabeculation at 80 hpf (Camenisch, Spicer et al. 2000, Patra, Diehl et al. 2011). To further investigate cardiac chamber ballooning after *has2*, *npnt* and *cdh5* knockdown, we analyzed the volume of the atrium and the ventricle at the maximal point of diastole during the cardiac cycle in 52 hpf embryos (Supp. Figure 1.1). Embryos injected with *has2* and *npnt* MOs showed no significant change in atrial or ventricular volume compared to their non-injected siblings (Supp Figure 1.1A, B) (NI n = 15, *has2*MO; n = 15, atrium p = 0.443, ventricle p = 0.9485, *npnt*MO; n = 10, atrium p = 0.6134, ventricle p = 0.4582). Interestingly, embryos injected with the *cdh5* MO demonstrated a decrease in atrial volume but no significant change in ventricular volume or total volume (total volume not shown) (Supp Figure 1.1A, B) (*cdh5*MO n = 15, atrium p = 0.009, ventricle p = 0.4182). To evaluate chamber shape, we computed the aspect ratio of the chambers by comparing chamber width to chamber length. The closer the aspect ratio is to 1, the more spherical the shape of the chamber. Values smaller than 1 indicate

shapes more cylindrical or elongated in nature. We find that non-injected siblings displayed an average atrial ratio of 0.663 and a ventricular ratio of 0.533, indicating the wildtype ventricle normally adopts a slightly more cylindrical shape than the atrium. In comparison, *has2* MO embryos showed atrial and ventricular ratios closer to 1, indicating each chamber adopted a more spherical shape than control embryos (Supp. Figure 1.1C, D) (*has2*MO atrium mean = 0.739, ventricle mean = 0.749, atrium p = 0.1146, ventricle p = <0.0001). Within the atrium, both *npnt* and *cdh5* MOs resulted in lower width/length ratios, indicating a more elongated chamber (Supp. Figure 1.1C) (*npnt*MO; atrium mean = 0.555, p = 0.0300, *cdh5*MO atrium mean = 0.555, p = 0.0141). Embryos depleted for *npnt* or *cdh5* showed increased width/length ratios within the ventricle, again indicating more spherical chambers than controls (Supp. Figure 1.1D) (*npnt*MO; ventricle mean = 0.668, p = 0.0114, *cdh5*MO; ventricle mean = 0.623, p = 0.0751). In sum, depleting or expanding the cardiac jelly altered the overall shape of the cardiac chambers without altering their overall volume.

We hypothesized that changes in chamber shape might correlate to changes in patterns of contraction within the chamber. To determine if the altered chamber shape affected the degree or dimensions of chamber contraction, we evaluated chamber shortening fraction. Zebrafish cardiac shortening fraction was originally conceived as a metric to assess cardiac function (Hoage, Ding et al. 2012, Yang, Hartjes et al. 2014). Better methods for assessing overall heart function have since been developed, but for our purposes the shortening fraction provides a means to evaluate the degree of contraction along specific axes of the chamber. From high speed videos, we isolated frames of the heart at peak systole and peak diastole and measured the shortening fraction of the width and the length of the chamber as previously described (Yang, Hartjes et al. 2014). Knockdown of *has2* or *npnt* had little effect on either the atrial or ventricular shortening fraction (Supp. Figure 1.2A,B) (*has2*MO; atrium width p = 0.755, atrium length p = 0.916, ventricle width p = 0.198, ventricle length p = 0.680, *npnt*MO; atrium width p = 0.717, atrium length p = 0.727, ventricle width p = 0.9150, ventricle length p = 0.8676).

Within the atrium, *cdh5* knockdown did not affect the atrial contraction along the width or length axes (Supp. Figure 1.2A width p = 0.987, length p = 0.0901). In contrast, *cdh5* knockdown hearts had no effect on the shortening fraction of ventricular length (Supp. Figure 1.2B, p = 0.340) but showed a decreased shortening fraction for the ventricular width (Supp. Figure 1.2B p = 0.0319). On the whole, these data provide little support for the hypothesis that altered chamber shape detrimentally affects contraction on either the lengthwise or widthwise axis of the cardiac chambers.

Table 2.1- Statistical analysis of chamber development after altering CJ

	Atrium		**Ventricle**	
Treatment	**Width p-value**	**Length p-value**	**Width p-value**	**Length p-value**
***has2* MO**	0.755	0.9156	0.1981	0.6805
***npnt* MO**	0.7174	0.7275	0.9150	0.8676
***cdh5* MO**	0.9867	0.0901	**0.0319**	0.3397

CJ changes in valve lead to improper cell differentiation

Prior studies identified AVC-specific endocardial gene expression (*alcam*, *notch1b*) and the adoption of cuboidal cell shape as two measurable characteristics to gauge the progression of valve cell differentiation (Beis, Bartman et al. 2005, Patra, Diehl et al. 2011, Lagendijk, Szabó et al. 2013). To investigate how well valve differentiation proceeded when the cardiac jelly was depleted, excessive or compromised, we used an Alcam antibody to label endothelial cells that have adopted a valve-specific fate (Figure 2.3). We found that embryos injected with *has2* MO showed a substantial decrease in the percentage of differentiated endocardial cells at 52 hpf, out of the total AVC endocardial cells (Figure 2.3B,B',B",E)(NI; n = 16, mean = 85%, *has2*MO n = 9, mean = 12.3%, p = <0.0001). In contrast, embryos injected with *npnt* MO had a substantial increase in the percentage of Alcam positive cells (Figure 2.3C,C',C",E) (*npnt*MO; n = 7, mean =

124%, p = 0.0004). This data, taken from dissected 52 hpf hearts to align with the rest of this study, was highly consistent with a prior study investigating 52 hpf images from a whole-mount stain (Patra, Diehl et al. 2011). These data indicate that the extent of CJ present at the AVC correlates with the number of differentiated valve cells.

cdh5 knockdown likewise resulted in a significant decrease in valve cell differentiation (Figure 2.3 D,D',D",E)(*cdh5*MO n = 8, mean = 27.7%, p = <0.0001). We noted a diffuse and abnormal sub-cellular distribution of the Alcam labeling in *cdh5* MO-treated embryos. Control embryos routinely demonstrated exclusive labeling at the cell periphery. Hence, only cells with peripheral Alcam were scored as differentiated. It is intriguing to speculate that depletion of a critical adherens junctions protein may have adversely affected the health of the AVC endocardium (Figure 2.3 D,D'). These data indicate that a reduced CJ and/or a compromised AVC endocardium is associated with a reduced number of differentiated valve cells.

We next analyzed whether the differentiated valve cells showed normal morphology. We analyzed the cell surface area and the circularity of Alcam-positive cells in all three types of CJ-manipulated embryos. We found no significant changes compared to their non-injected siblings for either criterion (Figure 2.3 F,G). These data indicate that regardless of the extent of CJ, any cells that exhibited the differentiated valve marker also displayed normal dimensions.

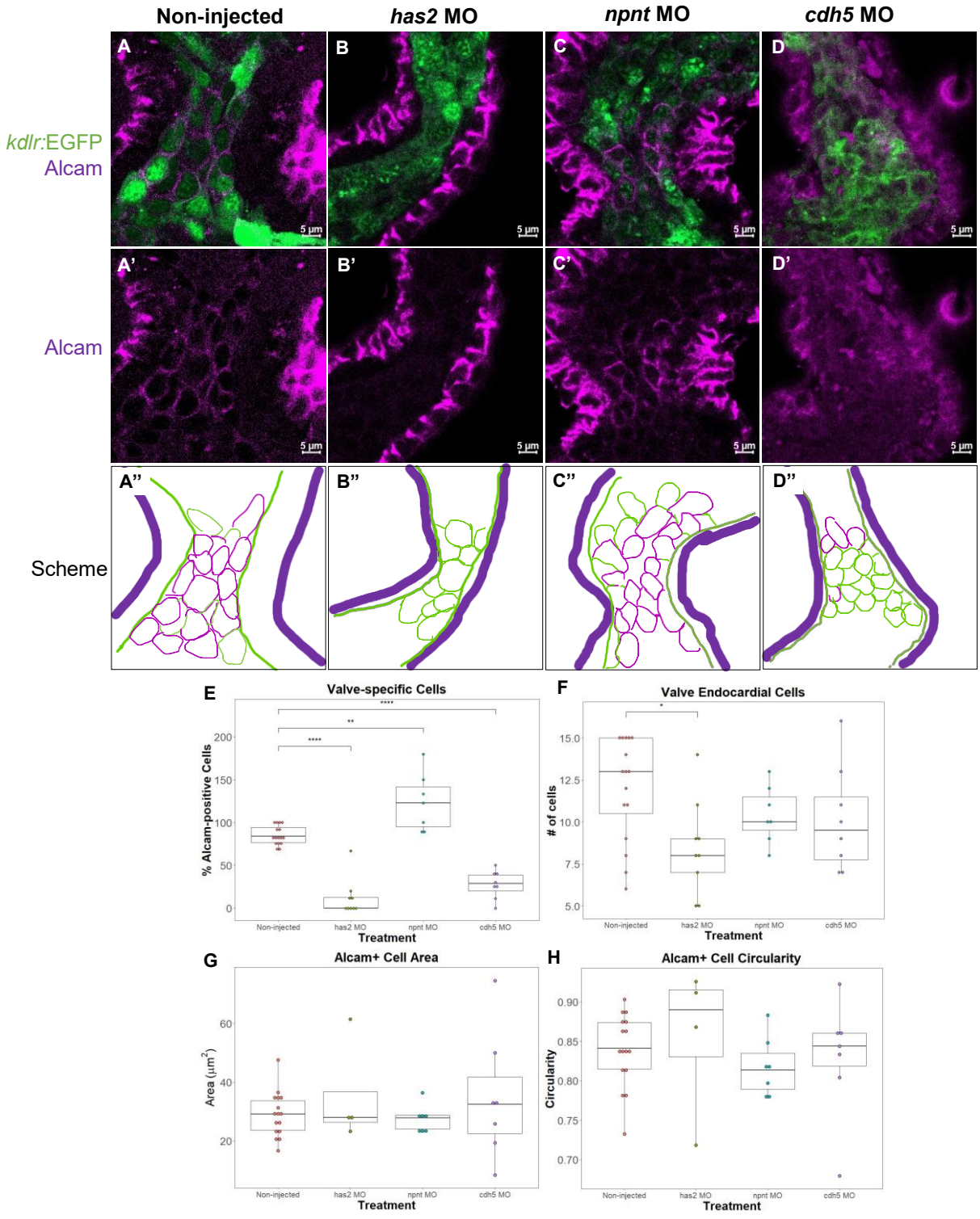

Figure 2.6. Valve cell specification is dependent on CJ width. **A**) Non-injected (NI) siblings, (**B**) *has2* MO, (**C**) *npnt* MO and (**D**) *cdh5* MO embryonic dissected hearts at 52 hpf and labeled using an Alcam antibody (**A'**, **B'**, **C'**, **D'**). Within the AVC region, cells that are green with a purple outline are considered "valve-specific" endocardial cells. The cell differentiation pattern is

illustrated as a scheme for all treatments (**A”**, **B”**, **C”**, **D”**). The percentage of valve specific cells (**E**) change with CJ width. The number of valve endocardial cells decreases with *has2* MO (**F**) Cells that do differentiate adapt wildtype characteristics such as cell area (**G**) and cell circularity (**H**). Images are pseudo colored. Scale bar measures 5 μm. Dunnett's comparison performed, * indicates $p \leq 0.05$, ** indicates $p \leq 0.01$, *** indicates $p \leq 0.001$, **** indicates $p < 0.00001$.

Blocking cardiac contraction reduces AVC valve differentiation

The poor endocardial differentiation observed in CJ-manipulated embryos suggested the hypothesis that contraction itself may impact valve development. To test this idea, we treated embryos with a non-muscle myosin inhibitor, blebbistatin (BLE), which serves to decouple the excitation-contraction process. Embryos subjected to BLE for 44 hrs were then scored to determine the proportion of Alcam-positive endocardial cells at the AVC. In embryos treated with BLE, significantly fewer AVC endocardial cells were Alcam-positive (Figure 2.4C,C',C",D) (WT n = 11, DMSO n = 10, BLE n =10, DMSO-BLE p = <0.0001, WT-BLE p =<0.0001, WT-DMSO p = 0.7081). BLE-treated embryos developed fewer AVC endocardial cells overall compared to controls (Figure 2.4E)(BLE n = 10, p = <0.0001). Thus, BLE-treatment showed results similar to *has2* knockdown (see Figure 2.3) in depleting the number of AVC endocardial cells. Conversely, *npnt* and *cdh5* MO embryos do not have a significant change in the number of endocardial cells (Figure 2.3F). Pairwise comparisons of the number of AVC endocardial cells between the BLE and knockdown experiments confirmed that BLE and has2 knockdown produced similar numbers of cells, whereas npnt and cdh5 knockdown embryos were much higher number than BLE-treated embryos (Figure 2.3F) (*npnt*MO n = 7 WT-*npnt*MO p = 0.2248 BLE-*npnt*MO p = <0.0001, *cdh5*MO n = 8 WT-*cdh5*MO p = 0.1213 p = BLE-*cdh5*MO p = <0.0001).

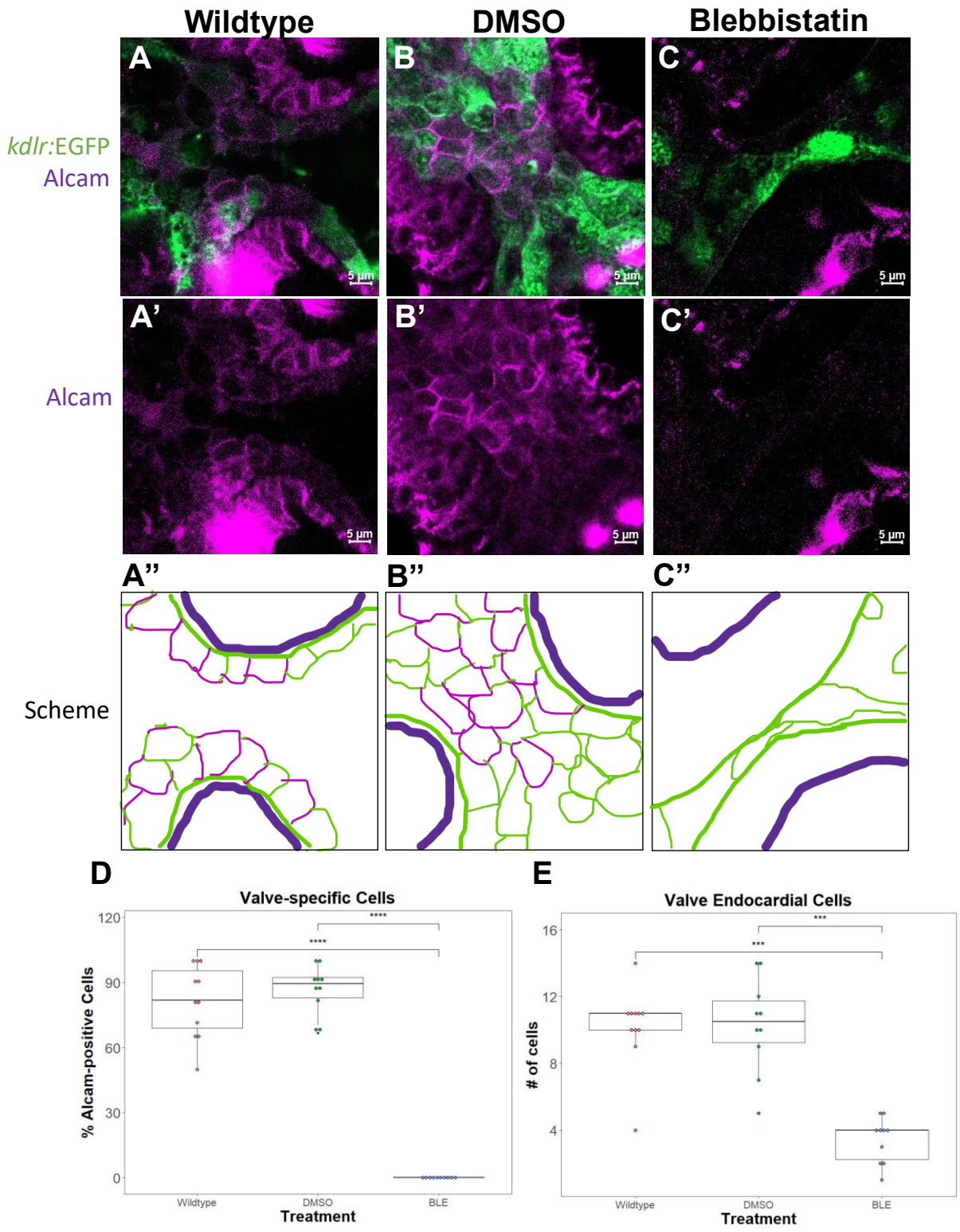

Figure 2.4. Valve cell differentiation relies on mechanical cues. (**A**) Wildtype siblings, (**B**) DMSO controls and (**C**) BLE-treated hearts were dissected at 52 hpf and immunolabel with an Alcam-specific antibody (**A'**, **B'**, **C'**). Endocardial cells (green) with a purple outline are considered

"valve-specific" cells. The percentage of valve-specific cells was calculated within the AVC region of all three treatments (**D**). The number of valve endocardial cells decreased with BLE treatment (**E**). Images are pseudo colored. Scale bar measures 5 µm. ANOVA testing was performed, * indicates $p \leq 0.05$, ** indicates $p \leq 0.01$, *** indicates $p \leq 0.001$, **** indicates $p < 0.00001$.

Table 2.2- Valve endocardial cell analysis

Comparison	P-value
NI – *has2* MO	0.0136
NI – *npnt* MO	0.4809
NI – *cdh5* MO	0.3134
WT – DMSO	0.1331
WT – BLE	<0.0001
DMSO – BLE	<0.0001
BLE – *has2* MO	0.0001
BLE – *npnt* MO	<0.0001
BLE – *cdh5* MO	<0.0001

Smaller valve opening as a result of altered CJ

Given that valve differentiation was abnormal in CJ-manipulated embryos, we next assessed valve (endocardial cushion) functionality in treated and control embryos. Using high-speed videos, we measured the diameter of the cardiac lumen at the AVC and plotted this value over the full cardiac cycle (Figure 2.5A). When compared to the non-injected siblings, embryos

treated with *has2*, *npnt*, and *cdh5* MOs showed a significantly decreased maximum valve aperture (Figure 2.5B)(NI n = 13, *has2*MO n = 11 p = 0.0030, *npnt*MO n = 13 p = 0.0496,

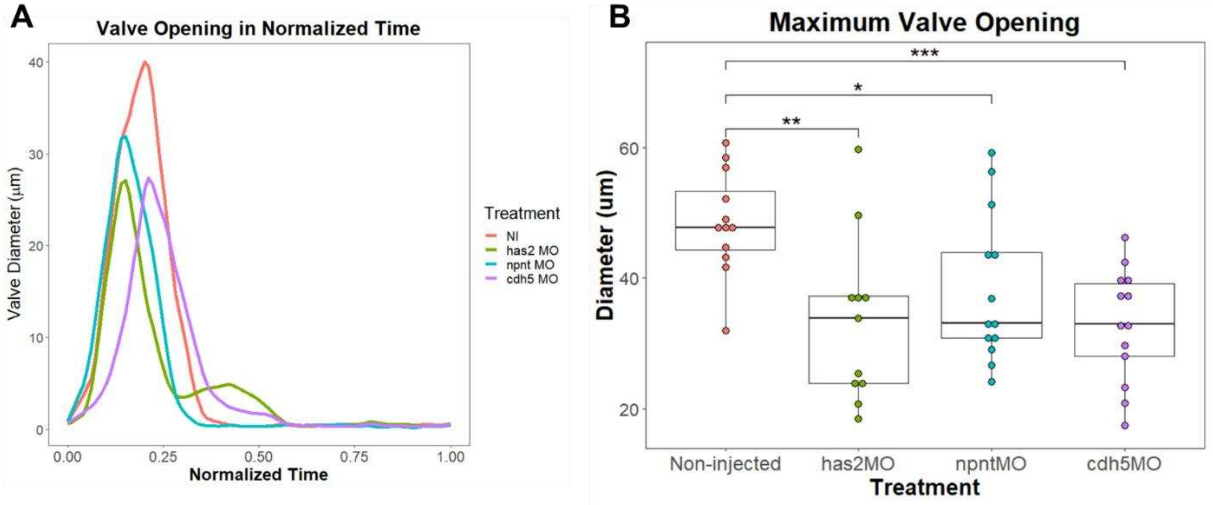

Figure 2.5. Altered CJ width affects maximum valve opening. The function of *in vivo* embryonic hearts are analyzed using high speed video technology. (**A**) The average valve diameter is plotted against a normalized time scale and regardless of CJ change, the valve cannot open as wide as the non-injected siblings. (**B**) Comparing the maximum valve opening of all videos also concludes that altering the CJ will reduce the maximum valve opening. Dunnett's comparison performed, * indicates $p \leq 0.05$, ** indicates $p \leq 0.01$, *** indicates $p \leq 0.001$, **** indicates $p < 0.00001$.

*cdh5*MO n = 13 p = 0.0014). This indicates a reduced ability of the AVC to fully open during atrial systole under any condition that modified the amount of CJ present. In addition, we noted that non-injected, *npnt*, and *cdh5* MO-treated embryos all demonstrated one peak over the course of a cardiac cycle, whereas the *has2* MO-treated embryos displayed two different peaks (Figure 2.5A). This suggested an additional functional defect specific to *has2*-depleted hearts, namely that endocardial cushions are not able to remain fully closed during ventricular systole, potentially allowing a degree of retrograde flow. Taken together, these data indicate that altering the CJ significantly alters valve cell differentiation, which in turn severely impacts the mechanics of the endocardial cushions, resulting in narrower apertures during atrial systole and less consistent occlusion by these tissues during ventricular systole. Moreover, these data provide some of the first specific evidence that the observed morphological and developmental

differences observed in CJ-manipulated embryos do indeed translate to aberrant behavior of the valves (Figure 2.7).

Disrupted cardiac jelly decreases heart function

Multiple sources associate abnormal heart morphology with decreased ability to function (Schroeder, Jackson et al. 2003, Auman, Coleman et al. 2007). To evaluate heart function, we took high speed videos of the 52 hpf embryonic heart and analyzed its mechanics using a spatiotemporal kymograph of the blood cells moving through the atrioventricular canal. *Has2* MO embryos showed no substantial change in heart rate compared to non-injected siblings (Figure 2.6A) (NI n = 13, *has2*MO n = 11, p = 0.7742). However, both *npnt* and *cdh5* MOs resulted in increased heart rates (*npnt*MO n = 13, *cdh5*MO n = 13, *npnt*MO p = 0.0055, *cdh5*MO p = <0.0001). The volume of blood moved through the AVC in one pump, i.e., stroke volume, decreased in all three morpholino gene knockdown models (Figure 2.6B)(*has2*MO p = 0.0001, *npnt*MO p = 0.0164, *cdh5*MO p = 0.0001). To evaluate total cardiac output the heart rate is multiplied by the stroke volume. Cardiac output was significantly decreased for all three MO-

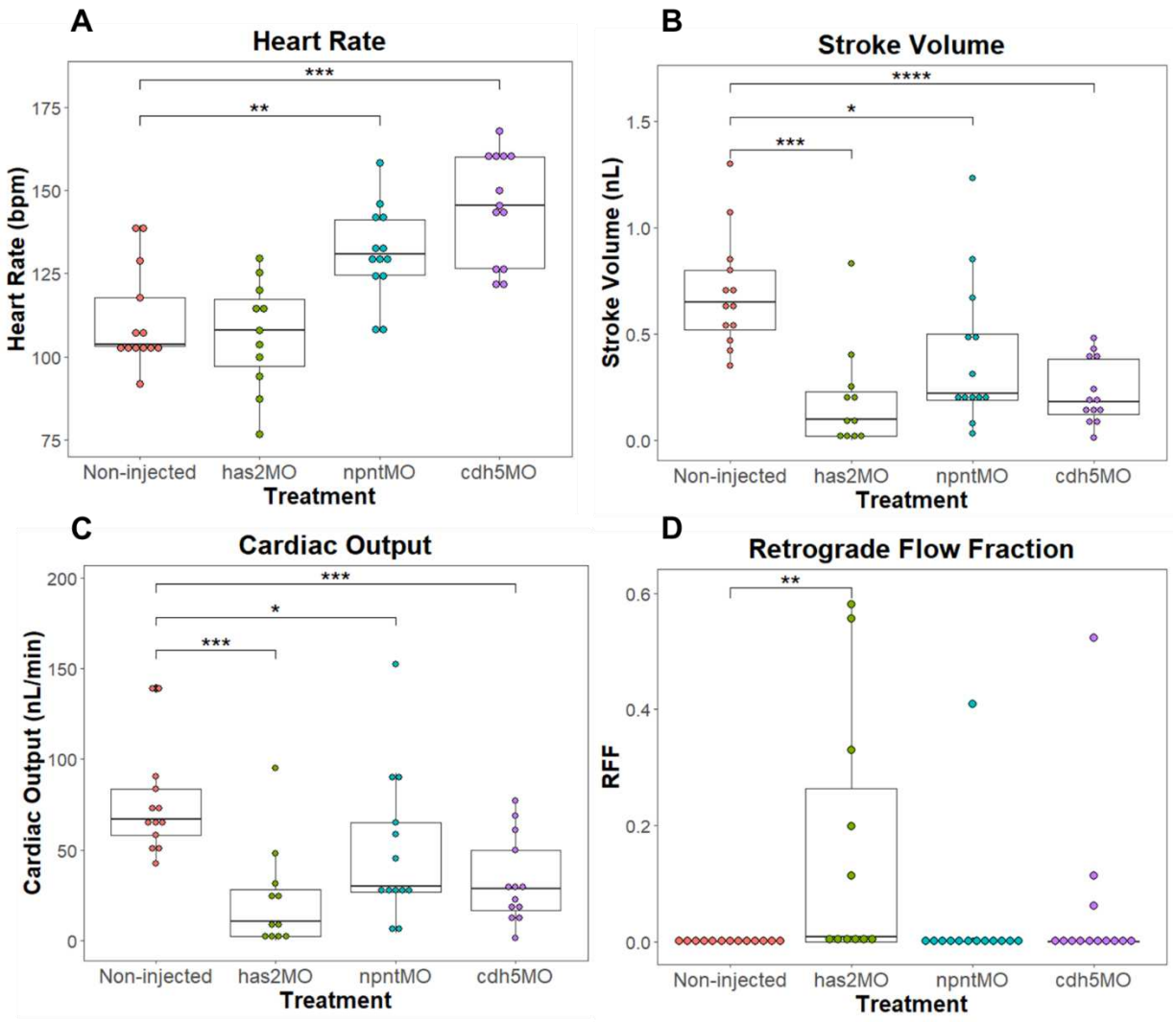

Figure 2.6. Heart function relies on proper CJ width. NI, *has2* MO, *npnt* MO and *cdh5* MO embryonic heart function was analyzed using high-speed video technology. (**A**) Heart rate increases with *npnt* and *cdh5* Mos. (**B**) Stroke volume significantly decreases with all three morpholino treatments. (**C**) Cardiac output (heart rate x stroke volume) also significantly decreases with all three morpholino treatments. (**D**) Reverse blood flow through the valve occurs more frequently in *has2* MO embryos. Dunnett's comparison performed, * indicates $p \leq 0.05$, ** indicates $p \leq 0.01$, *** indicates $p \leq 0.001$.

treated groups (Figure 2.6C) (*has2*MO p = 0.0006, *npnt*MO p = 0.0387, *cdh5*MO p = 0.0008). Another indication of valve integrity is the degree of retrograde flow. By 52 hpf, most of the blood moving through the valve travels in one direction (atrium to ventricle). However, if the endocardial cushions are not properly functioning, some blood cells will move in a retrograde fashion (ventricle to atrium). *Npnt* and *cdh5* knockdown embryos demonstrated sporadic

occurrences of retrograde flow, but *has2* knockdown embryos showed a significant increase in occurrences (Figure 2.6D) (*has2*MO p = 0.0210, *npnt*MO p = 0.8637, *cdh5*MO p = 0.6370). The two peaks observed in the valve opening plot of has2-depleted hearts (Figure 2.4A) are consistent with the greater frequency of retrograde flow. Overall, these data demonstrate a severe impact in cardiac function in response to any disruption in CJ development.

DISCUSSION

In summary, after evaluating processes prior to and after CJ development we have established that 1) the initial formation of cardiac jelly relies genetic expression but does not require mechanical stimuli, 2) if the cardiac jelly is altered, valve differentiation is severely impacted whereas chamber development has minor changes, 3) endocardial cushions with compromised differentiation open less during diastole, resulting in a functional deficiency for the heart, and finally 4) subsequent steps of AVC development (normal numbers of AVC endocardial cells, and the differentiation of AVC endocardial cells into Alcam-positive differentiating cells) require both the presence of CJ and the mechanical signals associated with cardiac contraction. This suggests that the cardiac jelly must be present to relay mechanical cues to surrounding valve cells (Figure 2.7).

A major goal of this study was to analyze the consequences for heart development after changing the width of the CJ between the endocardial and myocardial cell layers. This was accomplished by knockdown of genetic factors that comprise components of the CJ. Since *has2* encodes a synthase critical for the production of the large hyaluronic acid network in the CJ, the phenotype of reduced CJ under conditions of *has2* depletion is logical. Less is understood about

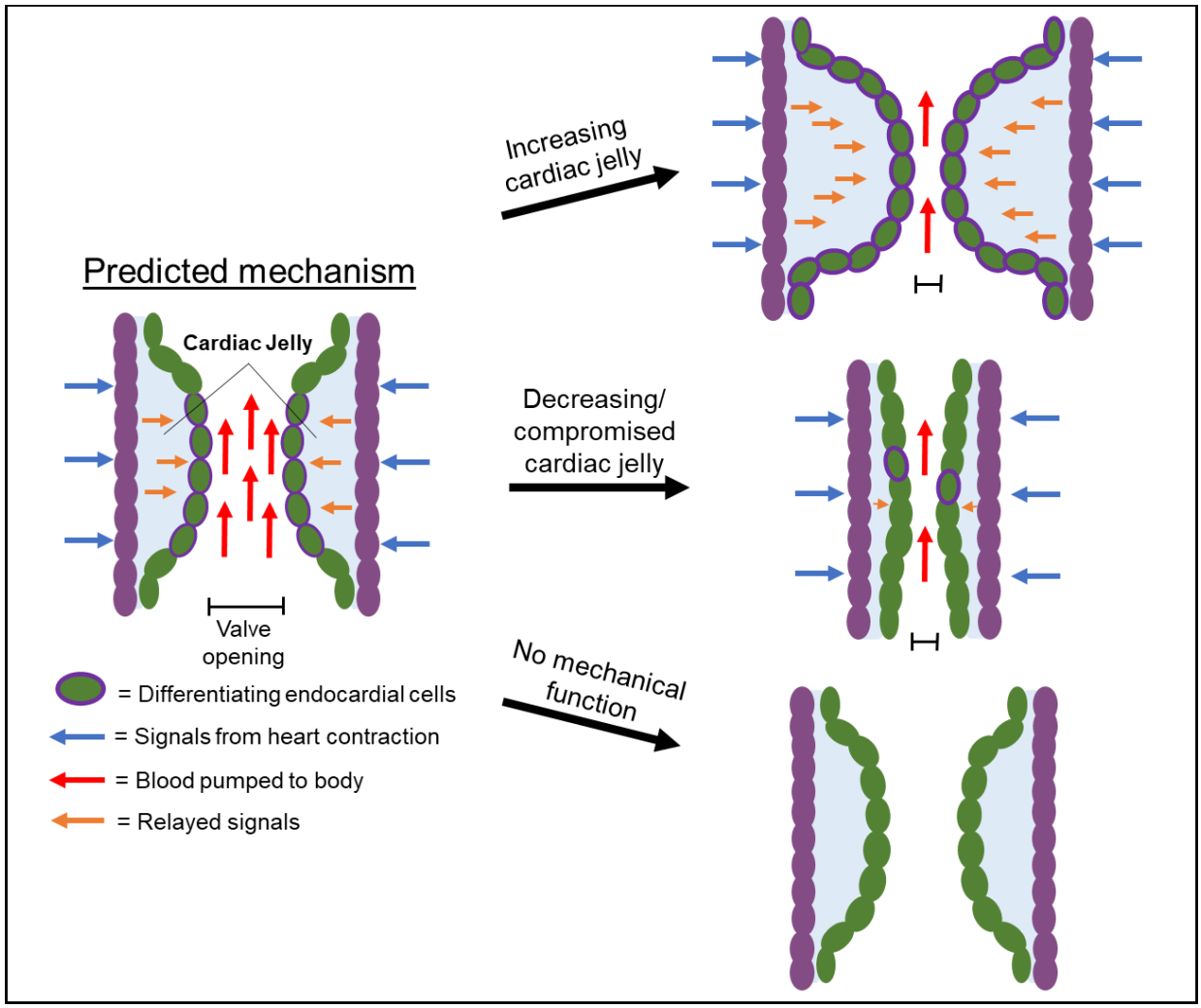

Figure 2.7. Graphical summary of proposed CJ mechanism. The cardiac jelly relays mechanical signals (orange arrows) from heart contractions (blue arrows) needed for valve differentiation (green circles with purple outlines) and function. The ability of the CJ to relay mechanical signals is altered when the CJ is extended, depleted and when there is no mechanical function. Valve opening is indicated by black bracket, blood flow through the valve is indicated by red arrows. Myocardial cell layer is purple and endocardial cell layer is green.

mechanisms underlying Npnt protein function, but its structure suggests a role in cell signals that involve the CJ structure. Npnt was first noted as a novel ECM protein containing an N-terminal signal peptide followed by 5 Epidermal Growth Factor-like repeats and an RGD, integrin recognition sequence with a C-terminal MAM domain. Npnt may interact with growth factors through its EGF repeats, and with integrins through its RGD domain. *In vitro* studies

show that due to its RGD domain, Npnt aides in the attachment of endocardial and myocardial cells (Patra, Ricciardi et al. 2012).

In this study, we confirmed that morpholino knockdown of *npnt* statistically increased the distance between the two cell layers in the endocardial cushions and increased the number of differentiating endocardial cells in the AVC, whereas *has2* knockdown had the opposite effect. These data are consistent with findings of (Patra, Diehl et al. 2011). We further show that these developmental aberrancies are accompanied by a significant decrease in valve opening which can reduce cardiac output, indicating that compromised function of both the early endocardial cushions that affects the efficiency of the heart as a pump. This study highlights that expansion of the AVC CJ causes a specific phenotype in the developing embryo, affecting valve differentiation and valve function most prominently, while leaving chambers functional. Importantly, we identify a reduced ability of the AVC to fully open as the likely cause of reduced cardiac output. We speculate that the increased bulk of the endocardial cushions contributes to the smaller AVC opening. Alternatively, increase CJ may cause the AVC to be less compliant.

A few other studies have identified factors other than Npnt that may be involved in signaling pathways impacting CJ width. Independent of Npnt function, Atrial Natriuretic Peptide (Nppa/anf) and Brain Natriuretic Peptide (Nppb) act redundantly to limit CJ deposition to the AVC rather than cardiac chamber (Patra, Ricciardi et al. 2012, Grassini, Lagendijk et al. 2018). Double mutants of Nppa/Nppb exhibited increased CJ width along with expanded expression of *bmp4* and *has2*, matching the *npnt* knockdown phenotype (Patra, Diehl et al. 2011, Grassini, Lagendijk et al. 2018). In addition, Transmembrane Protein 2 (Tmem2) may play a more direct role in controlling CJ expansion. Rather than regulating signaling upstream of *has2*, Tmem2 has an extracellular portion predicted to depolymerize HA within the CJ, as evidenced by *tmem2* mutants exhibiting excess HA within the endocardial cushions (Hernandez, Ryckebüsch et al. 2019).

Cdh5 is an adherens junction protein present in endocardial cells. Embryos knocked down for Chd5 showed decreased ECM density, raising the possibility that endocardial cushions were compromised (Mitchell, Brown et al. 2010). Here, we note a decrease in the distance between the endocardial and myocardial cell layers in chd5 knockdown embryos. Since Chd5 protein is not a component of the ECM itself, this observation suggests that endocardial integrity impacts CJ accumulation. In contrast to this 52 hpf phenotype, Mitchell et al, 2011 noted that *cdh5* knockdown increased endocardial/myocardial separation at 32 hpf, (Mitchell, Brown et al. 2010), The basis of this difference is unknown but we speculate that as the heart continues to develop, the impaired adherens junctions may be negatively affecting cell health, resulting in poor signaling for CJ accumulation.

A second major objective of this study was to determine whether alteration of CJ had any effects on valve function by 52hpf. The cardiac jelly has been proposed to act as mechanical support in the early stages of heart pumping prior to valve development (REF). Passive energy stored in the CJ layer during systole will power reopening of the heart tube during diastole. This hypothesis was further supported in CJ-deficient mice that exhibited poor heart function at initial stages of development (Barry 1948, Camenisch, Spicer et al. 2000, Camenisch, Biesterfeldt et al. 2001). Further studies show that hydration of the CJ is critical to help create a turgor pressure within the developing heart. The fibrous nature of the CJ in the early heart tube may provide a hydraulic skeleton that complements the mechanical function of the heart tube (Nakamura and Manasek 1978, Nakamura and Manasek 1978). Others have proposed this type of ECM-mediated hydraulic skeleton are not limited to only the developing heart tube may characterize all early embryonic ECMs (Patten, Kramer et al. 1948). This hypothesis suggests therefore, that if without the CJ, the valve does not contain the appropriate hydraulic skeleton, then endocardial cushions will be altered in their ability to open or to remain closed during the heartbeat. Interestingly, with an excess of CJ, the endocardial cushions also functioned less well than controls. We suggest that excessive hydraulic skeleton is too stiff,

reducing the valve width. Further investigation is needed to fully understand how this excess of CJ disrupts the mechanical functionality of the endocardial cushion.

Finally, we observed that mechanical stimuli provided by contraction of the heart is not necessary for the *formation* of the CJ. However, the subsequent steps of AVC endocardial cell differentiation require both the presence of CJ and the presence of contractions. These data support the hypothesis that the CJ plays a role in the relay of mechanical signals from the beating heart to the differentiating endocardial cells. We show that hearts that do not have any mechanical function have reduced valve cell differentiation and fewer endocardial cells overall, suggesting that endocardial cells must experience cues from mechanical stimuli for proper development. BLE treatment stops all cardiac contractions, and therefore also stops blood flow. The “mechanical stimuli” blocked by BLE treatment may relate to cues provided by cardiac contraction itself, or to stopping blood flow. Many studies have shown the importance blood flow has in development as well as contraction (Boselli, Freund et al. 2015, Goddard, Duchemin et al. 2017, Ahuja, Ostwald et al. 2022). Interestingly, *silent heart* mutants, a mechanically absent model, likewise develop a reduced number of AVC endocardial cells (Dietrich, Lombardo et al. 2014). This exact mechanism through which the CJ relays mechanical signals remains undetermined but could be influenced by CJ composition, structure, or some other cause. Perhaps the CJ width provides a necessary space between cells to aide in signaling. Bressan et al identified an intriguing correlation between the width of the CJ in the AVC and conduction speed. To transition from a peristaltic pump to an impedance pump (linear heart tube to cushion impedance), conduction velocity must change. A wildtype heart will have myocytes with fast-conducting inductive cues in the chambers and conduction delay in the AVC. Bressan et al noted that if the myocardial and endocardial cells in the AVC are too close together, no slow conduction occurs, but when the two cell layers are too far apart, conduction cues are also too slow (Bressan, Yang et al. 2014). This data suggests that signaling between the two cell layers

not only influences valve development but also myocyte conduction and ultimately valve function.

In sum, the cardiac jelly plays an important role in the transition of the AVC into functional valve tissue. Once formed, the CJ relies on mechanical and genetic expression to trigger differentiation in embryonic endocardial cushions. If the CJ is too thin or too thick, valve differentiation will be severely impacted leading to poor valve opening and function. When the CJ is depleted, mechanical cues from the beating heart are not properly sensed, leading to disrupted cell differentiation.

Chapter 3: Embryonic exposure to hyperglycemic conditions disrupts cardiac jelly development resulting in poor valve differentiation and function

SUMMARY

Aims: Congenital heart defects and maternal hyperglycemia have a significant association, yet exact mechanisms of developmental defects remain elusive. Studies in model organisms have found evidence that the valve is a candidate for developmental anomalies while an embryo is exposed to high-glucose concentrations. A small extracellular matrix called the cardiac jelly is known for its vital role in valve development and function. There are indications that primary components, such as hyaluronic acid, of the cardiac jelly have altered expression levels in embryos in hyperglycemic conditions. Very few studies have investigated the cardiac jelly specifically after exposure to high glucose concentrations. Due to the cardiac jelly's key role in valve development, there is a possibility that it is affected by hyperglycemic conditions leading to valve defects.

The objective of this work is to analyze if the cardiac jelly changes in embryos exposed to high glucose concentrations and evaluate the effects on valve development and function.

Methods and Results: Here we describe a zebrafish model exposed to multiple concentrations of D-glucose; 50, 150, 225, 300, 450, and 900 mg/dL. We found that embryos will absorb over 1.5-fold of the amount of normal glucose in 450 and 900 mg/dL D-glucose. This excessive absorption leads to an increase and decrease in cardiac jelly width, respectively. Due to this altered cardiac jelly, valve development is more impacted than chamber development. Endocardial cells within the valve have reduced differentiation with increase glucose concentrations. The valve also struggles to open as wide as it should, leading to a decrease in heart stroke volume at the highest glucose levels, 900 mg/dL. To compensate for this decrease in stroke volume, the heart beats faster to ensure adequate cardiac output within the embryo.

Conclusions: The cardiac jelly is more affected by hyperglycemic conditions than previously thought. Our results suggest that the high levels of glucose alter the cardiac jelly, leading to impaired valve development and function. With these data, the cardiac jelly should be more thoroughly investigated as a target to developmental defects in hyperglycemic mothers.

INTRODUCTION

In the United States, women with pregestational diabetes are at least four times more likely to have a pregnancy affected by a congenital heart defect (CHD) than women who do not have diabetes (Wren, Birrell et al. 2003, Simeone, Devine et al. 2015). Roughly 8% of CHDs that occur within the United States each year are due to poor blood sugar control prior to and in early pregnancy (Simeone, Devine et al. 2015). It is estimated that about 2,670 babies are born every year with maternal pregestational diabetes-associated CHDs such as atrial septal defects (ASDs), ventricular septal defects (VSDs) and atrioventricular septal defects (AVSDs). (Simeone, Devine et al. 2015) (Loffredo, Wilson et al. 2001) (Abu-Sulaiman and Subaih 2004).

Three possible diabetes mellitus diagnoses for females are recognized: diabetes mellitus type 1 (DM1), diabetes mellitus type 2 (DM2), and gestational diabetes mellitus (GDM). DM1 and DM2 are often preexisting conditions that need to be diligently controlled prior to and during early stages of pregnancy. GDM is hyperglycemia that develops during pregnancy and resolves after birth (McIntyre, Catalano et al. 2019). Both maternal pregestational diabetes and gestational diabetes are associated with CHDs with pregestational diabetes having a 2-6 times higher relative risk than gestational diabetes (Allen, Armson et al. 2007, Hoang, Marengo et al. 2017). Due to its late onset, expectant mothers without preexisting diabetes are not tested for gestational diabetes until roughly 20-28 weeks gestation, which is after the critical developmental period of the heart (3-7 weeks gestation) (Hoang, Marengo et al. 2017). However due to various studies linking CHDs with gestational diabetes, the American College of Obstetricians and Gynecologists recommends screening for undiagnosed diabetes mellitus prior to or in early pregnancy (Bulletins 2005). More research is needed to better understand the

teratogenicity of abnormally high levels of D-glucose in early pregnancy. A better understanding would encourage universal preconception care among reproductive-age females. The ability to closely monitor and control blood D-glucose levels during critical developmental stages would prevent roughly 4,731 birth defects a year in the United States (Peterson, Grosse et al. 2015).

Model organisms can be used to further elucidate the effect of hyperglycemia on developing embryos, including mice, rats, and (potentially) zebrafish. Zebrafish are frequently used to model disruptions of early development due to their transparent embryos, which develop rapidly and external to the body of the mother. Vertebrates including zebrafish and humans follow similar processes during the initial stages of heart development and deploy many of the same genetic modules. By 24 hours post fertilization (hpf) in zebrafish the early heart has formed a linear tube composed of two endothelial cell layers called the endocardium and the myocardium. The inner endocardium lines the lumen of the heart tube and the myocardium comprises the outside contractile layer of the tube (Stainier, Lee et al. 1993). Following the linear tube phase, starting around 36 hpf, the heart undergoes looping and chamber ballooning to develop an atrium, a ventricle and a constriction called the atrioventricular canal (AVC) which later develops into a valve. Within the AVC region, signals from the myocardium initiate extracellular matrix (ECM) secretion to establish a thick, dynamic layer of cardiac jelly (CJ), leading to formation of the endocardial cushions by 48 hpf (Männer and Yelbuz 2019). The endocardial cushions function as a primitive valve. When compressed, they prevent ventricular blood from flowing back into the atrium (Stainier 2001). When relaxed, they permit forward flow of blood from atrium to ventricle via the AVC.

Previous work demonstrated that the cardiac jelly influences heart patterning, structure, and function, and attains its maximum width just prior to endocardial migration at 52 hpf (Camenisch, Spicer et al. 2000, Patra, Diehl et al. 2011, Hatano, Kimata et al. 2012). After 52 hpf, endocardial cells move into the extracellular matrix and continue differentiating, eventually creating a mature valve leaflet (Männer and Yelbuz 2019). Ordinarily, zebrafish embryos

develop autonomously outside the body of the mother in a glucose-free aqueous environment. Intriguingly, embryos exposed to hyperglycemic aqueous conditions show aberrant developmental responses. In one study, 6 hpf zebrafish embryos exposed to 450 mg/dL D-glucose exhibited increased expression levels of *hyaluronan synthase 2* (*has2*), a key gene in endocardial cushion development, by 48 hpf (Camenisch, Spicer et al. 2000, Liang, Gui et al. 2010). Has2 synthesizes hyaluronic acid (HA), a major component of the cardiac jelly. Although *has2* expression is normally restricted to the AVC at 52 hpf, zebrafish embryos exposed to hyperglycemic conditions demonstrated abnormally expanded regions of *has2* expression extending into the ventricle (Liang, Gui et al. 2010, Patra, Diehl et al. 2011). Other studies using mouse endocardial explants have linked hyperglycemia to abnormal extracellular matrix development. High D-glucose levels resulted in decreased cardiac matrix metalloproteinase (MMP) activity which is necessary for mesenchymal cell invasion for the epithelial-to-mesenchymal transition (EMT) of endocardial cells into the endocardial cushion (Enciso, Gratzinger et al. 2003).

These studies suggest the hypothesis that hyperglycemic conditions change the quality or quantity of cardiac jelly present in the embryonic heart, which compromises the functional efficiency of the primitive valve. Moreover, even though zebrafish embryonic development is not placental, the initial evidence suggests that fish and mammal embryos may share certain parallel cellular responses to hyperglycemic conditions. If so, zebrafish might be exploited as an experimental system, since the external development of embryos means that their environment can be easily manipulated, and the effects easily observed.

To explore the consequences of hyperglycemia upon zebrafish heart development and gauge the sensitivity of zebrafish as a model for physiologic responses, we tested a range of D-glucose concentrations and evaluated the relationship between hyperglycemia, cardiac jelly presence, valve development and primitive valve function. We found that embryos which absorb over 2 times the normal D-glucose level demonstrate a significant reduction in AVC cardiac jelly.

Concomitantly, the AVC endocardial cells fail to uniformly complete valve-specific differentiation, and the primitive valve does not open as widely as controls. At least temporarily, embryos compensate for decreased blood flow through the valve by increasing heart rate.

In the United States, women with pregestational diabetes are at least 4 times more likely to have a pregnancy affected by a congenital heart defect (CHD) than women who do not have diabetes (Wren, Birrell et al. 2003, Simeone, Devine et al. 2015). Roughly 8% of CHDs that occur within the United States each year are due to poor blood sugar control prior to and in early pregnancy (Simeone, Devine et al. 2015). It is estimated that about 2,670 babies are born every year with maternal pregestational diabetes-associated CHDs such as atrial septal defects (ASDs), ventricular septal defects (VSDs) and atrioventricular septal defects (AVSDs) (Simeone, Devine et al. 2015) (Loffredo, Wilson et al. 2001) (Abu-Sulaiman and Subaih 2004).

Three possible diabetes mellitus diagnoses for females are recognized: diabetes mellitus type 1 (DM1), diabetes mellitus type 2 (DM2), and gestational diabetes mellitus (GDM). DM1 and DM2 are often preexisting conditions that need to be diligently controlled prior to and during early stages of pregnancy. GDM is hyperglycemia that develops during pregnancy and resolves after birth (McIntyre, Catalano et al. 2019). Both maternal pregestational diabetes and gestational diabetes are associated with CHDs with pregestational diabetes having a 2-6 times higher relative risk than gestational diabetes (Allen, Armson et al. 2007, Hoang, Marengo et al. 2017). Due to its late onset, expecting mothers without preexisting diabetes are not tested for gestational diabetes until roughly 20-28 weeks gestation, which is after the critical developmental period of the heart (3-7 weeks gestation) (Hoang, Marengo et al. 2017). However due to various studies linking CHDs with gestational diabetes, the American College of Obstetricians and Gynecologists recommends screening for undiagnosed diabetes mellitus prior to or in early pregnancy (Bulletins 2005). More research is needed to better understand the teratogenicity of abnormally high levels of D-glucose in early pregnancy. A better understanding would encourage universal preconception care among reproductive-age females. The ability to

closely monitor and control blood D-glucose during critical developmental stages would prevent roughly 4,731 birth defects a year in the United States (Peterson, Grosse et al. 2015).

Model organisms can be used to further elucidate the effect of hyperglycemia on developing embryos, including mice, rats, and (potentially) zebrafish. Zebrafish are frequently used to model disruptions of early development due to their transparent embryos, which develop rapidly and external to the body of the mother. Vertebrates including zebrafish and humans follow similar processes during the initial stages of heart development and deploy many of the same genetic modules. By 24 hours post fertilization (hpf) in zebrafish the early heart has formed a linear tube composed of two endothelial cell layers called the endocardium and the myocardium. The endocardium lines the lumen of the heart tube and the myocardium comprises the outside contractile layer of the tube (Stainier, Lee et al. 1993). Following the linear tube phase, starting around 36 hpf, the heart undergoes looping and chamber ballooning to develop an atrium, a ventricle and a constriction called the atrioventricular canal (AVC) which later develops into a valve. Within the AVC region, signals from the myocardium initiate extracellular matrix secretion to establish a thick, dynamic layer of cardiac jelly (CJ), leading to formation of the endocardial cushions by 48 hpf (Männer and Yelbuz 2019). The endocardial cushions function as a primitive valve. When compressed, they prevent ventricular blood from flowing back into the atrium (Stainier 2001). When relaxed, they permit forward flow of blood from atrium to ventricle via the AVC.

Previous work demonstrated that the cardiac jelly influences heart patterning, structure, and function, and attains its maximum width just prior to endocardial migration at 52 hpf (Camenisch, Spicer et al. 2000, Patra, Diehl et al. 2011, Hatano, Kimata et al. 2012). After 52 hpf, endocardial cells move into the extracellular matrix and continue differentiating, eventually creating a mature valve leaflet (Männer and Yelbuz 2019). Ordinarily, zebrafish embryos develop autonomously outside the body of the mother in a glucose-free aqueous environment. Intriguingly, embryos exposed to hyperglycemic aqueous conditions show aberrant

developmental responses. In one study, 6 hpf zebrafish embryos exposed to 450 mg/dL D-glucose exhibited increased expression levels of *hyaluronan synthase 2* (*has2*), a key gene in endocardial cushion development, by 48 hpf (Camenisch, Spicer et al. 2000, Liang, Gui et al. 2010). Has2 synthesizes hyaluronic acid (HA), a major component of the cardiac jelly. Although *has2* expression is normally restricted to the AVC at 52 hpf, zebrafish embryos exposed to hyperglycemic conditions demonstrated abnormally expanded regions of *has2* expression extending into the ventricle (Liang, Gui et al. 2010, Patra, Diehl et al. 2011). Other studies using mouse endocardial explants have linked hyperglycemia to abnormal extracellular matrix development. High D-glucose levels resulted in decreased cardiac matrix metalloproteinase (MMP) activity which is necessary for mesenchymal cell invasion for EMT of endocardial cells into the endocardial cushion (Enciso, Gratzinger et al. 2003).

These studies suggest the hypothesis that hyperglycemic conditions change the quality or quantity of cardiac jelly present in the embryonic heart, which compromises the functional efficiency of the primitive valve. Moreover, even though zebrafish embryonic development is not placental, the initial evidence suggests that fish and mammal embryos may share certain parallel cellular responses to hyperglycemic conditions. If so, zebrafish might be exploited as an experimental system, since the external development of embryos means that their environment can be easily manipulated, and the effects easily observed.

To explore the consequences of hyperglycemia upon zebrafish heart development and gauge the sensitivity of zebrafish as a model for physiologic responses, we tested a range of D-glucose concentrations and evaluated the relationship between hyperglycemia, cardiac jelly presence, valve development and primitive valve function. We found that embryos which absorb over 2 times the normal D-glucose level demonstrate a significant reduction in AVC cardiac jelly. Concomitantly, the AVC endocardial cells fail to uniformly complete valve-specific differentiation, and the primitive valve does not open as widely as controls. At least temporarily, embryos compensate for decreased blood flow through the valve by increasing heart rate.

METHODS

Zebrafish Husbandry

Zebrafish were raised as per Colorado State University Animal Care and Use Protocols. Zebrafish embryos were raised at 28.5°C.

Glucose application

Zebrafish embryos were raised at 28.5°C until 8 hpf in E3 medium, a standard buffered salt solution that lacks glucose. At 8 hpf embryos were either exposed to E3 medium containing 50, 150, 225, 300, 450, or 900 mg/dL D-(+)-Glucose, Dextrose (D-glucose) (Sigma-Aldrich CAS No: 50-88-7) along with L-(-)-glucose (L-glucose) (Santa Cruz Biotechnology, SC – 221793) or E3-only sibling controls and incubated at 28.5°C (Gleeson, Connaughton et al. 2007, Liang, Gui et al. 2010, Olsen, Sarras et al. 2010). At 24 hpf, embryos were dechorionated and the treatment or control media was refreshed. Embryos were placed back in a 28.5°C incubator until 52 hpf. Total exposure length was thus 44 hours.

Embryonic free D-glucose measurements

Zebrafish embryos were treated as previously described until 52 hpf and free D-glucose levels were analyzed using a protocol previously described (Singh, Castillo et al. 2019). D-glucose concentrations were measured using the Clarity BG1000 Blood Glucose Meter (VWR Cat No.: 7540-796) and corresponding Clarity BG1000 Blood Glucose Meter Strips (VWR Cat No.: 7540-798). The Clarity BG1000 Blood Glucose Meter will detect D-glucose but cannot detect L-glucose. Three technical replicates were measured from each tube along and the experiment was repeated two more times resulting in three biological replicates. Average fold change was calculated using average glucose measurement from embryos exposed to 0 mg/dL glucose.

Heart Looping, Chamber Volume and Valve Opening Analysis

Heart looping angle was measured using a video-extracted image of the heart depicting blood flowing though the valve. The angle was measured between the line parallel to blood flow

and the line bisecting the atrium (Johnson, Garrity et al. 2013). An image of each chamber was captured at peak diastole and the width and length of the chamber were measured. Volume was calculated using the formula for cylindrical volume (Yang, Hartjes et al. 2014). Looping angle and chamber volume measurements performed using Fiji-ImageJ software. Valve opening was measured by a spatiotemporal kymograph program (Johnson, Garrity et al. 2013).

Immunofluorescence

Immunofluorescence was performed on dissected Tg(fli1:eGFP) zebrafish hearts as previously described (Yang and Xu 2012). In short, hearts were dissected at 52 hpf in an L15-10% FBS solution. The hearts were then placed on a polylysine-coated glass slide. Hearts were fixed in 4% PFA and permeabilized with a 1% Triton-X solution. Rhodamine phalloidin labelling was performed using a 1:200 dilution of Alex-546 conjugated-phalloidin. Alcam labelling was performed using a zn8 antibody at 1:10 dilution. Embryos were washed 3X with PBST solution then incubated with Alexa-546 anti-goat IgG secondary antibody at a 1:200 dilution. 50% glycerol was added to the slide prior to a coverslip. Z-stack images were taken on the Zeiss LSM800 and analyzed.

Quantification of Cardiac Function

52 hpf embryos were mounted in low-melt agarose. Videos of live hearts were captured using a Photon SA3 camera at 1200 frames per second, across at least 3 cardiac cycles. Videos analysis was performed as previously described using a line scan and spatiotemporal kymographs to quantify blood cell movement along the line scan (Johnson, Garrity et al. 2013).

RESULTS

<u>Higher concentrations of D-glucose increase width between endocardial and myocardial layers at the AVC</u>

Our first objective was to expose zebrafish embryos to a range of D-glucose concentrations in E3 buffer and evaluate the efficacy of glucose absorption into embryo bodies. A literature search suggested two starting points for selecting glucose concentrations to

investigate. Gleeson and colleagues showed that adult zebrafish exhibited wildtype fasting blood glucose levels averaging 50 mg/dL (Gleeson, Connaughton et al. 2007, Olsen, Sarras et al. 2010). In initial experiments, sibling embryos were exposed to E3 buffer only, or E3 buffer containing 50 or 150 mg/dL of D-glucose, for 44 hours. Thus, this first pilot study compared the effects of incubating embryos in a glucose-free control environment versus exposing them to adult glucose values or three times that amount. After glucose treatment, embryos were rinsed and then homogenized. Under these incubation conditions, the free glucose measured from extracts of treated embryos showed little or no increase compared to control embryos (Figure 3.1) (50 mg/dL Mean = 1.11, 150 mg/dL Mean = 0.212). To analyze the effect on AVC development in embryo hearts, we measured the distance between the endocardial and myocardial cell layers to estimate the width of the cardiac jelly at the AVC. In embryos raised in glucose solutions of 50, 150 or 300 mg/dL, we found no significant change in cardiac jelly width within the inferior valve cushion (Figure 3.2 A,A',B,B',C,C',D,D') (0 mg/dL n = 18, 50mg/dL n =12 p = 0.857, 150 mg/dL n = 15 p = 0.343, 300 mg/dL n = 13 p = 0.201). For the superior valve cushion, there was no significant change for embryos incubated with the lower concentrations of glucose. However, one change stood out: a significant decrease in CJ width with the highest concentration of 300 mg/dL (Figure 3.2 D,D',E) (50 mg/dL p = 0.053, 150 mg/dL p = 0.1755, 300 mg/dL p = 0.0038).

Rat gestational diabetes models typically indicate an average maternal hyperglycemic fasting blood glucose of 450 mg/dL (Molin, Roest et al. 2004, Wentzel, Gäreskog et al. 2008, Liang, Gui et al. 2010). A study exposing zebrafish embryos to 450 mg/dL D-glucose for 12-24 hours detected pericardial edema, altered cardiac looping, blood toggling, and altered cardiac T-box gene expression (Liang, Gui et al. 2010). The levels of glucose absorbed by the embryos were not evaluated in this study. Thus, our second pilot study sought to build upon the findings of Liang et al by searching for a potential dose-dependent effect by using a range of 225 mg/dL, 450 mg/dL and 900 mg/dL D-glucose treatments lasting 44 hours. In this experimental series,

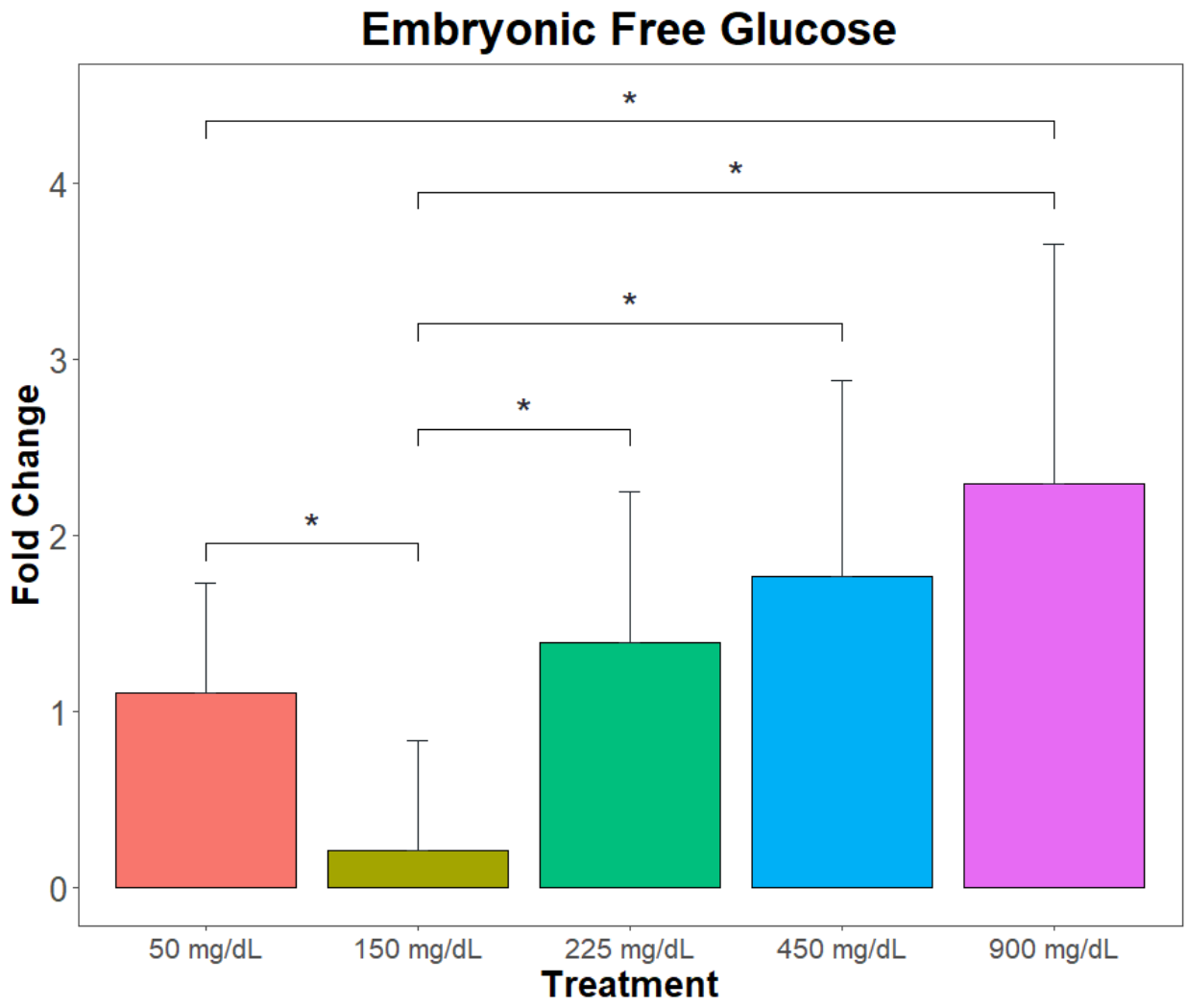

Figure 3.7. Free glucose from embryonic tissue with increasing hyperglycemic environments. Free glucose levels of embryonic tissue was measured at 52 hpf after exposure to 50, 150, 225, 450 and 900 mg/dL D-glucose. The average fold change was calculated using the average free glucose concentration from embryos exposed to 0 mg/dL D-glucose (34.2 mg/dL). Error bars represent standard deviation for each treatment.

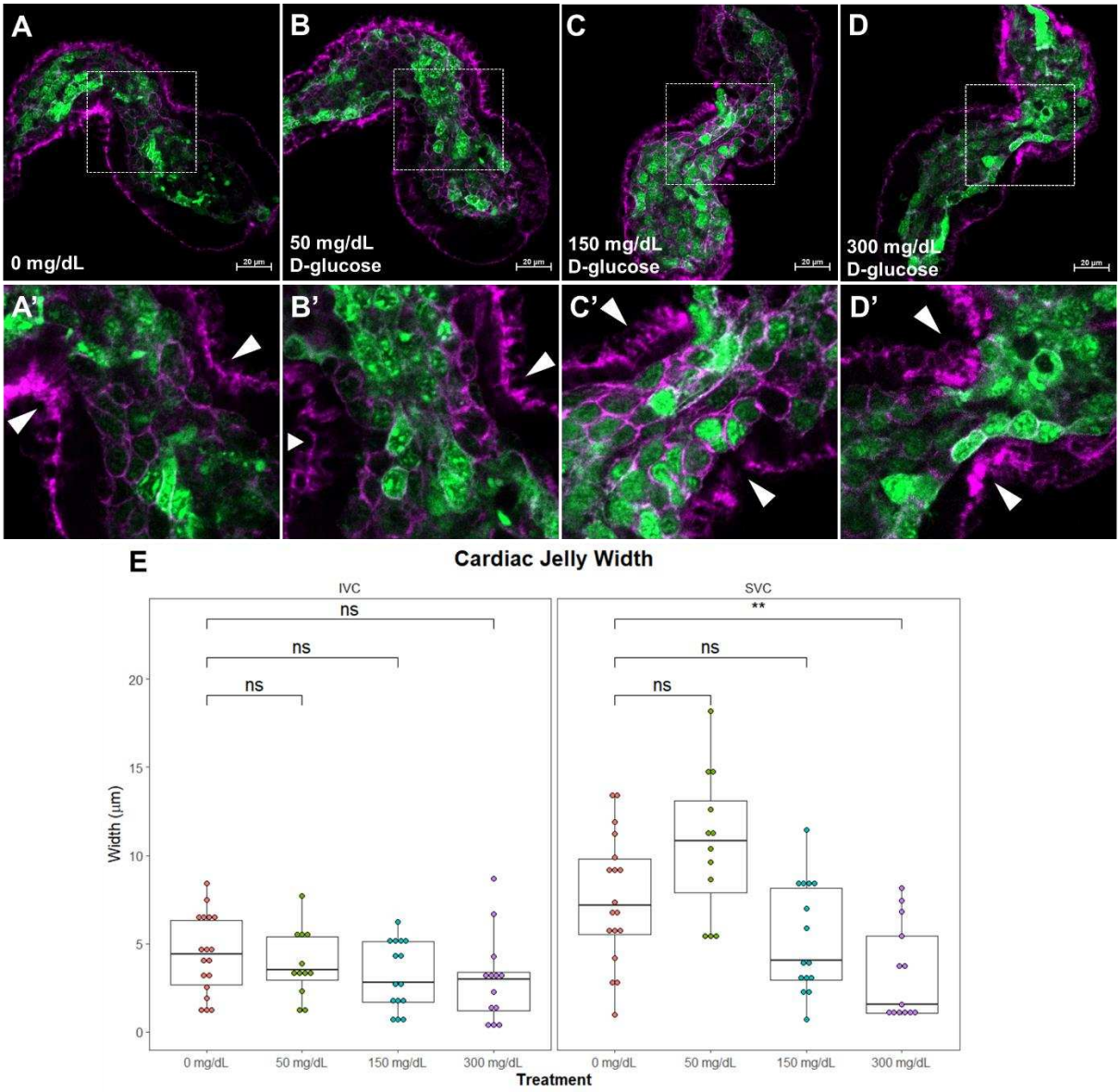

Figure 3.8. Lower concentrations of D-glucose have minimal effect on cardiac jelly. 52 hpf dissected embryonic hearts incubated in **(A)** 0 mg/dL D-glucose, **(B)** 50 mg/dL D-glucose, **(C)** 150 mg/dL D-glucose and **(D)** 300 mg/dL D-glucose. The distance between myocardial cells (purple, phalloidin) and endocardial cells (green, *kdrl*:EGFP) was measured for cardiac jelly width (**E**). Myocardial border of valve cushions indicated by white arrow heads. Images are pseudo colored. Scale bar measures 20 μm. Dunnett's comparison performed, ** indicates $p \leq 0.01$.

embryo body glucose absorption increased over controls for all three glucose concentrations, with embryos exposed to 450 mg/dL or 900 mg/dL showing over a 1.5 fold increase in free glucose levels over controls (Figure 3.1 C,C',D,D',E) (225mg/dL Mean = 1.39, 450 mg/dL Mean = 1.76, 900 mg/dL Mean = 2.29). These measurements confirmed the supposition that embryos

incubated in E3 solutions with elevated D-glucose levels would indeed absorb substantial glucose into their bodies.

Next, we measured CJ width of embryos with the highest exposures (450, 900 mg/dL). Notably, CJ width significantly increased in both valve cushions in the 450 mg/dL treatment (Figure 3.3 B,B',E) (0 mg/dL n = 24, 450 mg/dL n = 12 p (IVC) = 0.0003 p (SVC) = 0.013). When embryos were exposed to 900 mg/dL, CJ width in both cushions decreased significantly (Figure 3.3 C,C',E) (900 mg/dL n =8 p (IVC) = <0.0001 p (SVC) = 0.002). These results plus those above reflect a dose-dependent incidence of CJ defects in glucose-incubated embryo hearts.

To ensure that any difference we observed in the CJ was due to hyperglycemic conditions and not to a change in osmolarity, we exposed embryos to 900 mg/dL of L-glucose, a stereoisomer of D-glucose not used in physiological systems. L-glucose treatment produced no significant change to CJ width even at high concentrations (Figure 3.3 D,D',E) (L-glucose 900 mg/dL n = 10, p (IVC) = 0.116, p (SVC) = 0.214. The Liang et al, 2010 study likewise identified no generalized body defects due to L-glucose exposure (Liang, Gui et al. 2010). Overall, these data indicate that high osmolarity does not itself influence embryonic AVC development, and subsequent experiments did not include an L-glucose control.

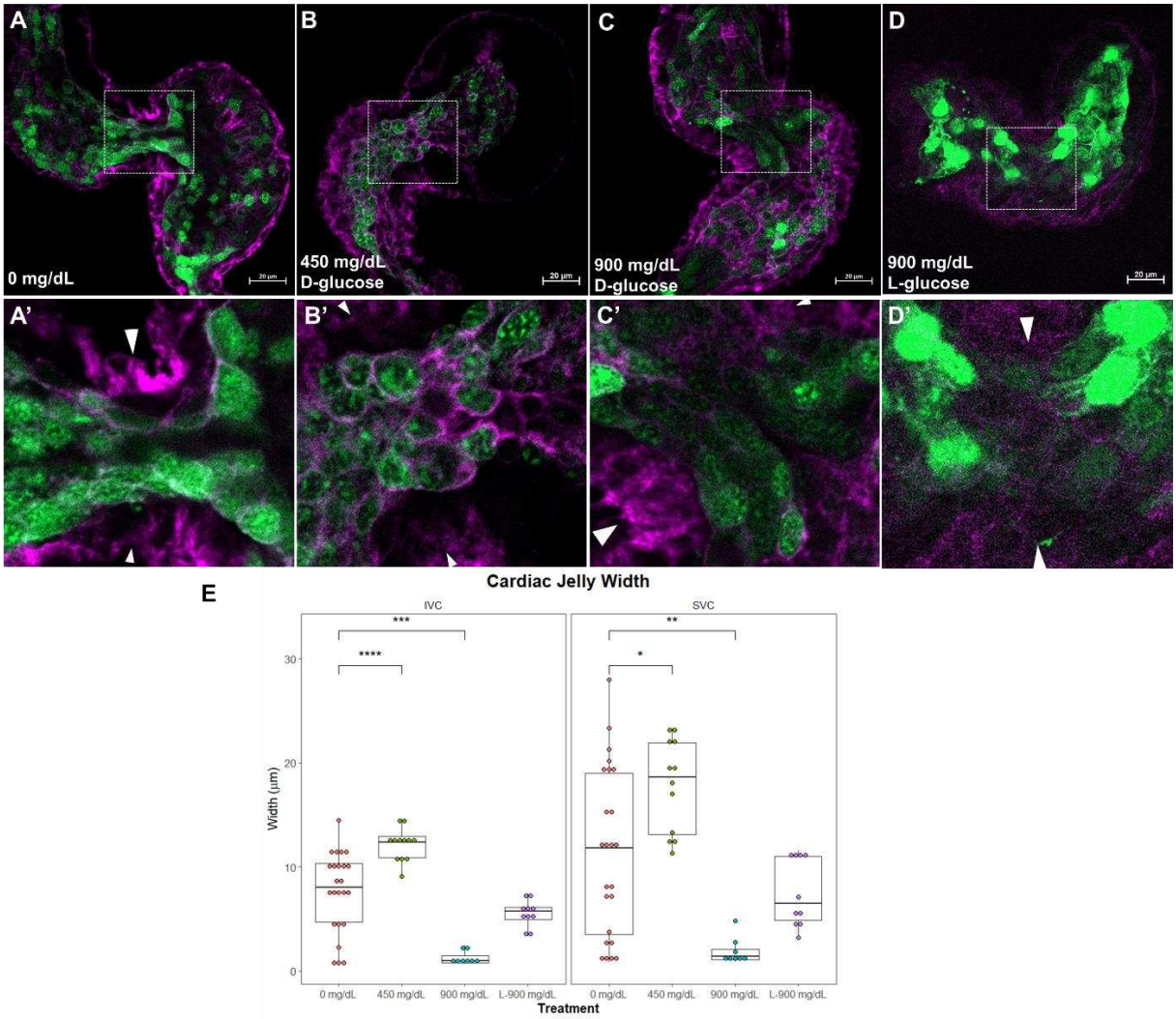

Figure 3.9. Higher concentrations of glucose in embryonic environment can alter cardiac jelly width. 52 hpf dissected embryonic hearts incubated in **(A)** 0 mg/dL D-glucose, **(B)** 450 mg/dL D-glucose, **(C)** 900 mg/dL D-glucose and **(D)** 900 mg/dL L-glucose. The distance between myocardial cells (purple, phalloidin) and endocardial cells (green, *kdrl*:EGFP) was measured for cardiac jelly width (**E**). Myocardial border of valve cushions indicated by white arrow heads. Images are pseudo colored. Scale bar measures 20 μm. Dunnett's comparison performed, * indicates $p \leq 0.05$, ** indicates $p \leq 0.01$, *** and **** indicates $p \leq 0.001$.

Hyperglycemic conditions have no overt effect on chamber volume or heart looping

Previous work reported that hyperglycemic incubation reduced cardiac looping and altered cardiac gene expression patterns in a manner consistent with delayed chamber development (Liang, Gui et al. 2010). However, the slight embryo-level developmental delay observed by these authors was not evident in our treatments. To investigate how hyperglycemic conditions influence general verses AVC-specific cardiac morphogenesis, we first measured

chamber volume and cardiac looping. To obtain quantitative data, we selected still images from the highspeed videos to measure chamber volume and looping angles at 52 hpf. We found very little difference in atrial, ventricular, and total heart volume with all three concentrations of D-glucose tested (Table 3.1, Figure 3.4 A,B,C,D). Additionally, we found very small changes in cardiac looping angle regardless of the D-glucose environment (Figure 3.4 D) (0 mg/dL Mean = 82.6, 225 mg/dL Mean = 92.3 p = 0.519, 450 mg/dL Mean = 93.9 p = 0.356, 900 mg/dL Mean = 98.5 p = 0.238). In summary, these data show no significant changes occurred in chamber development and cardiac looping after embryo exposure to hyperglycemic conditions. Thus, the effects of hyperglycemic conditions on AVC development are not secondary to global cardiac defects in the zebrafish system.

Table 3.1: Chamber Volume Analysis

		Atrial Volume		Ventricular Volume		Total Volume	
Treatment	N	Mean Volume ($10^5 \mu m^3$)	P-value	Mean Volume ($10^5 \mu m^3$)	P-value	Mean Volume ($10^5 \mu m^3$)	P-value
0 mg/dL D-glucose	14	1.12	---	0.67	---	1.80	---
225 mg/dL D-glucose	14	1.34	0.2719	0.595	0.6979	1.94	0.8155
450 mg/dL D-glucose	18	1.25	0.6031	0.590	0.6310	1.84	0.9782
900 mg/dL D-glucose	11	1.24	0.7284	0.9211	0.0554	2.16	0.2584

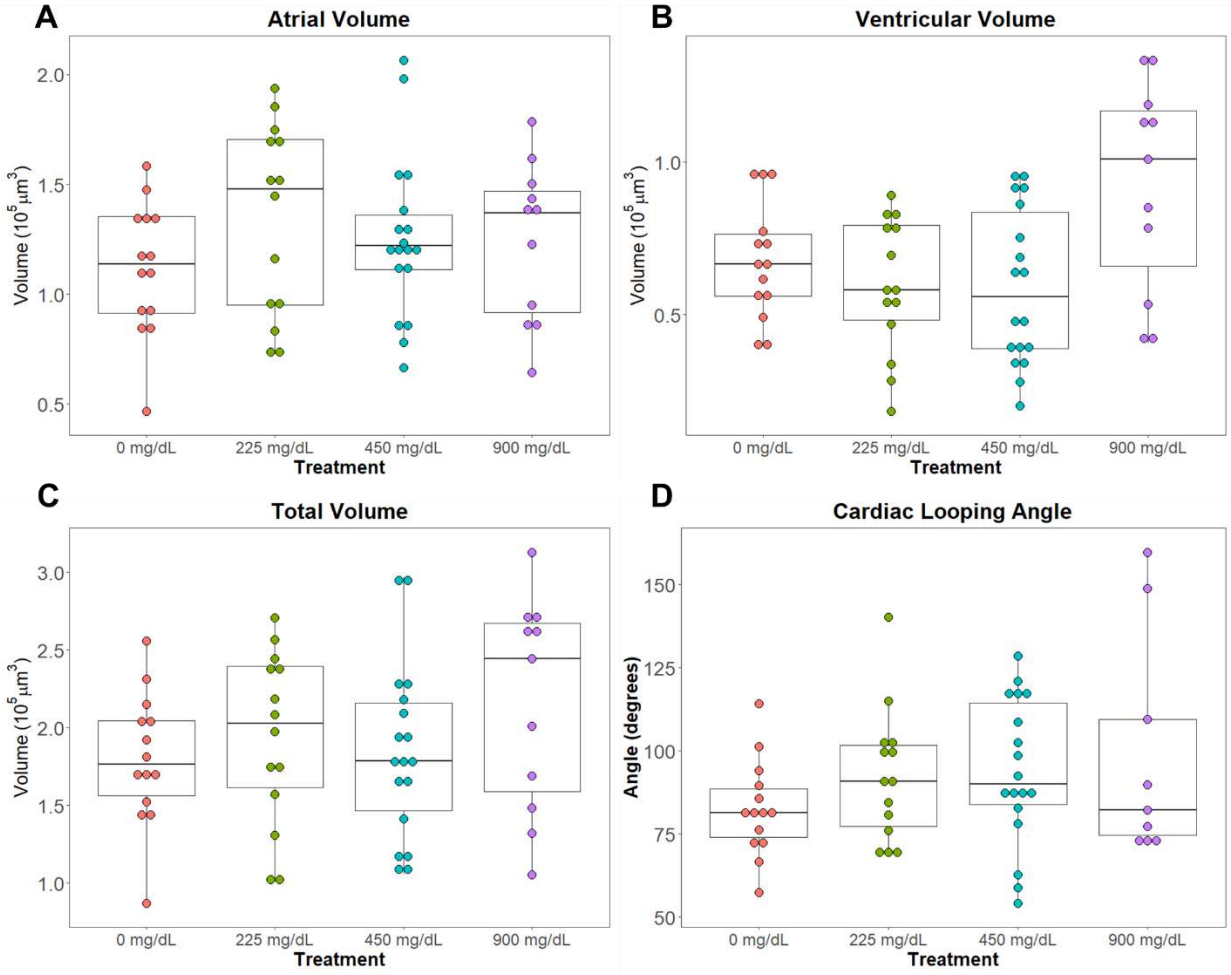

Figure 3.10. Hyperglycemic environments do not alter chamber morphology or looping angle. The volume of embryonic hearts was measured in the atrium **(A)**, the ventricle **(B)**, and combined for total volume **(C)** after exposure to 0, 225, 450, and 900 mg/dL D-glucose. Looping angle of the heart was also measured in embryos exposed to 0, 225, 450 and 900 mg/dL D-glucose **(D)**. Dunnett's comparison performed, no comparisons were significant so there are no asterisks present.

Valve-specific endocardial cell differentiation decreases with increasing hyperglycemic conditions

Focusing now on the AVC-related defects, we next investigated how valve-specific endocardial differentiation was affected by hyperglycemic conditions. Prior studies have established that the CJ is necessary for proper valve development (Chapter 2) (Camenisch, Spicer et al. 2000, Patra, Diehl et al. 2011, Grassini, Lagendijk et al. 2018). Due to altered CJ

from the high-glucose concentrations we predicted a change in valve-specific cell differentiation as well. Using immunofluorescence, we calculated the percentage of valve-specific endocardial cells expressing Alcam, a marker for cells undergoing valve differentiation in preparation for leaflet development. We observed dose-responsive significant decreases in valve-specific cell differentiation as environmental glucose concentrations increased (Figure 3.5) (0 mg/dL n = 9, 225 mg/dL n = 14 p = 0.020, 450 mg/dL n = 17 p = 0.022, 900 mg/dL n = 9.33 p = 0.009). These data support the hypothesis that exposure to high concentrations of glucose substantially disrupts valve-specific endocardial differentiation in conjunction with altered cardiac jelly.

Endocardial cushion defects lead to functional defects in the primitive valve, for which the embryo compensates by increasing heart rate

The effectiveness of endocardial cushions as a primitive valve is appraised by evaluating how well they occlude blood back-flow when compressed together during ventricular systole, plus how well they support forward blood flow by separating broadly during atrial systole. The retrograde flow fraction (the amount of blood moving backwards through the valve) is zero in a normal 52 hpf heart during ventricular systole. We found that exposure to any tested hyperglycemic condition did not significantly change retrograde flow fraction (Figure 3.6 A) (225 mg/dL p = 0.607, 450 mg/dL p = 0.607, 900 mg/dL p = 0.729). We next tracked the extent of AVC opening throughout the cardiac cycle. In embryos exposed to high glucose concentrations, the maximum valve opening decreased significantly compared to controls (Figure 3.6 B, C) (0

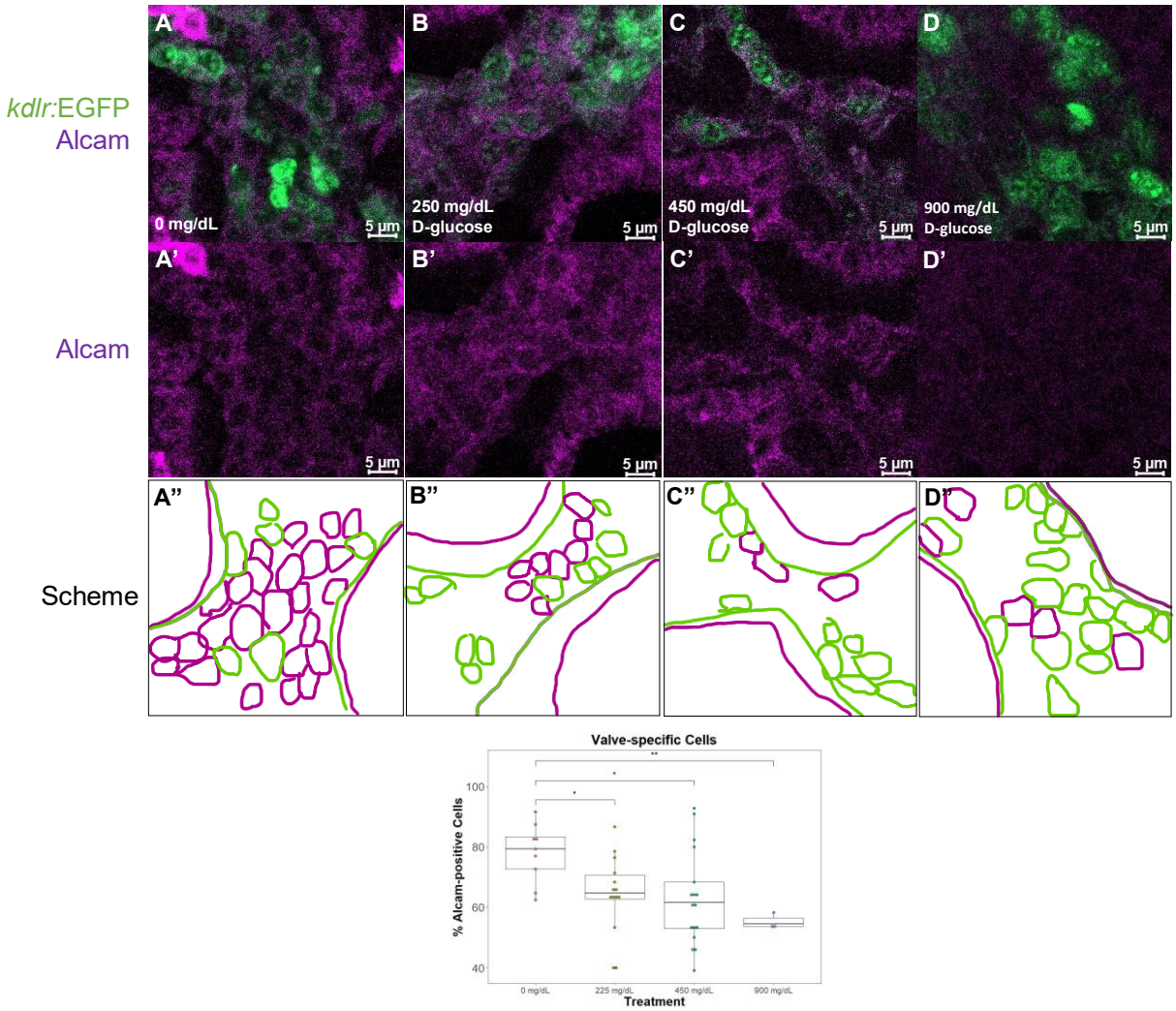

Figure 3.11. Valve cell differentiation decreases with increasing concentrations of glucose in the embryonic environment. Hearts from 52 hpf embryos exposed to **A**) 0 mg/dL D-glucose, (**B**) 225 mg/dL D-glucose, (**C**) 450 mg/dL D-glucose and (**D**) 900 mg/dL D-glucose were dissected and labeled using an Alcam antibody (**A'**, **B'**, **C'**, **D'**). Within the AVC region, cells that are green with a purple outline are considered "valve-specific" endocardial cells. The cell differentiation pattern is illustrated as a scheme for all treatments (**A"**, **B"**, **C"**, **D"**). The percentage of valve specific cells (**E**) change with increasing hyperglycemic conditions. Images are pseudo colored. Scale bar measures 5 µm. Dunnett's comparison performed, * indicates $p \leq 0.05$, ** indicates $p \leq 0.01$, *** indicates $p \leq 0.001$, **** indicates $p < 0.00001$.

mg/dL n = 24, 225 mg/dL n = 22 p = 0.088, 450 mg/dL n = 25 p = 0.032, 900 mg/dL n = 11 p = 0.016). Thus, our data support the hypothesis that the CJ and cellular phenotypes associated with hyperglycemic conditions have functional effects: they deter the opening of the cushions but do not alter its ability to compress and close.

We were curious whether cardiac stroke volume would be decreased in response to the lessened valve opening in treated embryos, given that the atrial and ventricular chamber volumes were normal. Using a high-speed camera and kymographic analysis we measured four parameters of heart function: heart rate, stroke volume, and cardiac output. Stroke volume is defined as the amount of blood that moves through the valve in a single stroke. We observed a dose-responsive (but non-significant) trend toward decreased stroke volume after exposure to 225 and 450 mg/dL D-glucose. The decrease achieved a significance in embryos subjected to 900 mg/dL D-glucose (Figure 3.6 C) (225 mg/dL $p = 0.346$, 450 mg/dL $p = 0.111$, 900 mg/dL $p = 0.022$). In parallel, heart rate significantly increased as glucose concentrations increased (Figure 3.6 D) (0 mg/dL $n = 10$, 225 mg/dL $n = 9$ $p = 0.005$, 450 mg/dL $n = 9$ $p = 0.0010$, 900 mg/dL $n = 11$ $p = <0.0001$). Total cardiac output, a measure that takes both of these changes into account ($CO = HR \times SV$), showed no net alteration across all treatments (Figure 3.6 E) ($p = 0.916$). These data suggest that, as glycemic conditions increased, embryos increased their heart rate to compensate for decreases in stroke volume (Figure 3.6E) (225 mg/dL $p = 0.842$, 450 mg/dL $p = 0.935$, 900 mg/dL $p = 0.916$).

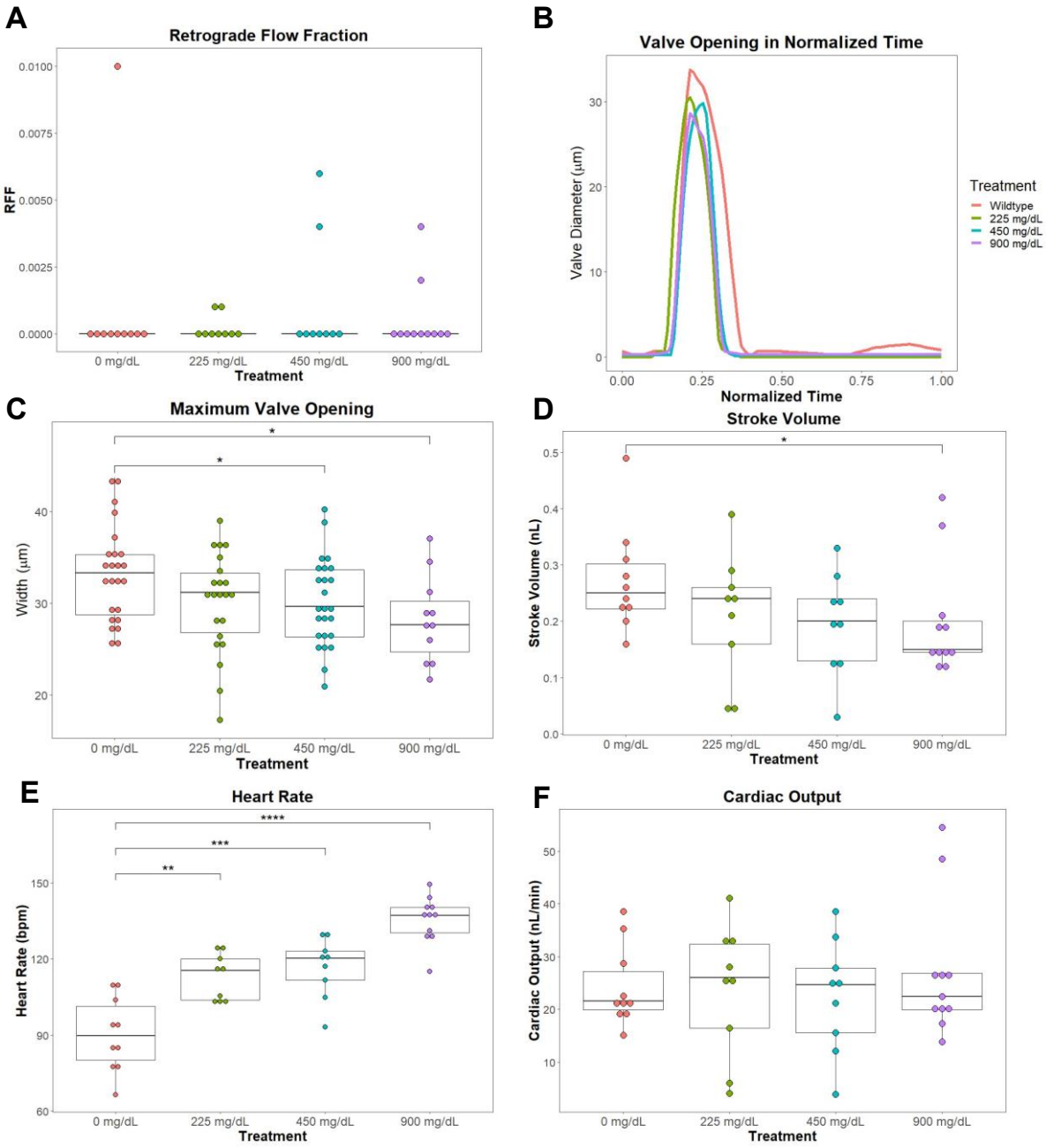

Figure 3.12. Heart rate increases to compensate for decreased stroke volume in hyperglycemic environments. Embryonic hearts were imaged using high-speed video technology and videos were analyzed using spatio-temporal graphs. Backwards movement of the cells was also analyzed and found to not be significantly different **(A).** Analysis of valve openings has shown that very hyperglycemic conditions result in smaller valve openings **(B, C)**. Shown is a representative valve opening trace of an embryo from each glucose concentration (**B**). Stroke volume decreased with very high levels of D-glucose in the environment **(D)**. Heart rate increases with high concentrations of glucose **(E)**. Cardiac output is the product of heart rate and stroke volume; and has no significant changes with any high-glucose environments **(F).** Wilcoxon Rank Sum test performed, * indicates $p \leq 0.05$, ** indicates $p \leq 0.01$, *** indicates $p \leq 0.001$, **** indicates $p < 0.00001$.

DISCUSSION

This study determined that a relationship exists between hyperglycemic embryonic environments, the AVC cardiac jelly, AVC valve-specific endocardial differentiation and primitive valve function. We demonstrate that embryo body glucose levels change in response to increased levels of D-glucose in the E3 buffer, indicating that zebrafish embryos are quite sensitive to their environment despite the fact that their ontogeny is non-placental and thus independent of the parental physiology. When incubated in high D-glucose concentrations (450 mg/dL and 900 mg/dL), embryo free glucose rose to over 1.5 times that of controls, whereas concentrations lower than 225 mg/dL generated little or no effect on the internal glucose content of embryos. Of the range of D-glucose concentrations we tested with zebrafish embryos, those extrapolated from the hyperglycemic rat model had a greater effect than concentrations extrapolated from hyperglycemic adult zebrafish models. Notably, the hyperglycemic environments that resulted in at least a 1.5-fold increase of free D-glucose in embryonic tissue (450 and 900 mg/dL) all induced a change in CJ width (aka the distance that separates the endo-myocardial layers in the AVC, Figure 3.3E) and a smaller valve opening (Figure 3.6E). Embryos that had over a 2-fold increase in free D-glucose were further impacted, showing a significant change in stroke volume. We conclude that there exists a threshold under which embryos can absorb D-glucose without functional consequences. Our data support the hypothesis that embryos which absorb over 1.5-fold the D-glucose concentration observed in adult fish are at risk of cardiac dysfunction.

We further show that zebrafish embryos develop AVC-specific rather than generalized cardiac phenotypes in response to a hyperglycemic environment. The three highest of the tested concentrations (300, 450 and 900 mg/dL) resulted in reduced CJ width in endocardial cushions of the AVC. Further analysis showed that valve-specific differentiation was significantly reduced by hyperglycemic environments although the chamber morphology and heart looping were not detectably affected.

Finally, these phenotypes produced a functionally compromised early valve performance. Valves developing in high D-glucose environments failed to open as fully as control embryos. As the concentrations of D-glucose increased, the smaller valve opening correlated with a trend of reduced stroke volume, which became significant at 900 mg/dL. Concomitantly, embryos demonstrated a dose-responsive increase in heart rate, statistically significant even at the 225 mg/dL concentration. These data suggest that embryos increased their heart rate as a means to compensate for decreased stroke volume. In sum, we propose that hyperglycemic environments alter the CJ significantly enough to decrease endocardial cushion differentiation, interfering with valve development and reducing primitive valve function. Our findings are the first to implicate the CJ as a structure affected by hyperglycemia. They suggest that embryonic CJ development and endocardial EMT should be investigated as a potential cause of valve-related cardiac defects triggered by maternal diabetes in mammals.

Maternal diabetes and altered cardiac function have been linked in prior studies in humans. A study with 63 diabetic pregnancies found first trimester fetuses exhibited diastolic dysfunction (stiffening of ventricles), and overall decreased myocardial function (Turan, Turan et al. 2011). This coincides with a meta-analysis on different studies of pregnancies affected by diabetes mellitus where impaired diastolic function was observed in diabetic pregnancies in 22/28 studies (Depla, De Wit et al. 2021). However, decreased myocardial function is usually diagnosed using ultrasound technology. At earlier stages of pregnancy, defects leading to impaired function are not as readily observed via ultrasound so other measures of cardiac distress are necessary. Cord blood is analyzed for specific markers indicating cardiac dysfunction at earlier stages (Lee-Tannock, Hay et al. 2022). A recent study found elevated levels of the amino terminal segment of B-type natriuretic peptide's prohormone (NT pro-BNP) in women with diabetes mellitus. It was not apparent why natriuretic peptide levels were elevated, but they could be indication of subtle cardiac dysfunction (Lee-Tannock, Hay et al. 2022). Zebrafish Natriuretic Peptide B (Nppb) plays a key role in embryonic cardiac jelly

development within the endocardial cushion. *Nppb* mutants exhibited expanded cardiac jelly within the endocardial cushions along with blood regurgitation, indicating poor valve health (Grassini, Lagendijk et al. 2018). Natriuretic peptides have a closer relationship with maternal diabetes and cardiac jelly development than previously thought and would be an excellent candidate for future studies.

A second goal of this study was to evaluate whether heart development in zebrafish embryos raised in hyperglycemic solutions in a petri dish showed parallels relative to mammalian embryos nurtured in hyperglycemic conditions in utero. At least two intriguing parallels exist. First, in humans, studies detected decreased expression of *bmp4*, a key CJ regulator, in embryos of diabetic pregnancy, suggesting CJ abundance might be affected although endocardial cushion width was not analyzed (Kumar, Dheen et al. 2007). In zebrafish embryos, we find that hyperglycemic environments led to reduced CJ width at the AVC, indicating less robust endocardial cushion development. Next, in mammals, endocardial cells undergo an epithelial to mesenchymal transition (EMT) to form the leaflet structure. Previous studies in mice have linked hyperglycemia to decreased EMT. The marker Msx1 is expressed in endocardial cells during EMT, and it has been found that Msx1 expression is downregulated in hyperglycemic conditions resulting in defective endocardial cushions (Enciso, Gratzinger et al. 2003). In zebrafish embryos, hyperglycemic environments likewise abrogated valve-specific cell differentiation, as measured by the presence of fewer Alcam-expressing endocardial cells at the time shortly before they fold into the surrounding CJ to form a leaflet (Pestel, Ramadass et al. 2016). To the extent that similar tissues and similar cellular pathways are impaired by hyperglycemia in mammals and fish, zebrafish will be useful model. Given that zebrafish embryo bodies show dose-responsive, isomer-specific, AVC-specific effects to glucose levels present in their E3 incubation buffer, they offer a simple experimental set-up with which a variety of drugs or genetic manipulations may be tested to determine if the hyperglycemia-induced effects can be counteracted.

Chapter 4: Reflection

The key to any research is to reflect upon what you have done by celebrating the successes, identifying the errors, and thinking of the future directions the project can go in. Looking back at the work presented in this dissertation, there are a few points that should be discussed further.

The majority of the research performed in chapter 2 used a morpholino (MO) technique to knock-down gene expression in zebrafish embryos. Currently, scientists have been discussing the use of mutant lines as opposed to morpholino knock-down. Morpholinos only stay in zebrafish embryo for the first 72 hours of development. Due to this temporary effect, it will be difficult to decipher permanent damage done to heart after morpholino knockdown. Perhaps defects within the developing heart are so severe that they persist beyond 72 hpf. Due to the dynamic nature of the extracellular matrix within the developing heart, CJ-related defects at an early stage in the embryo could correct themselves later on. Using mutant lines instead of morpholinos could provide better insight into long-term effects of altering the cardiac jelly and the associated defects.

Regardless of their temporary effects, morpholinos have the potential to induce more severe phenotypes than mutants. There are a few reasons why this could occur. In mutants, maternal wildtype mRNAs can rescue zygotic mutant phenotypes whereas MOs could block the translation of maternal mRNAs (Kok, Shin et al. 2015, Stainier, Raz et al. 2017). Previous studies have clarified that *has2*, *npnt*, and *cdh5* MOs result in less protein abundance, but they have not specified if that protein product was a result of maternal or zygotic mRNAs (Bakkers, Kramer et al. 2004, Mitchell, Brown et al. 2010, Patra, Diehl et al. 2011). It is also possible that morpholinos have off-target effects, but scientists will design multiple MOs including a scrambled MO to ensure that any phenotypes are due to inhibited transcription of the target mRNA (Kok, Shin et al. 2015). In mutants, the hypomorphic quality of the mutant allele could

also result in less severe phenotypes as compared to the morpholino technique (Kok, Shin et al. 2015). Another explanation to a less-severe phenotype in mutants is the possibility of genetic compensation that is not possible in a morpholino knock-down model. Although both a morpholino knock-down or a mutant model have benefits and cots, it is important to compare MO phenotypes with mutant phenotypes to support these findings.

In order to compare our *has2* MO data with *has2* mutant phenotypes, we attempted to use a Zebrafish International Resource Center (ZIRC)-generated mutation line as well as create our own CRISPR-Cas9 induced mutant line. We obtained mutant line sa22788 from ZIRC. This line contains a point mutation with a splice site consequence. As a result, exon 2 will be spliced during RNA processing, leaving a 3-exon transcript, rather than a wildtype 4-exon transcript. However, *has2* contains two transcript variants. What we call variant 1, has 4 exons and will act as described with the splice site mutation. Variant 2 contains a 5' flanking sequence instead of exon 1. Due to this flanking sequence, exon 2 will not be spliced with a splice site mutation. We determined that embryonic heart does not express variant 1 rather it expresses variant 2. The *has2* sa22788 line is not an effective null mutant line.

After discovering the ineffective mutant line, we attempted to create a CRISPR-Cas9 mutant line. Using the free online software, ChopChop, 4 guide RNAs (gRNA) were designed. The software was able to grade each gRNA by its specificity, helping us avoid off-target effects. All gRNAs were targeted toward exon 2, which is in both *has2* transcript variants. Two of the designed sgRNA could be used together to create a large deletion within *has2* exon 2. Once the gRNAs are designed, sgRNA oligos must be assembled to be injected with Cas9 protein to induce a mutation. We had immense issues with constructing entire sgRNA oligo, primarily due to gRNA degradation. After an exhaustive effort we decided to put this project on hold in order to complete morpholino-based experiments. In order to avoid this issue, it would be wise to reach out to labs that have successfully completed this technique for assistance in creating the constructs.

Once of the most common comments on this research were about labeling the cardiac jelly (CJ) directly, instead of evaluating its width by measuring the distance between the surrounding cell layers. With this in mind, we wanted to find or create a transgenic model that would label the CJ. Our first option was a hyaluronic acid (HA) transgenic line created by De Angelis et al. that used the HA-binding domain of Neurocan to GFP (*Tg(ubi:ssNcan-EGFP)*). HA is one of the most prominent components of the CJ resulting in this transgene labeling cardiac jelly in zebrafish embryos by Grassini et al. (De Angelis, Lagendijk et al. 2017, Grassini, Lagendijk et al. 2018). We attempted to receive this line, but the lab that created the line is located in Australia making the shipping of embryos or adult zebrafish quite difficult and expensive. In one fortuitous circumstance, a member of the lab was traveling to the United States for a conference and brought embryos with them to ship to Colorado. However, the embryos did not survive shipping. We then received the plasmid used for this transgenic line and we attempted to create our own *Tg(ubi:ssNcan-EGFP)* line but again we did not get any positive results. Another option was to try and label another prominent component of the CJ, Chondroitin sulfate. We purchased an antibody for use in immunofluorescence studies in dissected hearts. Again, we had issues finding the correct protocol to accurately label the CJ in the heart. Future experiments would benefit from using a transgenic line or antibody. More questions can be answered if we are able to see the CJ directly and analyze how it changes.

The work performed in chapter 3 did not experience any major setbacks however there are aspects that could be improved, and it is beneficial to brainstorm future directions this project could move toward. The purpose of this study was to expose zebrafish embryos to a high-glucose environment and evaluate phenotypes as a result. The hyperglycemic environment was created by using various concentrations of D-glucose in the typical embryonic medium, E3. These results aimed to mimic what a developing embryo would experience in a mother with pre-existing or gestational diabetes mellitus. However, these two hyperglycemic environments may not be considered equal. Soaking zebrafish embryos in glucose-treated water is not necessarily

the same as an embryo exposed to maternal blood with elevated levels of glucose. Due to the external fertilization nature of zebrafish, soaking the embryos is the closest scientists can get to mimicking maternal diabetes using this model. Adult diabetic zebrafish models do exist and can be used to evaluate the effects of high blood glucose levels and oocyte health but that is the furthest extent those models could be used in context of this project.

To further our understanding of how hyperglycemic conditions alter the cardiac jelly, it would be beneficial to evaluate what components of the CJ are changed. An RT-qPCR analysis on *has2*, *npnt* and other genes known to code for CJ components would illuminate how the composition of the CJ changes with various D-glucose concentrations. We would also like to understand why the CJ is affected by glucose. HA, a glycosaminoglycan, is a primary component of the CJ at the point of our study. Glycosaminoglycans are composed of repeating disaccharide units which could be disrupted by excessive glucose in the system (Williams and Black III 2015). Diving deeper into the molecular mechanisms that may be disrupted in the cardiac jelly after exposure to high-glucose concentrations could explain why we see the CJ and valve phenotypes.

This reflection is to provide clarity for future work based on the findings described in Chapter 2 and Chapter 3. Regardless of the failures and desired improvements mentioned, this project was performed with the best intentions to achieve high-quality results leading to reliable and well-supported conclusions. Future work related to this project will hopefully illuminate more about heart development and why it is the peanut butter to the cardiac jelly.

References

Abu-Sulaiman, R. M. and B. Subaih (2004). "Congenital heart disease in infants of diabetic mothers: echocardiographic study." Pediatr Cardiol **25**(2): 137-140.
Ahuja, N., P. Ostwald, D. Bark and D. Garrity (2020). "Biomechanical Cues Direct Valvulogenesis." J Cardiovasc Dev Dis **7**(2).
Ahuja, N., P. Ostwald, A. Gendernalik, E. Guzzolino, L. Pitto, D. Bark and D. M. Garrity (2022). "Myocardial Afterload Is a Key Biomechanical Regulator of Atrioventricular Myocyte Differentiation in Zebrafish." J Cardiovasc Dev Dis **9**(1).
Albers, E. L., D. P. Bichell and B. McLaughlin (2010). "New approaches to neuroprotection in infant heart surgery." Pediatr Res **68**(1): 1-9.
Alfano, D., A. Altomonte, C. Cortes, M. Bilio, R. G. Kelly and A. Baldini (2019). "Tbx1 regulates extracellular matrix-cell interactions in the second heart field." Hum Mol Genet **28**(14): 2295-2308.
Allen, V. M., B. A. Armson, G. COMMITTEE and M. F. M. COMMITTEE (2007). "Teratogenicity associated with pre-existing and gestational diabetes." J Obstet Gynaecol Can **29**(11): 927-934.
Anderson, B. R., K. N. Stevens, S. C. Nicolson, S. B. Gruber, T. L. Spray, G. Wernovsky and P. J. Gruber (2013). "Contemporary outcomes of surgical ventricular septal defect closure." J Thorac Cardiovasc Surg **145**(3): 641-647.
Ang, Y. S., R. N. Rivas, A. J. S. Ribeiro, R. Srivas, J. Rivera, N. R. Stone, K. Pratt, T. M. A. Mohamed, J. D. Fu, C. I. Spencer, N. D. Tippens, M. Li, A. Narasimha, E. Radzinsky, A. J. Moon-Grady, H. Yu, B. L. Pruitt, M. P. Snyder and D. Srivastava (2016). "Disease Model of GATA4 Mutation Reveals Transcription Factor Cooperativity in Human Cardiogenesis." Cell **167**(7): 1734-1749.e1722.
Auman, H. J., H. Coleman, H. E. Riley, F. Olale, H. J. Tsai and D. Yelon (2007). "Functional modulation of cardiac form through regionally confined cell shape changes." PLoS Biol **5**(3): e53.
Baasanjav, S., L. Al-Gazali, T. Hashiguchi, S. Mizumoto, B. Fischer, D. Horn, D. Seelow, B. R. Ali, S. A. Aziz, R. Langer, A. A. Saleh, C. Becker, G. Nürnberg, V. Cantagrel, J. G. Gleeson, D. Gomez, J. B. Michel, S. Stricker, T. H. Lindner, P. Nürnberg, K. Sugahara, S. Mundlos and K. Hoffmann (2011). "Faulty initiation of proteoglycan synthesis causes cardiac and joint defects." Am J Hum Genet **89**(1): 15-27.
Bakkers, J., C. Kramer, J. Pothof, N. E. Quaedvlieg, H. P. Spaink and M. Hammerschmidt (2004). "Has2 is required upstream of Rac1 to govern dorsal migration of lateral cells during zebrafish gastrulation." Development **131**(3): 525-537.
Baldini, A. (2004). "DiGeorge syndrome: an update." Curr Opin Cardiol **19**(3): 201-204.
Baldwin, H. S. and M. Solursh (1989). "Degradation of hyaluronic acid does not prevent looping of the mammalian heart in situ." Dev Biol **136**(2): 555-559.
Barry, A. (1948). "The functional significance of the cardiac jelly in the tubular heart of the chick embryo." Anat Rec **102**(3): 289-298.
Bartlett, H., G. J. Veenstra and D. L. Weeks (2010). "Examining the cardiac NK-2 genes in early heart development." Pediatr Cardiol **31**(3): 335-341.
Bassat, E., Y. E. Mutlak, A. Genzelinakh, I. Y. Shadrin, K. Baruch Umansky, O. Yifa, D. Kain, D. Rajchman, J. Leach, D. Riabov Bassat, Y. Udi, R. Sarig, I. Sagi, J. F. Martin, N. Bursac, S. Cohen and E. Tzahor (2017). "The extracellular matrix protein agrin promotes heart regeneration in mice." Nature **547**(7662): 179-184.
Bassili, A., S. A. Mokhtar, N. I. Dabous, S. R. Zaher, M. M. Mokhtar and A. Zaki (2000). "Risk factors for congenital heart diseases in Alexandria, Egypt." Eur J Epidemiol **16**(9): 805-814.

Basson, C. T., D. R. Bachinsky, R. C. Lin, T. Levi, J. A. Elkins, J. Soults, D. Grayzel, E. Kroumpouzou, T. A. Traill, J. Leblanc-Straceski, B. Renault, R. Kucherlapati, J. G. Seidman and C. E. Seidman (1997). "Mutations in human TBX5 cause limb and cardiac malformation in Holt-Oram syndrome." Nat Genet **15**(1): 30-35.
Beis, D., T. Bartman, S. W. Jin, I. C. Scott, L. A. D'Amico, E. A. Ober, H. Verkade, J. Frantsve, H. A. Field, A. Wehman, H. Baier, A. Tallafuss, L. Bally-Cuif, J. N. Chen, D. Y. Stainier and B. Jungblut (2005). "Genetic and cellular analyses of zebrafish atrioventricular cushion and valve development." Development **132**(18): 4193-4204.
Benson, D. W., G. M. Silberbach, A. Kavanaugh-McHugh, C. Cottrill, Y. Zhang, S. Riggs, O. Smalls, M. C. Johnson, M. S. Watson, J. G. Seidman, C. E. Seidman, J. Plowden and J. D. Kugler (1999). "Mutations in the cardiac transcription factor NKX2.5 affect diverse cardiac developmental pathways." J Clin Invest **104**(11): 1567-1573.
Biben, C. and R. P. Harvey (1997). "Homeodomain factor Nkx2-5 controls left/right asymmetric expression of bHLH gene eHand during murine heart development." Genes Dev **11**(11): 1357-1369.
Boselli, F., J. B. Freund and J. Vermot (2015). "Blood flow mechanics in cardiovascular development." Cell Mol Life Sci **72**(13): 2545-2559.
Bragança, J., J. J. Eloranta, S. D. Bamforth, J. C. Ibbitt, H. C. Hurst and S. Bhattacharya (2003). "Physical and functional interactions among AP-2 transcription factors, p300/CREB-binding protein, and CITED2." J Biol Chem **278**(18): 16021-16029.
Brandenberger, R., A. Schmidt, J. Linton, D. Wang, C. Backus, S. Denda, U. Müller and L. F. Reichardt (2001). "Identification and characterization of a novel extracellular matrix protein nephronectin that is associated with integrin alpha8beta1 in the embryonic kidney." J Cell Biol **154**(2): 447-458.
Bressan, M., P. B. Yang, J. D. Louie, A. M. Navetta, R. J. Garriock and T. Mikawa (2014). "Reciprocal myocardial-endocardial interactions pattern the delay in atrioventricular junction conduction." Development **141**(21): 4149-4157.
Brown, D. R., L. A. Samsa, L. Qian and J. Liu (2016). "Advances in the Study of Heart Development and Disease Using Zebrafish." J Cardiovasc Dev Dis **3**(2).
Brun, H., R. A. B. Bugge, L. K. R. Suther, S. Birkeland, R. Kumar, E. Pelanis and O. J. Elle (2019). "Mixed reality holograms for heart surgery planning: first user experience in congenital heart disease." Eur Heart J Cardiovasc Imaging **20**(8): 883-888.
Bulletins, A. C. o. P. (2005). "ACOG Practice Bulletin. Clinical Management Guidelines for Obstetrician-Gynecologists. Number 60, March 2005. Pregestational diabetes mellitus." Obstet Gynecol **105**(3): 675-685.
Camenisch, T. D., J. Biesterfeldt, T. Brehm-Gibson, J. Bradley and J. A. McDonald (2001). "Regulation of cardiac cushion development by hyaluronan." Exp Clin Cardiol **6**(1): 4-10.
Camenisch, T. D., A. P. Spicer, T. Brehm-Gibson, J. Biesterfeldt, M. L. Augustine, A. Calabro, S. Kubalak, S. E. Klewer and J. A. McDonald (2000). "Disruption of hyaluronan synthase-2 abrogates normal cardiac morphogenesis and hyaluronan-mediated transformation of epithelium to mesenchyme." J Clin Invest **106**(3): 349-360.
Carey, A. H., D. Kelly, S. Halford, R. Wadey, D. Wilson, J. Goodship, J. Burn, T. Paul, A. Sharkey and J. Dumanski (1992). "Molecular genetic study of the frequency of monosomy 22q11 in DiGeorge syndrome." Am J Hum Genet **51**(5): 964-970.
Carmichael, S. L., G. M. Shaw, W. Yang, B. Abrams and E. J. Lammer (2007). "Maternal stressful life events and risks of birth defects." Epidemiology **18**(3): 356-361.
Caton, A. R., E. M. Bell, C. M. Druschel, M. M. Werler, A. E. Lin, M. L. Browne, L. A. McNutt, P. A. Romitti, A. A. Mitchell, R. S. Olney, A. Correa and N. B. D. P. Study (2009). "Antihypertensive medication use during pregnancy and the risk of cardiovascular malformations." Hypertension **54**(1): 63-70.

Chan, T. F., A. Poon, A. Basu, N. R. Addleman, J. Chen, A. Phong, P. H. Byers, T. E. Klein and P. Y. Kwok (2008). "Natural variation in four human collagen genes across an ethnically diverse population." Genomics **91**(4): 307-314.
Chelliah, A., A. J. Moon-Grady, S. Peyvandi, J. S. Chiu, J. E. Bost, D. Schidlow, S. J. Carroll, B. Davey, A. Divanovic, L. Hornberger, L. W. Howley, A. Kavanaugh-McHugh, J. P. Kovalchin, S. M. Levasseur, C. L. Lindblade, S. A. Morris, D. Ngwezi, J. D. Pruetz, M. D. Puchalski, J. Rychik, C. Samai, T. A. Tacy, W. Tworetzky, M. M. Vernon, J. Yeh and M. T. Donofrio (2021). "Contemporary Outcomes in Tetralogy of Fallot With Absent Pulmonary Valve After Fetal Diagnosis." J Am Heart Assoc **10**(12): e019713.
Chin, A. J., P. M. Weinberg and G. Barber (1990). "Subcostal two-dimensional echocardiographic identification of anomalous attachment of septum primum in patients with left atrioventricular valve underdevelopment." J Am Coll Cardiol **15**(3): 678-681.
Christianson, A., C. P. Howson and B. Modell (2006). March of Dimes: global report on birth defects, the hidden toll of dying and disabled children. White Plains, New York, March of Dimes Birth Defects Foundation.
Clancy, R. R., S. A. McGaurn, G. Wernovsky, J. W. Gaynor, T. L. Spray, W. I. Norwood, M. L. Jacobs and J. E. Goin (2003). "Risk of seizures in survivors of newborn heart surgery using deep hypothermic circulatory arrest." Pediatrics **111**(3): 592-601.
Correa, A., S. M. Gilboa, L. M. Besser, L. D. Botto, C. A. Moore, C. A. Hobbs, M. A. Cleves, T. J. Riehle-Colarusso, D. K. Waller and E. A. Reece (2008). "Diabetes mellitus and birth defects." Am J Obstet Gynecol **199**(3): 237.e231-239.
d'Udekem, Y., A. J. Iyengar, A. D. Cochrane, L. E. Grigg, J. M. Ramsay, G. R. Wheaton, D. J. Penny and C. P. Brizard (2007). "The Fontan procedure: contemporary techniques have improved long-term outcomes." Circulation **116**(11 Suppl): I157-164.
De Angelis, J. E., A. K. Lagendijk, H. Chen, A. Tromp, N. I. Bower, K. A. Tunny, A. J. Brooks, J. Bakkers, M. Francois, A. S. Yap, C. Simons, C. Wicking, B. M. Hogan and K. A. Smith (2017). "Tmem2 Regulates Embryonic Vegf Signaling by Controlling Hyaluronic Acid Turnover." Dev Cell **40**(2): 123-136.
Del Monte-Nieto, G., M. Ramialison, A. A. S. Adam, B. Wu, A. Aharonov, G. D'Uva, L. M. Bourke, M. E. Pitulescu, H. Chen, J. L. de la Pompa, W. Shou, R. H. Adams, S. K. Harten, E. Tzahor, B. Zhou and R. P. Harvey (2018). "Control of cardiac jelly dynamics by NOTCH1 and NRG1 defines the building plan for trabeculation." Nature **557**(7705): 439-445.
Depla, A. L., L. De Wit, T. J. Steenhuis, M. G. Slieker, D. N. Voormolen, P. G. Scheffer, R. De Heus, B. B. Van Rijn and M. N. Bekker (2021). "Effect of maternal diabetes on fetal heart function on echocardiography: systematic review and meta-analysis." Ultrasound Obstet Gynecol **57**(4): 539-550.
Derrick, C. J. and E. S. Noël (2021). "The ECM as a driver of heart development and repair." Development **148**(5).
Derrick, C. J., J. Sanchez-Posada, F. Hussein, F. Tessadori, E. J. Pollitt, A. M. Savage, R. N. Wilkinson, T. J. Chico, F. J. van Eeden, J. Bakkers and E. Noel (2019). Asymmetric Hapln1a drives regionalised cardiac ECM expansion and promotes heart morphogenesis during zebrafish development, bioRxiv.
Derrick, C. J., J. Sánchez-Posada, F. Hussein, F. Tessadori, E. J. G. Pollitt, A. M. Savage, R. N. Wilkinson, T. J. Chico, F. J. van Eeden, J. Bakkers and E. S. Noël (2022). "Asymmetric Hapln1a drives regionalized cardiac ECM expansion and promotes heart morphogenesis in zebrafish development." Cardiovasc Res **118**(1): 226-240.
Dietrich, A. C., V. A. Lombardo, J. Veerkamp, F. Priller and S. Abdelilah-Seyfried (2014). "Blood flow and Bmp signaling control endocardial chamber morphogenesis." Dev Cell **30**(4): 367-377.
Diz, O. M., R. Toro, S. Cesar, O. Gomez, G. Sarquella-Brugada and O. Campuzano (2021). "Personalized Genetic Diagnosis of Congenital Heart Defects in Newborns." J Pers Med **11**(6).

Duong, T. B., P. Ravisankar, Y. C. Song, J. T. Gafranek, A. B. Rydeen, T. E. Dohn, L. A. Barske, J. G. Crump and J. S. Waxman (2018). "Nr2f1a balances atrial chamber and atrioventricular canal size via BMP signaling-independent and -dependent mechanisms." Dev Biol **434**(1): 7-14.
Enciso, J. M., D. Gratzinger, T. D. Camenisch, S. Canosa, E. Pinter and J. A. Madri (2003). "Elevated glucose inhibits VEGF-A-mediated endocardial cushion formation: modulation by PECAM-1 and MMP-2." J Cell Biol **160**(4): 605-615.
Erikssen, G., K. Liestøl, E. Seem, S. Birkeland, K. J. Saatvedt, T. N. Hoel, G. Døhlen, H. Skulstad, J. L. Svennevig, E. Thaulow and H. L. Lindberg (2015). "Achievements in congenital heart defect surgery: a prospective, 40-year study of 7038 patients." Circulation **131**(4): 337-346; discussion 346.
Errami, M., C. L. Galindo, A. T. Tassa, J. M. Dimaio, J. A. Hill and H. R. Garner (2008). "Doxycycline attenuates isoproterenol- and transverse aortic banding-induced cardiac hypertrophy in mice." J Pharmacol Exp Ther **324**(3): 1196-1203.
Familiari, A., M. Morlando, A. Khalil, S. E. Sonesson, C. Scala, G. Rizzo, G. Del Sordo, C. Vassallo, M. Elena Flacco, L. Manzoli, A. Lanzone, G. Scambia, G. Acharya and F. D'Antonio (2017). "Risk Factors for Coarctation of the Aorta on Prenatal Ultrasound: A Systematic Review and Meta-Analysis." Circulation **135**(8): 772-785.
Fedak, P. W., S. Verma, T. E. David, R. L. Leask, R. D. Weisel and J. Butany (2002). "Clinical and pathophysiological implications of a bicuspid aortic valve." Circulation **106**(8): 900-904.
Feinstein, J. A., D. W. Benson, A. M. Dubin, M. S. Cohen, D. M. Maxey, W. T. Mahle, E. Pahl, J. Villafañe, A. B. Bhatt, L. F. Peng, B. A. Johnson, A. L. Marsden, C. J. Daniels, N. A. Rudd, C. A. Caldarone, K. A. Mussatto, D. L. Morales, D. D. Ivy, J. W. Gaynor, J. S. Tweddell, B. J. Deal, A. K. Furck, G. L. Rosenthal, R. G. Ohye, N. S. Ghanayem, J. P. Cheatham, W. Tworetzky and G. R. Martin (2012). "Hypoplastic left heart syndrome: current considerations and expectations." J Am Coll Cardiol **59**(1 Suppl): S1-42.
Fraisse, A., M. Latchman, S. R. Sharma, S. Bayburt, P. Amedro, G. di Salvo and A. E. Baruteau (2018). "Atrial septal defect closure: indications and contra-indications." J Thorac Dis **10**(Suppl 24): S2874-S2881.
Freund, J. B., J. G. Goetz, K. L. Hill and J. Vermot (2012). "Fluid flows and forces in development: functions, features and biophysical principles." Development **139**(7): 1229-1245.
Friedl, P. and D. Gilmour (2009). "Collective cell migration in morphogenesis, regeneration and cancer." Nat Rev Mol Cell Biol **10**(7): 445-457.
Garavito-Aguilar, Z. V., H. E. Riley and D. Yelon (2010). "Hand2 ensures an appropriate environment for cardiac fusion by limiting Fibronectin function." Development **137**(19): 3215-3220.
Garne, E., M. Loane, H. Dolk, I. Barisic, M. C. Addor, L. Arriola, M. Bakker, E. Calzolari, C. Matias Dias, B. Doray, M. Gatt, K. K. Melve, V. Nelen, M. O'Mahony, A. Pierini, H. Randrianaivo-Ranjatoelina, J. Rankin, A. Rissmann, D. Tucker, C. Verellun-Dumoulin and A. Wiesel (2012). "Spectrum of congenital anomalies in pregnancies with pregestational diabetes." Birth Defects Res A Clin Mol Teratol **94**(3): 134-140.
Garrity, D. M., S. Childs and M. C. Fishman (2002). "The heartstrings mutation in zebrafish causes heart/fin Tbx5 deficiency syndrome." Development **129**(19): 4635-4645.
Gatti, G., B. Benussi, P. Currò, G. Forti, E. Rauber, A. Minati, M. Gabrielli, U. Tognolli, G. Sinagra and A. Pappalardo (2017). "The Risk of Neurological Dysfunctions after Deep Hypothermic Circulatory Arrest with Retrograde Cerebral Perfusion." J Stroke Cerebrovasc Dis **26**(12): 3009-3019.
Gleeson, M., V. Connaughton and L. S. Arneson (2007). "Induction of hyperglycaemia in zebrafish (Danio rerio) leads to morphological changes in the retina." Acta Diabetol **44**(3): 157-163.

Glessner, J. T., A. G. Bick, K. Ito, J. Homsy, L. Rodriguez-Murillo, M. Fromer, E. Mazaika, B. Vardarajan, M. Italia, J. Leipzig, S. R. DePalma, R. Golhar, S. J. Sanders, B. Yamrom, M. Ronemus, I. Iossifov, A. J. Willsey, M. W. State, J. R. Kaltman, P. S. White, Y. Shen, D. Warburton, M. Brueckner, C. Seidman, E. Goldmuntz, B. D. Gelb, R. Lifton, J. Seidman, H. Hakonarson and W. K. Chung (2014). "Increased frequency of de novo copy number variants in congenital heart disease by integrative analysis of single nucleotide polymorphism array and exome sequence data." Circ Res **115**(10): 884-896.
Goddard, L. M., A. L. Duchemin, H. Ramalingan, B. Wu, M. Chen, S. Bamezai, J. Yang, L. Li, M. P. Morley, T. Wang, M. Scherrer-Crosbie, D. B. Frank, K. A. Engleka, S. C. Jameson, E. E. Morrisey, T. J. Carroll, B. Zhou, J. Vermot and M. L. Kahn (2017). "Hemodynamic Forces Sculpt Developing Heart Valves through a KLF2-WNT9B Paracrine Signaling Axis." Dev Cell **43**(3): 274-289.e275.
Gonzalez, D. C., J. Ory, R. Blachman-Braun, S. Nackeeran, J. C. Best and R. Ramasamy (2022). "Advanced Paternal Age and Sperm DNA Fragmentation: A Systematic Review." World J Mens Health **40**(1): 104-115.
Grassini, D. R., A. K. Lagendijk, J. E. De Angelis, J. Da Silva, A. Jeanes, N. Zettler, N. I. Bower, B. M. Hogan and K. A. Smith (2018). "Nppa and Nppb act redundantly during zebrafish cardiac development to confine AVC marker expression and reduce cardiac jelly volume." Development **145**(12).
Grego-Bessa, J., L. Luna-Zurita, G. del Monte, V. Bolós, P. Melgar, A. Arandilla, A. N. Garratt, H. Zang, Y. S. Mukouyama, H. Chen, W. Shou, E. Ballestar, M. Esteller, A. Rojas, J. M. Pérez-Pomares and J. L. de la Pompa (2007). "Notch signaling is essential for ventricular chamber development." Dev Cell **12**(3): 415-429.
Gross, R. E. (1939). "SURGICAL MANAGEMENT OF THE PATENT DUCTUS ARTERIOSUS: WITH SUMMARY OF FOUR SURGICALLY TREATED CASES." Ann Surg **110**(3): 321-356.
Gunawan, F., A. Gentile, R. Fukuda, A. T. Tsedeke, V. Jiménez-Amilburu, R. Ramadass, A. Iida, A. Sehara-Fujisawa and D. Y. R. Stainier (2019). "Focal adhesions are essential to drive zebrafish heart valve morphogenesis." J Cell Biol **218**(3): 1039-1054.
Hatano, S., K. Kimata, N. Hiraiwa, M. Kusakabe, Z. Isogai, E. Adachi, T. Shinomura and H. Watanabe (2012). "Versican/PG-M is essential for ventricular septal formation subsequent to cardiac atrioventricular cushion development." Glycobiology **22**(9): 1268-1277.
Heckel, E., F. Boselli, S. Roth, A. Krudewig, H.-G. Belting, G. Charvin and J. Vermot (2015). "Oscillatory Flow Modulates Mechanosensitive klf2a Expression through trpv4 and trpp2 during Heart Valve Development | Elsevier Enhanced Reader." Current Biology **25**(10): 1354-1361.
Hernandez, L., L. Ryckebüsch, C. Wang, R. Ling and D. Yelon (2019). "Tmem2 restricts atrioventricular canal differentiation by regulating degradation of hyaluronic acid." Dev Dyn **248**(12): 1195-1210.
Hoage, T., Y. Ding and X. Xu (2012). "Quantifying cardiac functions in embryonic and adult zebrafish." Methods Mol Biol **843**: 11-20.
Hoang, T. T., L. K. Marengo, L. E. Mitchell, M. A. Canfield and A. J. Agopian (2017). "Original Findings and Updated Meta-Analysis for the Association Between Maternal Diabetes and Risk for Congenital Heart Disease Phenotypes." Am J Epidemiol **186**(1): 118-128.
Holst, K. A., S. M. Said, T. J. Nelson, B. C. Cannon and J. A. Dearani (2017). "Current Interventional and Surgical Management of Congenital Heart Disease: Specific Focus on Valvular Disease and Cardiac Arrhythmias." Circ Res **120**(6): 1027-1044.
Hu, B., Y. Gao, L. Davies, S. Woo, J. Topczewski, J. R. Jessen and F. Lin (2018). "Glypican 4 and Mmp14 interact in regulating the migration of anterior endodermal cells by limiting extracellular matrix deposition." Development **145**(17).
Huveneers, S., H. Truong, R. Fässler, A. Sonnenberg and E. H. Danen (2008). "Binding of soluble fibronectin to integrin alpha5 beta1 - link to focal adhesion redistribution and contractile shape." J Cell Sci **121**(Pt 15): 2452-2462.

Hyde, A. S., E. L. Farmer, K. E. Easley, K. van Lammeren, V. M. Christoffels, J. J. Barycki, J. Bakkers and M. A. Simpson (2012). "UDP-glucose dehydrogenase polymorphisms from patients with congenital heart valve defects disrupt enzyme stability and quaternary assembly." J Biol Chem **287**(39): 32708-32716.
Jacobs, J. P., D. M. Shahian, R. S. D'Agostino, J. E. Mayer, B. D. Kozower, V. Badhwar, V. H. Thourani, M. L. Jacobs, H. A. Gaissert, F. G. Fernandez and K. S. Naunheim (2018). "The Society of Thoracic Surgeons National Database 2018 Annual Report." Ann Thorac Surg **106**(6): 1603-1611.
Jessen, J. R. (2015). "Recent advances in the study of zebrafish extracellular matrix proteins." Dev Biol **401**(1): 110-121.
Jessen, J. R., J. Topczewski, S. Bingham, D. S. Sepich, F. Marlow, A. Chandrasekhar and L. Solnica-Krezel (2002). "Zebrafish trilobite identifies new roles for Strabismus in gastrulation and neuronal movements." Nat Cell Biol **4**(8): 610-615.
Johnson, B., D. Bark, I. Van Herck, D. Garrity and L. P. Dasi (2015). "Altered mechanical state in the embryonic heart results in time-dependent decreases in cardiac function." Biomech Model Mechanobiol **14**(6): 1379-1389.
Johnson, B. M., D. M. Garrity and L. P. Dasi (2013). "The Transitional Cardiac Pumping Mechanics in the Embryonic Heart." Cardiovasc Eng Technol **4**(3): 246-255.
Just, S., S. Hirth, I. M. Berger, M. C. Fishman and W. Rottbauer (2016). "The mediator complex subunit Med10 regulates heart valve formation in zebrafish by controlling Tbx2b-mediated Has2 expression and cardiac jelly formation." Biochem Biophys Res Commun **477**(4): 581-588.
Khalil, A., S. Bennet, B. Thilaganathan, D. Paladini, P. Griffiths and J. S. Carvalho (2016). "Prevalence of prenatal brain abnormalities in fetuses with congenital heart disease: a systematic review." Ultrasound Obstet Gynecol **48**(3): 296-307.
Kim, Y. Y., K. Gauvreau, E. A. Bacha, M. J. Landzberg and O. J. Benavidez (2011). "Risk factors for death after adult congenital heart surgery in pediatric hospitals." Circ Cardiovasc Qual Outcomes **4**(4): 433-439.
Kirkham, F. J. (1998). "Recognition and prevention of neurological complications in pediatric cardiac surgery." Pediatr Cardiol **19**(4): 331-345.
Knöll, R., R. Postel, J. Wang, R. Krätzner, G. Hennecke, A. M. Vacaru, P. Vakeel, C. Schubert, K. Murthy, B. K. Rana, D. Kube, G. Knöll, K. Schäfer, T. Hayashi, T. Holm, A. Kimura, N. Schork, M. R. Toliat, P. Nürnberg, H. P. Schultheiss, W. Schaper, J. Schaper, E. Bos, J. Den Hertog, F. J. van Eeden, P. J. Peters, G. Hasenfuss, K. R. Chien and J. Bakkers (2007). "Laminin-alpha4 and integrin-linked kinase mutations cause human cardiomyopathy via simultaneous defects in cardiomyocytes and endothelial cells." Circulation **116**(5): 515-525.
Kodo, K., T. Nishizawa, M. Furutani, S. Arai, E. Yamamura, K. Joo, T. Takahashi, R. Matsuoka and H. Yamagishi (2009). "GATA6 mutations cause human cardiac outflow tract defects by disrupting semaphorin-plexin signaling." Proc Natl Acad Sci U S A **106**(33): 13933-13938.
Kok, F. O., M. Shin, C. W. Ni, A. Gupta, A. S. Grosse, A. van Impel, B. C. Kirchmaier, J. Peterson-Maduro, G. Kourkoulis, I. Male, D. F. DeSantis, S. Sheppard-Tindell, L. Ebarasi, C. Betsholtz, S. Schulte-Merker, S. A. Wolfe and N. D. Lawson (2015). "Reverse genetic screening reveals poor correlation between morpholino-induced and mutant phenotypes in zebrafish." Dev Cell **32**(1): 97-108.
Kuciene, R. and V. Dulskiene (2009). "Maternal socioeconomic and lifestyle factors during pregnancy and the risk of congenital heart defects." Medicina (Kaunas) **45**(11): 904-909.
Kumar, S. D., S. T. Dheen and S. S. Tay (2007). "Maternal diabetes induces congenital heart defects in mice by altering the expression of genes involved in cardiovascular development." Cardiovasc Diabetol **6**: 34.
Lagendijk, A. K., A. Szabó, R. M. Merks and J. Bakkers (2013). "Hyaluronan: a critical regulator of endothelial-to-mesenchymal transition during cardiac valve formation." Trends Cardiovasc Med **23**(5): 135-142.

Le Gloan, L., L. A. Mercier, A. Dore, F. Marcotte, R. Ibrahim, F. P. Mongeon, A. Asgar, J. Miro, N. Poirier and P. Khairy (2011). "Recent advances in adult congenital heart disease." Circ J **75**(10): 2287-2295.
Lee-Tannock, A., K. Hay and S. Kumar (2022). "Differences in biomarkers of cardiac dysfunction in cord blood between normal pregnancies and pregnancies complicated by maternal diabetes." Aust N Z J Obstet Gynaecol **62**(1): 79-85.
Li, D. K., C. Yang, S. Andrade, V. Tavares and J. R. Ferber (2011). "Maternal exposure to angiotensin converting enzyme inhibitors in the first trimester and risk of malformations in offspring: a retrospective cohort study." BMJ **343**: d5931.
Li, Q. Y., R. A. Newbury-Ecob, J. A. Terrett, D. I. Wilson, A. R. Curtis, C. H. Yi, T. Gebuhr, P. J. Bullen, S. C. Robson, T. Strachan, D. Bonnet, S. Lyonnet, I. D. Young, J. A. Raeburn, A. J. Buckler, D. J. Law and J. D. Brook (1997). "Holt-Oram syndrome is caused by mutations in TBX5, a member of the Brachyury (T) gene family." Nat Genet **15**(1): 21-29.
Liang, J., Y. Gui, W. Wang, S. Gao, J. Li and H. Song (2010). "Elevated glucose induces congenital heart defects by altering the expression of tbx5, tbx20, and has2 in developing zebrafish embryos." Birth Defects Res A Clin Mol Teratol **88**(6): 480-486.
Lincoln, J. and V. Garg (2014). "Etiology of valvular heart disease-genetic and developmental origins." Circ J **78**(8): 1801-1807.
Lindsay, E. A., F. Vitelli, H. Su, M. Morishima, T. Huynh, T. Pramparo, V. Jurecic, G. Ogunrinu, H. F. Sutherland, P. J. Scambler, A. Bradley and A. Baldini (2001). "Tbx1 haploinsufficieny in the DiGeorge syndrome region causes aortic arch defects in mice." Nature **410**(6824): 97-101.
Lints, T. J., L. M. Parsons, L. Hartley, I. Lyons and R. P. Harvey (1993). "Nkx-2.5: a novel murine homeobox gene expressed in early heart progenitor cells and their myogenic descendants." Development **119**(3): 969.
Liu, S. A., H. Zhou, X. F. Zhou, J. F. Hu, M. T. Chen, W. J. Hu, H. L. Tang, L. Yan, J. W. Li, R. Z. Li, Y. B. Li, J. Y. Wang, W. Zhang, B. K. Zhang, Q. F. Zhang, J. Y. Yao, C. Chen, W. Q. Shi, L. X. Xia, B. Y. Cui, W. M. Cui, N. Kang, M. Jiang, L. J. Pan, Z. F. Zang, Y. X. Fan, F. C. Fan and H. J. Yu (2009). "[Mental health assessment among scattered residents after Wenchuan earthquake in Anxian, Sichuan province]." Zhonghua Yu Fang Yi Xue Za Zhi **43**(5): 380-384.
Liu, Y., S. Chen, L. Zühlke, G. C. Black, M. K. Choy, N. Li and B. D. Keavney (2019). "Global birth prevalence of congenital heart defects 1970-2017: updated systematic review and meta-analysis of 260 studies." Int J Epidemiol **48**(2): 455-463.
Lobo, I. (2008). "Birth Defects: Causes and Statistics." Nature Education **1**(1).
Loffredo, C. A., P. D. Wilson and C. Ferencz (2001). "Maternal diabetes: an independent risk factor for major cardiovascular malformations with increased mortality of affected infants." Teratology **64**(2): 98-106.
Love, A. M., D. J. Prince and J. R. Jessen (2018). "Vangl2-dependent regulation of membrane protrusions and directed migration requires a fibronectin extracellular matrix." Development **145**(22).
Lyons, I., L. M. Parsons, L. Hartley, R. Li, J. E. Andrews, L. Robb and R. P. Harvey (1995). "Myogenic and morphogenetic defects in the heart tubes of murine embryos lacking the homeo box gene Nkx2-5." Genes Dev **9**(13): 1654-1666.
Ma, L., M. F. Lu, R. J. Schwartz and J. F. Martin (2005). "Bmp2 is essential for cardiac cushion epithelial-mesenchymal transition and myocardial patterning." Development **132**(24): 5601-5611.
Mai, C. T., J. L. Isenburg, M. A. Canfield, R. E. Meyer, A. Correa, C. J. Alverson, P. J. Lupo, T. Riehle-Colarusso, S. J. Cho, D. Aggarwal, R. S. Kirby and N. B. D. P. Network (2019). "National population-based estimates for major birth defects, 2010-2014." Birth Defects Res **111**(18): 1420-1435.

Malfait, F., S. Symoens, P. Coucke, L. Nunes, S. De Almeida and A. De Paepe (2006). "Total absence of the alpha2(I) chain of collagen type I causes a rare form of Ehlers-Danlos syndrome with hypermobility and propensity to cardiac valvular problems." J Med Genet **43**(7): e36.
Mammoto, T., E. Jiang, A. Jiang and A. Mammoto (2013). "Extracellular matrix structure and tissue stiffness control postnatal lung development through the lipoprotein receptor-related protein 5/Tie2 signaling system." Am J Respir Cell Mol Biol **49**(6): 1009-1018.
Marino, B. S., P. H. Lipkin, J. W. Newburger, G. Peacock, M. Gerdes, J. W. Gaynor, K. A. Mussatto, K. Uzark, C. S. Goldberg, W. H. Johnson, J. Li, S. E. Smith, D. C. Bellinger, W. T. Mahle and C. o. C. D. i. t. Y. American Heart Association Congenital Heart Defects Committee, C.uncil on Cardiovascular Nursing, and Stroke Council (2012). "Neurodevelopmental outcomes in children with congenital heart disease: evaluation and management: a scientific statement from the American Heart Association." Circulation **126**(9): 1143-1172.
Marín-García, J. (2009). "Advances in molecular genetics of congenital heart disease." Rev Esp Cardiol **62**(3): 242-245.
Mavroudis, C., C. L. Backer, L. M. Kohr, B. J. Deal, J. Stinios, A. J. Muster and D. F. Wax (1999). "Bidirectional Glenn shunt in association with congenital heart repairs: the 1(1/2) ventricular repair." Ann Thorac Surg **68**(3): 976-981; discussion 982.
Mavroudis, C., J. A. Dearani and R. H. Anderson (2019). Ventricular Septal Defect. Atlas of Adult Congenital Heart Surgery, Springer, Cham**:** 91-115.
McIntyre, H. D., P. Catalano, C. Zhang, G. Desoye, E. R. Mathiesen and P. Damm (2019). "Gestational diabetes mellitus." Nat Rev Dis Primers **5**(1): 47.
Miller, A., T. Riehle-Colarusso, C. Siffel, J. L. Frías and A. Correa (2011). "Maternal age and prevalence of isolated congenital heart defects in an urban area of the United States." Am J Med Genet A **155A**(9): 2137-2145.
Mitchell, I. C., T. S. Brown, L. S. Terada, J. F. Amatruda and F. E. Nwariaku (2010). "Effect of vascular cadherin knockdown on zebrafish vasculature during development." PLoS One **5**(1): e8807.
Mittal, A., M. Pulina, S. Y. Hou and S. Astrof (2013). "Fibronectin and integrin alpha 5 play requisite roles in cardiac morphogenesis." Dev Biol **381**(1): 73-82.
Molin, D. G., P. A. Roest, H. Nordstrand, L. J. Wisse, R. E. Poelmann, U. J. Eriksson and A. C. Gittenberger-De Groot (2004). "Disturbed morphogenesis of cardiac outflow tract and increased rate of aortic arch anomalies in the offspring of diabetic rats." Birth Defects Res A Clin Mol Teratol **70**(12): 927-938.
Moon, A. (2008). "Mouse models of congenital cardiovascular disease." Curr Top Dev Biol **84**: 171-248.
Mould, A. P., J. A. McLeish, J. Huxley-Jones, A. C. Goonesinghe, A. F. Hurlstone, R. P. Boot-Handford and M. J. Humphries (2006). "Identification of multiple integrin beta1 homologs in zebrafish (Danio rerio)." BMC Cell Biol **7**: 24.
Mozaffarian, D., E. J. Benjamin, A. S. Go, D. K. Arnett, M. J. Blaha, M. Cushman, S. de Ferranti, J. P. Després, H. J. Fullerton, V. J. Howard, M. D. Huffman, S. E. Judd, B. M. Kissela, D. T. Lackland, J. H. Lichtman, L. D. Lisabeth, S. Liu, R. H. Mackey, D. B. Matchar, D. K. McGuire, E. R. Mohler, C. S. Moy, P. Muntner, M. E. Mussolino, K. Nasir, R. W. Neumar, G. Nichol, L. Palaniappan, D. K. Pandey, M. J. Reeves, C. J. Rodriguez, P. D. Sorlie, J. Stein, A. Towfighi, T. N. Turan, S. S. Virani, J. Z. Willey, D. Woo, R. W. Yeh, M. B. Turner and A. H. A. S. C. a. S. S. Subcommittee (2015). "Heart disease and stroke statistics--2015 update: a report from the American Heart Association." Circulation **131**(4): e29-322.
Mundell, N. A. and J. R. Jessen (2013). Extracellular Matrix Remodeling in Zebrafish Development. Extracellular Matrix in Development. Berlin Heidelberg, Springer-Verlag**:** 187-218.
Murakami, M., M. Nakagawa, E. N. Olson and O. Nakagawa (2005). "A WW domain protein TAZ is a critical coactivator for TBX5, a transcription factor implicated in Holt-Oram syndrome." Proc Natl Acad Sci U S A **102**(50): 18034-18039.

Männer, J. and T. M. Yelbuz (2019). "Functional Morphology of the Cardiac Jelly in the Tubular Heart of Vertebrate Embryos." J Cardiovasc Dev Dis **6**(1).
Nair, R., A. V. Ngangan, M. L. Kemp and T. C. McDevitt (2012). "Gene expression signatures of extracellular matrix and growth factors during embryonic stem cell differentiation." PLoS One **7**(10): e42580.
Nakamura, A. and F. J. Manasek (1978). "Cardiac jelly fibrils: their distribution and organization." Birth Defects Orig Artic Ser **14**(7): 229-250.
Nakamura, A. and F. J. Manasek (1978). "Experimental studies of the shape and structure of isolated cardiac jelly." J Embryol Exp Morphol **43**: 167-183.
Necas, J., L. Bartosikova, P. Brauner and J. Kolar (2008). Hyaluronic acid (hyaluronan): a review, Veterinarni Medicina. **53:** 397-411.
Nimura, K., K. Ura, H. Shiratori, M. Ikawa, M. Okabe, R. J. Schwartz and Y. Kaneda (2009). "A histone H3 lysine 36 trimethyltransferase links Nkx2-5 to Wolf-Hirschhorn syndrome." Nature **460**(7252): 287-291.
Norwood, W. I., P. Lang and D. D. Hansen (1983). "Physiologic repair of aortic atresia-hypoplastic left heart syndrome." N Engl J Med **308**(1): 23-26.
Notari, M., A. Ventura-Rubio, S. J. Bedford-Guaus, I. Jorba, L. Mulero, D. Navajas, M. Martí and Á. Raya (2018). "The local microenvironment limits the regenerative potential of the mouse neonatal heart." Sci Adv **4**(5): eaao5553.
Ntostis, P., D. Iles, G. Kokkali, T. Vaxevanoglou, E. Kanavakis, A. Pantou, J. Huntriss, K. Pantos and H. M. Picton (2021). "The impact of maternal age on gene expression during the GV to MII transition in euploid human oocytes." Hum Reprod **37**(1): 80-92.
Nyboe, C., Z. Karunanithi, J. E. Nielsen-Kudsk and V. E. Hjortdal (2018). "Long-term mortality in patients with atrial septal defect: a nationwide cohort-study." Eur Heart J **39**(12): 993-998.
Olsen, A. S., M. P. Sarras and R. V. Intine (2010). "Limb regeneration is impaired in an adult zebrafish model of diabetes mellitus." Wound Repair Regen **18**(5): 532-542.
Oster, M. E., C. H. Kim, A. S. Kusano, J. D. Cragan, P. Dressler, A. R. Hales, W. T. Mahle and A. Correa (2014). "A population-based study of the association of prenatal diagnosis with survival rate for infants with congenital heart defects." Am J Cardiol **113**(6): 1036-1040.
Oster, M. E., K. A. Lee, M. A. Honein, T. Riehle-Colarusso, M. Shin and A. Correa (2013). "Temporal trends in survival among infants with critical congenital heart defects." Pediatrics **131**(5): e1502-1508.
Pagnozzi, L. A. and J. T. Butcher (2017). "Mechanotransduction Mechanisms in Mitral Valve Physiology and Disease Pathogenesis." Front Cardiovasc Med **4**: 83.
Patel, S. S. and T. L. Burns (2013). "Nongenetic risk factors and congenital heart defects." Pediatr Cardiol **34**(7): 1535-1555.
Patra, C., F. Diehl, F. Ferrazzi, M. J. van Amerongen, T. Novoyatleva, L. Schaefer, C. Mühlfeld, B. Jungblut and F. B. Engel (2011). "Nephronectin regulates atrioventricular canal differentiation via Bmp4-Has2 signaling in zebrafish." Development **138**(20): 4499-4509.
Patra, C., F. Ricciardi and F. B. Engel (2012). "The functional properties of nephronectin: an adhesion molecule for cardiac tissue engineering." Biomaterials **33**(17): 4327-4335.
Patten, B. M., T. C. Kramer and A. Barry (1948). "Valvular action in the embryonic chick heart by localized apposition of endocardial masses." Anat Rec **102**(3): 299-311.
Pereira, F. A., Y. Qiu, G. Zhou, M. J. Tsai and S. Y. Tsai (1999). "The orphan nuclear receptor COUP-TFII is required for angiogenesis and heart development." Genes Dev **13**(8): 1037-1049.
Pestel, J., R. Ramadass, S. Gauvrit, C. Helker, W. Herzog and D. Y. Stainier (2016). "Real-time 3D visualization of cellular rearrangements during cardiac valve formation." Development **143**(12): 2217-2227.
Peterson, C., S. D. Grosse, R. Li, A. J. Sharma, H. Razzaghi, W. H. Herman and S. M. Gilboa (2015). "Preventable health and cost burden of adverse birth outcomes associated with pregestational diabetes in the United States." Am J Obstet Gynecol **212**(1): 74.e71-79.

Pfitzer, C., P. C. Helm, L. M. Rosenthal, F. Berger, U. M. M. Bauer and K. R. Schmitt (2018). "Dynamics in prevalence of Down syndrome in children with congenital heart disease." Eur J Pediatr **177**(1): 107-115.
Prince, D. J. and J. R. Jessen (2019). "Dorsal convergence of gastrula cells requires Vangl2 and an adhesion protein-dependent change in protrusive activity." Development **146**(22).
Quélin, C., C. Bendavid, C. Dubourg, C. de la Rochebrochard, J. Lucas, C. Henry, S. Jaillard, P. Loget, L. Loeuillet, D. Lacombe, J. M. Rival, V. David, S. Odent and L. Pasquier (2009). "Twelve new patients with 13q deletion syndrome: genotype-phenotype analyses in progress." Eur J Med Genet **52**(1): 41-46.
Rambeau, P., E. Faure, A. Théron, J. F. Avierinos, C. Jopling, S. Zaffran and A. Faucherre (2017). "Reduced aggrecan expression affects cardiac outflow tract development in zebrafish and is associated with bicuspid aortic valve disease in humans." Int J Cardiol **249**: 340-343.
Rana, M. S., M. Théveniau-Ruissy, C. De Bono, K. Mesbah, A. Francou, M. Rammah, J. N. Domínguez, M. Roux, B. Laforest, R. H. Anderson, T. Mohun, S. Zaffran, V. M. Christoffels and R. G. Kelly (2014). "Tbx1 coordinates addition of posterior second heart field progenitor cells to the arterial and venous poles of the heart." Circ Res **115**(9): 790-799.
Rao, P. S. (2012). Congenital Heart Defects - A Review. Congenital Heart Disease: Selected Aspects. P. S. Rao. Janeza Trdine 9, 51000 Rijeka, Croatia, InTech**:** 3-46.
Rao, P. S. and A. D. Harris (2017). "Recent advances in managing septal defects: atrial septal defects." F1000Res **6**: 2042.
Rao, P. S. and A. D. Harris (2018). "Recent advances in managing septal defects: ventricular septal defects and atrioventricular septal defects." F1000Res **7**.
Rasouli, S. J. and D. Y. R. Stainier (2017). "Regulation of cardiomyocyte behavior in zebrafish trabeculation by Neuregulin 2a signaling." Nature Communications **8**(1): 1-11.
Reifenstein, G. H., S. A. Levine and R. E. Gross (1947). "Coarctation of the aorta; a review of 104 autopsied cases of the adult type, 2 years of age or older." Am Heart J **33**(2): 146-168.
Ricard-Blum, S. (2011). "The collagen family." Cold Spring Harb Perspect Biol **3**(1): a004978.
Robinson, S. W., C. D. Morris, E. Goldmuntz, M. D. Reller, M. A. Jones, R. D. Steiner and C. L. Maslen (2003). "Missense mutations in CRELD1 are associated with cardiac atrioventricular septal defects." Am J Hum Genet **72**(4): 1047-1052.
Rowland, J. M. and A. G. Hendrickx (1983). "Corticosteroid teratogenicity." Adv Vet Sci Comp Med **27**: 99-128.
Russell, M. W., M. O. Raeker, S. B. Geisler, P. E. Thomas, T. A. Simmons, J. A. Bernat, T. Thorsson and J. W. Innis (2014). "Functional analysis of candidate genes in 2q13 deletion syndrome implicates FBLN7 and TMEM87B deficiency in congenital heart defects and FBLN7 in craniofacial malformations." Hum Mol Genet **23**(16): 4272-4284.
Rydeen, A. B. and J. S. Waxman (2016). "Cyp26 Enzymes Facilitate Second Heart Field Progenitor Addition and Maintenance of Ventricular Integrity." PLoS Biol **14**(11): e2000504.
S, C., A. JE and K. AA (2010). "Deep hypothermic circulatory arrest." Continuing Education in Anesthesia Critical Care & Pain **10**(5): 138-142.
Schoeneberg, L. and D. A. Adebo (2021). Dextro-Transposition of the Great Arteries. Pediatric Cardiac CT in Congenital Heart Disease, Springer, Cham**:** 129-135.
Schroeder, J. A., L. F. Jackson, D. C. Lee and T. D. Camenisch (2003). "Form and function of developing heart valves: coordination by extracellular matrix and growth factor signaling." J Mol Med (Berl) **81**(7): 392-403.
Schwarzbauer, J. E. and J. L. Sechler (1999). "Fibronectin fibrillogenesis: a paradigm for extracellular matrix assembly." Curr Opin Cell Biol **11**(5): 622-627.
Segert, J., I. Schneider, I. M. Berger, W. Rottbauer and S. Just (2018). "Mediator complex subunit Med12 regulates cardiac jelly development and AV valve formation in zebrafish." Prog Biophys Mol Biol **138**: 20-31.

Shirai, M., K. Imanaka-Yoshida, M. D. Schneider, R. J. Schwartz and T. Morisaki (2009). "T-box 2, a mediator of Bmp-Smad signaling, induced hyaluronan synthase 2 and Tgfbeta2 expression and endocardial cushion formation." Proc Natl Acad Sci U S A **106**(44): 18604-18609.
Shoff, C., T. C. Yang and S. A. Matthews (2012). "What has geography got to do with it? Using GWR to explore place-specific associations with prenatal care utilization." GeoJournal **77**(3): 331-341.
Shuler, C. O., G. B. Black and J. M. Jerrell (2013). "Population-based treated prevalence of congenital heart disease in a pediatric cohort." Pediatr Cardiol **34**(3): 606-611.
Silva, A. C., C. Pereira, A. C. R. G. Fonseca, P. Pinto-do-Ó and D. S. Nascimento (2020). "Bearing My Heart: The Role of Extracellular Matrix on Cardiac Development, Homeostasis, and Injury Response." Front Cell Dev Biol **8**: 621644.
Silversides, C. K., A. C. Lionel, G. Costain, D. Merico, O. Migita, B. Liu, T. Yuen, J. Rickaby, B. Thiruvahindrapuram, C. R. Marshall, S. W. Scherer and A. S. Bassett (2012). "Rare copy number variations in adults with tetralogy of Fallot implicate novel risk gene pathways." PLoS Genet **8**(8): e1002843.
Simeone, R. M., O. J. Devine, J. A. Marcinkevage, S. M. Gilboa, H. Razzaghi, B. H. Bardenheier, A. J. Sharma and M. A. Honein (2015). "Diabetes and congenital heart defects: a systematic review, meta-analysis, and modeling project." Am J Prev Med **48**(2): 195-204.
Singh, A., H. A. Castillo, J. Brown, J. Kaslin, K. M. Dwyer and Y. Gibert (2019). "High glucose levels affect retinal patterning during zebrafish embryogenesis." Sci Rep **9**(1): 4121.
Sinning, A. R. (1998). "Role of vitamin A in the formation of congenital heart defects." Anat Rec **253**(5): 147-153.
Siu, S. C. and C. K. Silversides (2010). "Bicuspid aortic valve disease." J Am Coll Cardiol **55**(25): 2789-2800.
Smith, K. A., I. C. Joziasse, S. Chocron, M. Van Dinther, V. Guryev, M. C. Verhoeven, H. Rehmann, J. J. Van Der Smagt, P. A. Doevendans, E. Cuppen, B. J. Mulder, P. Ten Dijke and J. Bakkers (2009). "Dominant-Negative ALK2 Allele Associates With Congenital Heart Defects." Circulation **119**(24): 3062-3069.
Soemedi, R., I. J. Wilson, J. Bentham, R. Darlay, A. Töpf, D. Zelenika, C. Cosgrove, K. Setchfield, C. Thornborough, J. Granados-Riveron, G. M. Blue, J. Breckpot, S. Hellens, S. Zwolinkski, E. Glen, C. Mamasoula, T. J. Rahman, D. Hall, A. Rauch, K. Devriendt, M. Gewillig, J. O' Sullivan, D. S. Winlaw, F. Bu'Lock, J. D. Brook, S. Bhattacharya, M. Lathrop, M. Santibanez-Koref, H. J. Cordell, J. A. Goodship and B. D. Keavney (2012). "Contribution of global rare copy-number variants to the risk of sporadic congenital heart disease." Am J Hum Genet **91**(3): 489-501.
Spector, L. G., J. S. Menk, J. H. Knight, C. McCracken, A. S. Thomas, J. M. Vinocur, M. E. Oster, J. D. St Louis, J. H. Moller and L. Kochilas (2018). "Trends in Long-Term Mortality After Congenital Heart Surgery." J Am Coll Cardiol **71**(21): 2434-2446.
Stainier, D. Y. (2001). "Zebrafish genetics and vertebrate heart formation." Nat Rev Genet **2**(1): 39-48.
Stainier, D. Y., R. K. Lee and M. C. Fishman (1993). "Cardiovascular development in the zebrafish. I. Myocardial fate map and heart tube formation." Development **119**(1): 31-40.
Stainier, D. Y. R., E. Raz, N. D. Lawson, S. C. Ekker, R. D. Burdine, J. S. Eisen, P. W. Ingham, S. Schulte-Merker, D. Yelon, B. M. Weinstein, M. C. Mullins, S. W. Wilson, L. Ramakrishnan, S. L. Amacher, S. C. F. Neuhauss, A. Meng, N. Mochizuki, P. Panula and C. B. Moens (2017). "Guidelines for morpholino use in zebrafish." PLoS Genet **13**(10): e1007000.
Steed, E., N. Faggianelli, S. Roth, C. Ramspacher, J. P. Concordet and J. Vermot (2016). "klf2a couples mechanotransduction and zebrafish valve morphogenesis through fibronectin synthesis." Nat Commun **7**: 11646.
Steimle, J. D. and I. P. Moskowitz (2017). "TBX5: A Key Regulator of Heart Development." Curr Top Dev Biol **122**: 195-221.

Stoller, J. Z., L. Huang, C. C. Tan, F. Huang, D. D. Zhou, J. Yang, B. D. Gelb and J. A. Epstein (2010). "Ash2l interacts with Tbx1 and is required during early embryogenesis." Exp Biol Med (Maywood) **235**(5): 569-576.
Straight, A. F., A. Cheung, J. Limouze, I. Chen, N. J. Westwood, J. R. Sellers and T. J. Mitchison (2003). "Dissecting temporal and spatial control of cytokinesis with a myosin II Inhibitor." Science **299**(5613): 1743-1747.
Strate, I., F. Tessadori and J. Bakkers (2015). "Glypican4 promotes cardiac specification and differentiation by attenuating canonical Wnt and Bmp signaling." Development **142**(10): 1767-1776.
Streissguth, A. P., F. L. Bookstein, H. M. Barr, P. D. Sampson, K. O'Malley and J. K. Young (2004). "Risk factors for adverse life outcomes in fetal alcohol syndrome and fetal alcohol effects." J Dev Behav Pediatr **25**(4): 228-238.
Stuckey, D. (1956). "Congenital heart defects following maternal rubella during pregnancy." Br Heart J **18**(4): 519-522.
Sun, L., Z. Zou, P. Collodi, F. Xu, X. Xu and Q. Zhao (2005). "Identification and characterization of a second fibronectin gene in zebrafish." Matrix Biol **24**(1): 69-77.
Sun, Z., S. S. Guo and R. Fässler (2016). "Integrin-mediated mechanotransduction." J Cell Biol **215**(4): 445-456.
Sylva, M., M. J. van den Hoff and A. F. Moorman (2014). "Development of the human heart." Am J Med Genet A **164A**(6): 1347-1371.
Sztal, T., S. Berger, P. D. Currie and T. E. Hall (2011). "Characterization of the laminin gene family and evolution in zebrafish." Dev Dyn **240**(2): 422-431.
Thisse, B., V. Heyer, A. Lux, V. Alunni, A. Degrave, I. Seiliez, J. Kirchner, J. P. Parkhill and C. Thisse (2004). "Spatial and temporal expression of the zebrafish genome by large-scale in situ hybridization screening." Methods Cell Biol **77**: 505-519.
Thorsson, T., W. W. Russell, N. El-Kashlan, R. Soemedi, J. Levine, S. B. Geisler, T. Ackley, A. Tomita-Mitchell, J. A. Rosenfeld, A. Töpf, M. Tayeh, J. Goodship, J. W. Innis, B. Keavney and M. W. Russell (2015). "Chromosomal Imbalances in Patients with Congenital Cardiac Defects: A Meta-analysis Reveals Novel Potential Critical Regions Involved in Heart Development." Congenit Heart Dis **10**(3): 193-208.
Tien, E. S., J. W. Davis and J. P. Vanden Heuvel (2004). "Identification of the CREB-binding protein/p300-interacting protein CITED2 as a peroxisome proliferator-activated receptor alpha coregulator." J Biol Chem **279**(23): 24053-24063.
Tikkanen, J. and O. P. Heinonen (1990). "Risk factors for cardiovascular malformations in Finland." Eur J Epidemiol **6**(4): 348-356.
Trinh, L. A. and D. Y. Stainier (2004). "Fibronectin regulates epithelial organization during myocardial migration in zebrafish." Dev Cell **6**(3): 371-382.
Turan, S., O. M. Turan, J. Miller, C. Harman, E. A. Reece and A. A. Baschat (2011). "Decreased fetal cardiac performance in the first trimester correlates with hyperglycemia in pregestational maternal diabetes." Ultrasound Obstet Gynecol **38**(3): 325-331.
Tuysuz, B., R. Mosig, G. Altun, S. Sancak, M. J. Glucksman and J. A. Martignetti (2009). "A novel matrix metalloproteinase 2 (MMP2) terminal hemopexin domain mutation in a family with multicentric osteolysis with nodulosis and arthritis with cardiac defects." Eur J Hum Genet **17**(5): 565-572.
Ueda, Y., S. Miki, K. Kusuhara, Y. Okita, T. Tahata and K. Yamanaka (1992). "Deep hypothermic systemic circulatory arrest and continuous retrograde cerebral perfusion for surgery of aortic arch aneurysm." Eur J Cardiothorac Surg **6**(1): 36-41; discussion 42.
van der Linde, D., E. E. Konings, M. A. Slager, M. Witsenburg, W. A. Helbing, J. J. Takkenberg and J. W. Roos-Hesselink (2011). "Birth prevalence of congenital heart disease worldwide: a systematic review and meta-analysis." J Am Coll Cardiol **58**(21): 2241-2247.

van der Ven, J. P. G., E. van den Bosch, A. J. C. C. Bogers and W. A. Helbing (2019). "Current outcomes and treatment of tetralogy of Fallot." F1000Res **8**.
Verhoeven, M. C., C. Haase, V. M. Christoffels, G. Weidinger and J. Bakkers (2011). "Wnt signaling regulates atrioventricular canal formation upstream of BMP and Tbx2." Birth Defects Res A Clin Mol Teratol **91**(6): 435-440.
Verma, S. and S. C. Siu (2014). "Aortic dilatation in patients with bicuspid aortic valve." N Engl J Med **370**(20): 1920-1929.
Vida, V. L., H. Berggren, W. J. Brawn, W. Daenen, D. Di Carlo, R. Di Donato, H. L. Lindberg, A. F. Corno, J. Fragata, M. J. Elliott, V. Hraska, L. Kiraly, F. Lacour-Gayet, B. Maruszewski, J. Rubay, H. Sairanen, G. Sarris, A. Urban, C. Van Doorn, G. Ziemer and G. Stellin (2007). "Risk of surgery for congenital heart disease in the adult: a multicentered European study." Ann Thorac Surg **83**(1): 161-168.
Vincentz, J. W., R. M. Barnes and A. B. Firulli (2011). "Hand factors as regulators of cardiac morphogenesis and implications for congenital heart defects." Birth Defects Res A Clin Mol Teratol **91**(6): 485-494.
Virani, S. S., A. Alonso, E. J. Benjamin, M. S. Bittencourt, C. W. Callaway, A. P. Carson, A. M. Chamberlain, A. R. Chang, S. Cheng, F. N. Delling, L. Djousse, M. S. V. Elkind, J. F. Ferguson, M. Fornage, S. S. Khan, B. M. Kissela, K. L. Knutson, T. W. Kwan, D. T. Lackland, T. T. Lewis, J. H. Lichtman, C. T. Longenecker, M. S. Loop, P. L. Lutsey, S. S. Martin, K. Matsushita, A. E. Moran, M. E. Mussolino, A. M. Perak, W. D. Rosamond, G. A. Roth, U. K. A. Sampson, G. M. Satou, E. B. Schroeder, S. H. Shah, C. M. Shay, N. L. Spartano, A. Stokes, D. L. Tirschwell, L. B. VanWagner, C. W. Tsao and A. H. A. C. o. E. a. P. S. C. a. S. S. Subcommittee (2020). "Heart Disease and Stroke Statistics-2020 Update: A Report From the American Heart Association." Circulation **141**(9): e139-e596.
Wang, X., Q. Yu, Q. Wu, Y. Bu, N. N. Chang, S. Yan, X. H. Zhou, X. Zhu and J. W. Xiong (2013). "Genetic interaction between pku300 and fbn2b controls endocardial cell proliferation and valve development in zebrafish." J Cell Sci **126**(Pt 6): 1381-1391.
Wentzel, P., M. Gäreskog and U. J. Eriksson (2008). "Decreased cardiac glutathione peroxidase levels and enhanced mandibular apoptosis in malformed embryos of diabetic rats." Diabetes **57**(12): 3344-3352.
Williams, C. and L. D. Black III (2015). The Role of Extracellular Matrix in Cardiac Development. Biomaterials for Cardiac Regeneration, SpringerLink**:** 1-35.
Williams, J. S., J. Y. Hsu, C. C. Rossi and K. B. Artinger (2018). "Requirement of zebrafish pcdh10a and pcdh10b in melanocyte precursor migration." Dev Biol.
Wren, C., G. Birrell and G. Hawthorne (2003). "Cardiovascular malformations in infants of diabetic mothers." Heart **89**(10): 1217-1220.
Wyatt, R. A., J. Y. Keow, N. D. Harris, C. A. Haché, D. H. Li and B. D. Crawford (2009). "The zebrafish embryo: a powerful model system for investigating matrix remodeling." Zebrafish **6**(4): 347-354.
Wypij, D., J. W. Newburger, L. A. Rappaport, A. J. duPlessis, R. A. Jonas, G. Wernovsky, M. Lin and D. C. Bellinger (2003). "The effect of duration of deep hypothermic circulatory arrest in infant heart surgery on late neurodevelopment: the Boston Circulatory Arrest Trial." J Thorac Cardiovasc Surg **126**(5): 1397-1403.
Wünnemann, F., A. Ta-Shma, C. Preuss, S. Leclerc, P. P. van Vliet, A. Oneglia, M. Thibeault, E. Nordquist, J. Lincoln, F. Scharfenberg, C. Becker-Pauly, P. Hofmann, K. Hoff, E. Audain, H. H. Kramer, W. Makalowski, A. Nir, S. S. Gerety, M. Hurles, J. Comes, A. Fournier, H. Osinska, J. Robins, M. Pucéat, O. Elpeleg, M. P. Hitz, G. Andelfinger and M. L. C. p. investigators (2020). "Loss of ADAMTS19 causes progressive non-syndromic heart valve disease." Nat Genet **52**(1): 40-47.

Yahalom-Ronen, Y., D. Rajchman, R. Sarig, B. Geiger and E. Tzahor (2015). "Reduced matrix rigidity promotes neonatal cardiomyocyte dedifferentiation, proliferation and clonal expansion." Elife **4**.
Yahata, T., W. Shao, H. Endoh, J. Hur, K. R. Coser, H. Sun, Y. Ueda, S. Kato, K. J. Isselbacher, M. Brown and T. Shioda (2001). "Selective coactivation of estrogen-dependent transcription by CITED1 CBP/p300-binding protein." Genes Dev **15**(19): 2598-2612.
Yang, J., S. L. Carmichael, M. Canfield, J. Song, G. M. Shaw and N. B. D. P. Study (2008). "Socioeconomic status in relation to selected birth defects in a large multicentered US case-control study." Am J Epidemiol **167**(2): 145-154.
Yang, J., K. A. Hartjes, T. J. Nelson and X. Xu (2014). "Cessation of contraction induces cardiomyocyte remodeling during zebrafish cardiogenesis." Am J Physiol Heart Circ Physiol **306**(3): H382-395.
Yang, J. and X. Xu (2012). "Immunostaining of dissected zebrafish embryonic heart." J Vis Exp(59): e3510.
Yang, Y. Q., L. Gharibeh, R. G. Li, Y. F. Xin, J. Wang, Z. M. Liu, X. B. Qiu, Y. J. Xu, L. Xu, X. K. Qu, X. Liu, W. Y. Fang, R. T. Huang, S. Xue and G. Nemer (2013). "GATA4 loss-of-function mutations underlie familial tetralogy of fallot." Hum Mutat **34**(12): 1662-1671.
Yauck, J. S., M. E. Malloy, K. Blair, P. M. Simpson and D. G. McCarver (2004). "Proximity of residence to trichloroethylene-emitting sites and increased risk of offspring congenital heart defects among older women." Birth Defects Res A Clin Mol Teratol **70**(10): 808-814.
Yoo, S. J., T. Spray, E. H. Austin, T. J. Yun and G. S. van Arsdell (2017). "Hands-on surgical training of congenital heart surgery using 3-dimensional print models." J Thorac Cardiovasc Surg **153**(6): 1530-1540.
Yue, X., T. M. Schultheiss, E. A. McKenzie and R. D. Rosenberg (2004). "Role of heparan sulfate in dextral heart looping in chick." Glycobiology **14**(8): 745-755.
Zaidi, S. and M. Brueckner (2017). "Genetics and Genomics of Congenital Heart Disease." Circ Res **120**(6): 923-940.
Zatyka, M., M. Priestley, E. J. Ladusans, A. E. Fryer, J. Mason, F. Latif and E. R. Maher (2005). "Analysis of CRELD1 as a candidate 3p25 atrioventicular septal defect locus (AVSD2)." Clin Genet **67**(6): 526-528.
Zhang, M., W. Luo, L. Wang, X. Chen, N. Bao and Z. Xu (2020). "Causes of Death after Congenital Heart Surgery in Children." Congenital Heart Disease **15**(5): 377-386.
Zhao, L., S. H. Ni, X. Y. Liu, D. Wei, F. Yuan, L. Xu, Xin-Li, R. G. Li, X. K. Qu, Y. J. Xu, W. Y. Fang, Y. Q. Yang and X. B. Qiu (2014). "Prevalence and spectrum of Nkx2.6 mutations in patients with congenital heart disease." Eur J Med Genet **57**(10): 579-586.
Zhao, Q., X. Liu and P. Collodi (2001). "Identification and characterization of a novel fibronectin in zebrafish." Exp Cell Res **268**(2): 211-219.

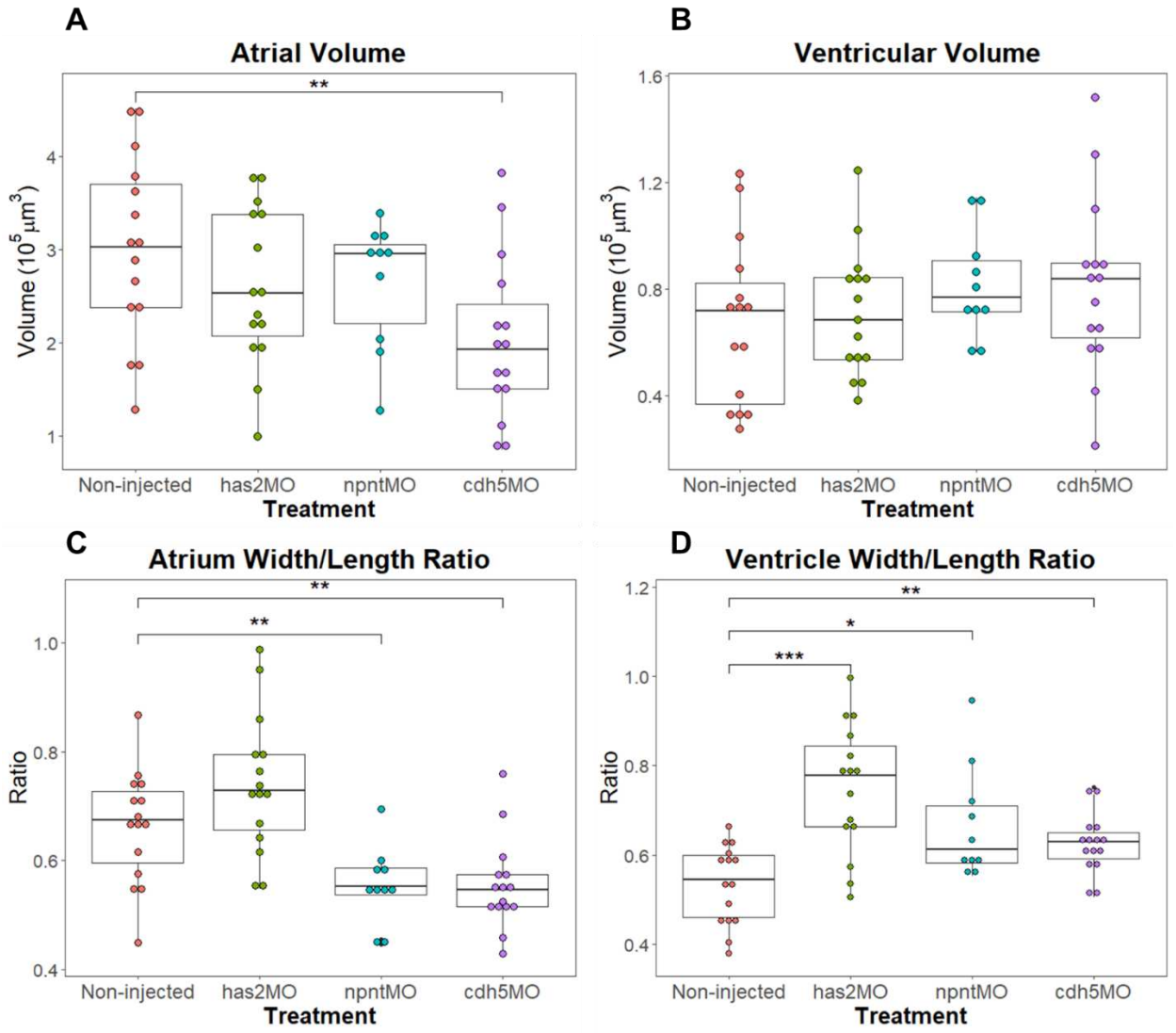

Supplemental Figure 1.1. Changes to cardiac jelly does not alter chamber volume but affects chamber shape. After injection of *has2, npnt,* and *cdh5 morpholinos,* the volume of embryonic hearts was measured in the atrium (**A**), the ventricle (**B**). The ratio of the width and length of each chamber was also calculated (**C**, **D**). Dunnett's comparison performed, * indicates $p \leq 0.05$, ** indicates $p \leq 0.01$, *** and **** indicates $p \leq 0.001$.

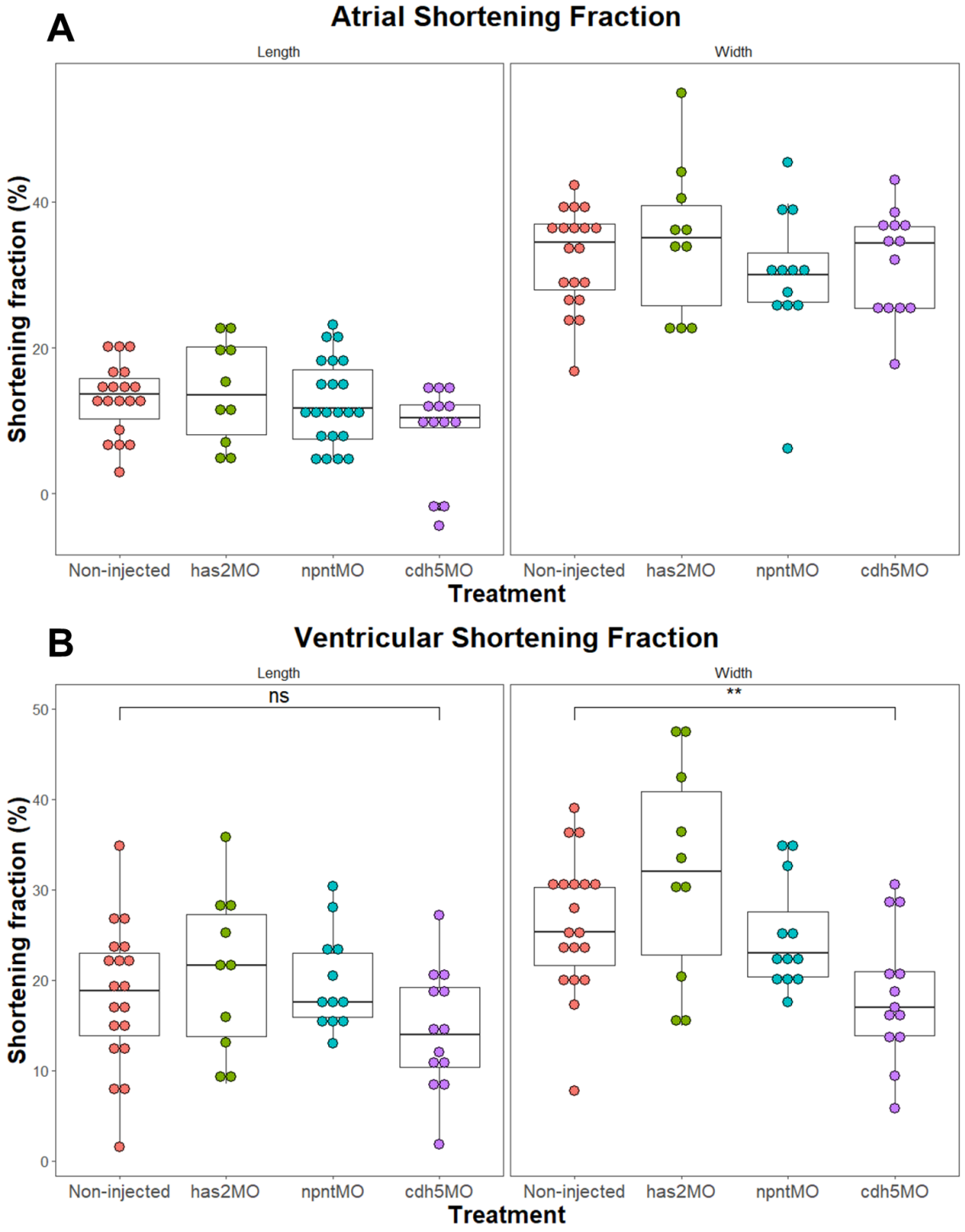

Supplemental Figure 1.2. Minimal change in ventricular shortening fraction after CJ alteration. The shortening fraction across the length and width of the atrium (A) and ventricle (B) were calculated. No change in atrial shortening fraction was calculated with any morpholino injection. There is a significant decrease in ventricle width decrease after *cdh5* morpholino injection. Dunnett's comparison performed, "ns" indicates no significance, ** indicates $p \leq 0.01$